1-2022

The Effect of Climate Change, Human Activity, and Water Management Interventions on Environmental and Socio-Economic Outcomes in the Mekong Delta Region

Huynh Truong Gia Nguyen
Montclair State University

The Effect of Climate Change, Human Activity, and Water Management Interventions on Environmental and Socio-Economic Outcomes in the Mekong Delta Region

A DISSERTATION

Submitted to the Faculty of

Montclair State University in partial fulfillment

of the requirements

for the degree of Doctor of Philosophy

by

Huynh Truong Gia Nguyen

Montclair State University

Montclair, New Jersey

January 2022

Dissertation Chair: Dr. Pankaj Lal

MONTCLAIR STATE UNIVERSITY

THE GRADUATE SCHOOL

DISSERTATION APPROVAL

We hereby approve the Dissertation

THE EFFECT OF CLIMATE CHANGE, HUMAN ACTIVITY, AND WATER MANAGEMENT INTERVENTIONS ON ENVIRONMENTAL AND SOCIO-ECONOMIC OUTCOMES IN THE MEKONG DELTA REGION

of

Huynh Truong Gia Nguyen

Candidate for the Degree:

Doctor of Philosophy

Graduate Program:

Environmental Management

Dissertation Committee:

[redacted]

Dr. Pankaj Lal
Dissertation Chair

[redacted]

Dr. Michelle Zhu

[redacted]

Dr. Yang Deng

[redacted]

Dr. Josh Galster

[redacted]

Dr. Kenneth Bagstad

[redacted]

Dr. Scott Herness
Vice Provost for Research and
Dean of the Graduate School

Jan. 12, 2022
Date

ABSTRACT

The Vietnam Mekong Delta (VMD) is the southernmost part of the Mekong River watershed basin and plays a critical role in Vietnam's socio-economic and ecological wellbeing. Because of both climate change and anthropogenic activities, such as hydropower dam construction and overwhelming water extraction, the area has recently experienced severe droughts, changing rainfall patterns, and decreasing water resources, collectively heightening disaster risks. Understanding the interactions among these evolving factors is key to preserving resources in the VMD and similarly afflicted regions. Therefore, this dissertation included three objectives. The first objective was to estimate potential impacts of changes in the available water resources in the research area by predicting soil moisture and drought risk in the Mekong Delta using the Variable Infiltration Capacity (VIC) model. The second objective was to develop and validate an Artificial Neural Networks (ANNs) that would be able to predict soil moisture in the Mekong Delta. This process entailed using historical soil moisture data and comparing those data with the ANNs predicted model data. The third objective was to evaluate the willingness of the inhabitants of the VMD to engage in potential tradeoffs to avoid potential disaster risk in the region and to use this information to assist the Vietnamese government in developing environmental policies in the VMD. The VIC model showed that land cover change would have minimal impact on soil moisture in the area, that an increase in cropland would result in a decrease in soil moisture, and that there would be notable differences in soil moisture during the wet versus dry season. Also, the model showed that there would be severe drought in the period between the wet and dry season along the VMD's western coastline. The ANNs model resulted in a high correlation between the historical data and the predicted soil moisture. In brief, both the VIC model and the ANN model have the ability to predict soil moisture. After the Vietnamese government introduced a flood management system, altering the natural flood pattern, VMD residents of both the area immediately downstream from the flood management structures and those who lived farther downstream were negatively affected socioeconomically. We conducted a survey of residents of the VMD and found that residents were willing to trade off some short-term benefits for long-term stability, but the residents farthest downstream were more willing to

accept tradeoffs than those residing immediately below the flood management system, as those farther downstream were more negatively affected by the new flood plan.

ACKNOWLEDGEMENTS

I would like to acknowledge a great many people for the support and guidance necessary for this dissertation. This work would not have been possible without the guidance of my dissertation advisor Dr. Pankaj Lal, and without my doctoral committee consisting of Dr. Deng, Dr. Galster, Dr. Zhu and Dr. Bagstad.

This work constantly challenged my abilities and understanding, and thus assistance and mentoring from Erik Lyttek, Meghann Smith, Sydney Oluoch, Taylor Wieczerak, Archana Prasad, Nicole Provost, and many others were critical in finishing this document. Support from family and friends, including my grandparents and parents, Dr. Trinh Thuc Hien, Nguyen Thi Kim Nga, and Dr. William Sullivan was instrumental in keeping me sane and pushing me forward.

The authors gratefully acknowledge the support of Montclair State University, the Clean Energy and Sustainability Analytics Center, and Nong Lam University. Finally, I would like to acknowledge the National Science Foundation, and the Vietnam Education Foundation, both of whom partially funded this research.

CONTENTS

LIST OF FIGURES

LIST OF TABLES

LIST OF ABBREVIATIONS

CHAPTER 1. INTRODUCTION

1. The Mekong River Delta

The Mekong River, which originates in China at the Tibetan Plateau, then flows downstream through Myanmar, Laos, Thailand, and Cambodia before draining into the East Sea (also known as the South China Sea) in Vietnam. The Mekong River is more than 4,000 kilometers in length, with an annual mean discharge of river water of approximately 475 km^3 (Mekong River Commission [MRC], 2005). The hydrologic characteristics of the Mekong River are complex due to extensive watershed areas covering various geographic features. According to the Vietnamese government's Ministry of Natural Resources and Environment (MONRE) (2010), the Mekong River gains its water mainly from precipitation via runoff processes. As a result, the different regions along the river contribute different volumes of water annually. The Mekong River Basin (Figure 1), with a surface area of 795,000 km^2, is the most significant watershed basin in Southeast Asia and is divided into two parts: The Upper Mekong River Basin (UMB) and the Lower Mekong River Basin (LMB) (Thompson et al., 2014, Tanaka, 2003, MRC, 2010). The Lower Mekong River Basin is also called the Mekong Delta, extending from central Cambodia to the southern part of Vietnam, where the Mekong River empties into the East Sea (MRC, 2017).

Figure 1. The Mekong River Basin (Modified from Beilfuss and Tran, 2016)

While the LMB supplies a substantial amount of water to the river's total annual flow, the UMB contributes a small portion to the total annual flow during the rainy season. However, 24% of the total river flow is dependent on ice melt in the Tibetan Plateau in China during the dry season (MONRE, 2010, MRC, 2017). Figure 2 illustrates the volume of water delivered to the Mekong River from its catchments (MONRE, 2010).

The Mekong River has brought substantial economic benefits to the countries it flows through. For example, the enriched alluvial water brings natural fertilizer to the Mekong Delta via sedimentation processes. In addition, the Mekong River is the home to numerous native wild freshwater species, such as giant Mekong catfish, aquatic snail, and the rare river dolphin (Campbell, 2016). Several studies have estimated that there are approximately 900 freshwater species in the Mekong River, making it the second most biodiverse river ecosystem on Earth (Campbell, 2016; Ziv et al., 2012).

Figure 2. The contributions of Mekong River's catchments to the total annual river flow. The number in the green box illustrates the amount of water (in billion cubic meters) that are contributed to the main flow of the river annually (Modified from MONRE, 2010).

2. Hydropower dam construction and its impact on water flow in the Mekong River

A key anthropogenic activity that disrupts the Mekong River streamflow is hydropower dam construction. The total estimated hydropower potential of 53,000 megawatts (MW) has driven countries along the Mekong River to the dam construction race (International Centre for Environmental Management (ICEM), 2010). Indeed, there has been a remarkable increase in upstream hydropower development in several countries along the Mekong River (i.e., China, Laos, Thailand, and Cambodia). In 2011, it was reported that 77 dams had been built in the Mekong River catchments. Among these, eleven dams have been constructed along the free flow mainstream of the LMB (Orr J. et al., 2012). Nguyen (2014) had reported that 136 hydropower plants have been built in the catchments. An example of the challenges associated with dam development is the unilateral decision of Laos to build the Don Sahong Dam, ignoring all concerns raised by other MRC members about the dams' impacts on the region's socio-economic and ecological features (Trandem, 2015). Figure 3 illustrates the locations of dams that have been proposed along the mainstream of the Mekong River, reported by MRC (2010).

There is a strong correlation between dam construction and the discharge declines along the Mekong Delta because the average discharge flows have been significantly lower in the post-dam period (1992–2010) compared to the pre-dam period (1960–1991). The dams also severely affect the river's ecological webs because they have altered the river's flow and sedimentation deposits (Orr et al., 2012; Piman & Shrestha, 2017). As a result, the water level in the river and its branches have recently decreased and threatened critical species' habitats, decreasing the biodiversity of aquatic flora and fauna. Also, the livelihoods of people living near water bodies have been affected by reduced water accessibility and water-based resource production, such as crop irrigation (Orr et al., 2012). Overconsumption of water extracted from the Mekong River has caused water depletion in the region, especially to the approximately 60 million people living in the LMB (MRC, 2005, Orr et al., 2012).

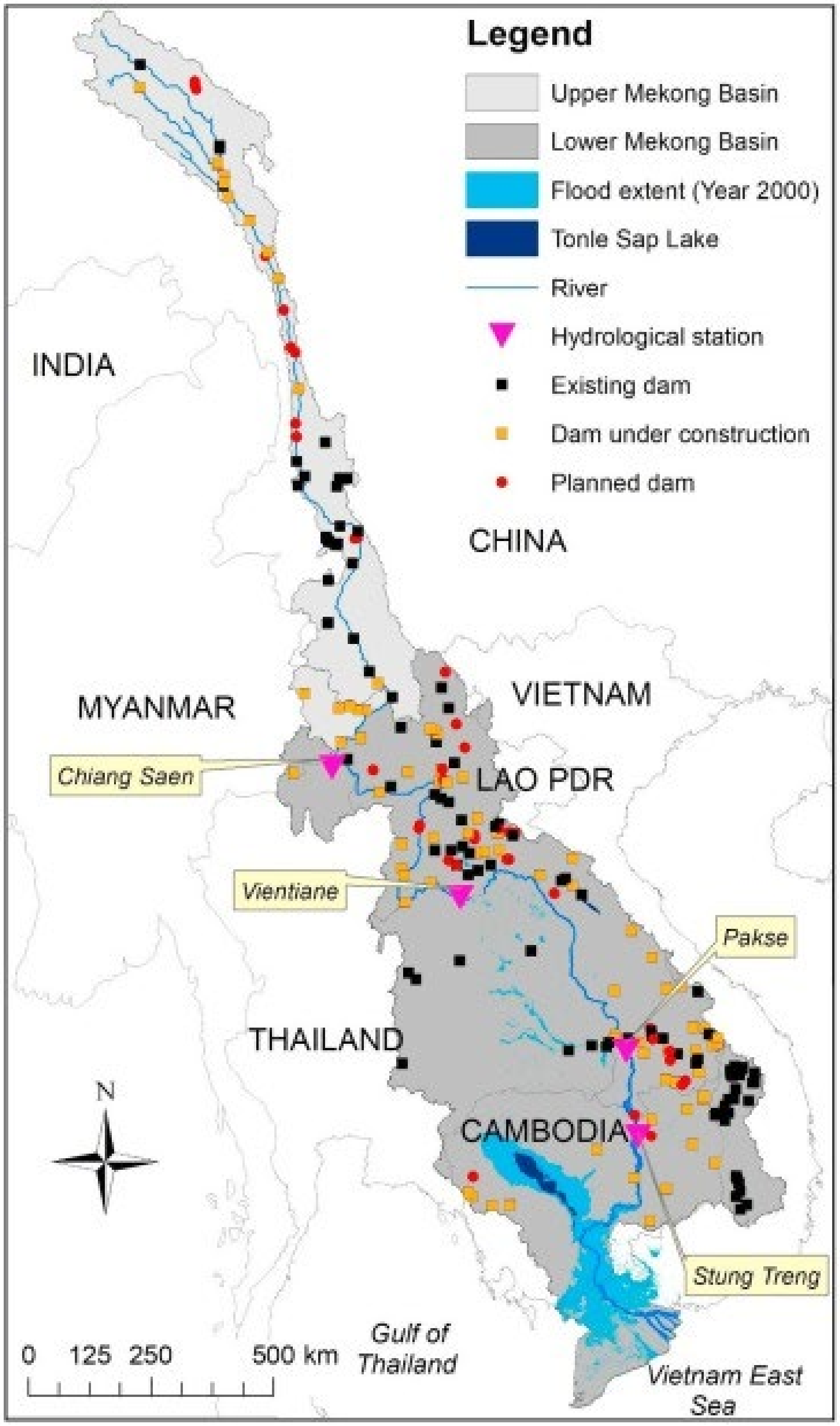

Figure 3. The hydropower dam locations that have been built or are planned to be built in the Mekong River Basin (Hecht et al., 2018)

Several studies (Zhang et al., 2015, Lu et al., 2014, Lee et al., 2014) reported that water consumption plays a significant role in drought development in the Mekong area. These studies, funded by the Nature Conservancy, identified the factors that affect changes in flow pattern such as dam construction, land cover change, climate change, and the increase in water consumption along the river (Conservation Gateway, 2021). In 2014, the MRC reported that the total amount of water used for irrigation along the LMB was approximately 12% of the Mekong water flow.

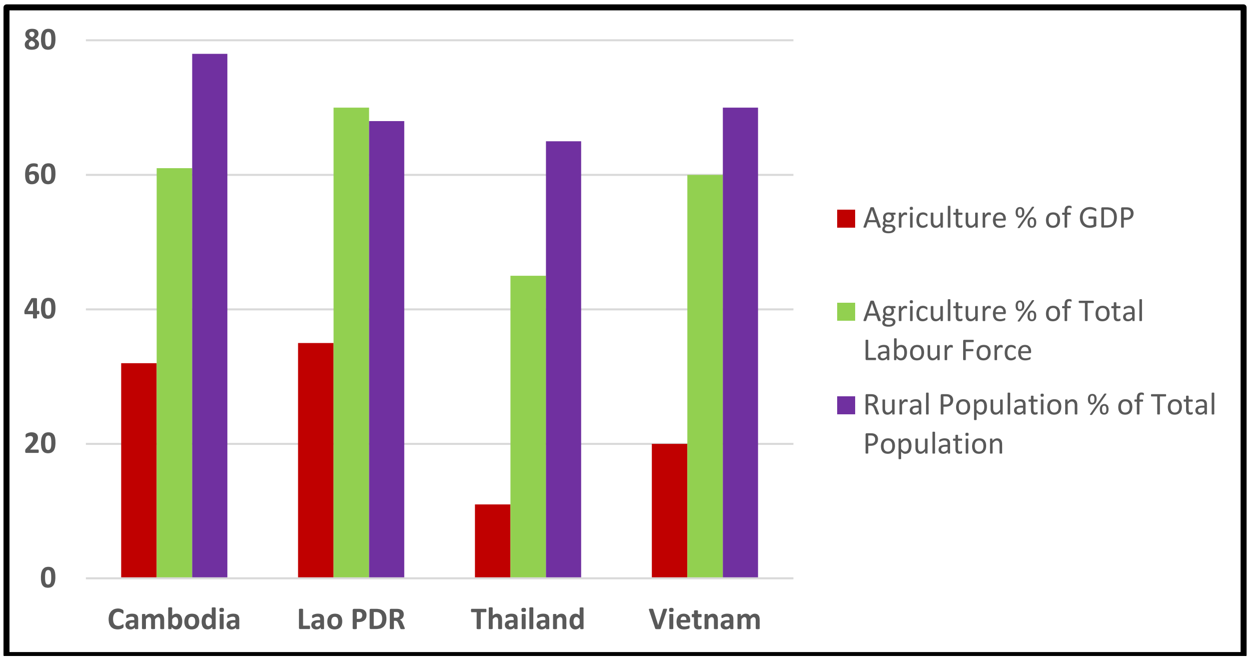

Figure 4. The contribution of agriculture to four countries of the LMB (Modified from MRC, 2014)

Figure 4 demonstrates how agricultural activities influence the economies of Cambodia, Laos, Thailand, and Vietnam. Freshwater requirements for irrigation are projected to increase exponentially as the LMB population is projected to grow to 90 million by 2050 (United Nations, 2006). In areas with aggressive irrigation systems, farmers could grow three paddy cycles annually, but the process would consume a tremendous amount of water.

Figure 5. Total rice yield by province. Source: MRC 2014

Figure 5 shows the total spatial distribution of paddy rice yield in the LMB. The highest rice yield areas were in Thailand and Vietnam, where irrigation measures maximize paddy yields. However, in these two countries, poor irrigation system design, inappropriate application, and low maintenance have resulted in an excess of 20% of water usage for irrigation (MRC, 2014).

Since sharing water management data among countries along the Mekong River has been a concern, the MRC was established with the goal of integrating water resources management. However, the lack of data sharing among the MRC members has further complicated the issue of ownership rights along the river (Thu, 2015). Southeast Asian countries have used the Mekong River for irrigation for centuries. In recent years, however, the Chinese government has influenced the river's management by monetarily investing in dam development in Cambodia. Sithirith and Gillen (2017) suggested "If one examines the Mekong through the lens of Cambodia it increasingly looks more like a Chinese river than a mainland Southeast Asian River".

3. Vietnam's Mekong Delta

Since the Vietnam's Mekong Delta (VMD) plays an essential role in the socio-economic and ecological aspects of the region. Any social or environmental modifications can drastically affect the region. There were two such attempts applied to the regions to enhance the development of this region. First, the post-1975 land reform program was initiated in an effort to rebuild the southern socio-economic status after the Vietnam War. Second, dyke structures were constructed during the 2000s with the hope of protecting agricultural land from inundations (Trung et al., 2007, Wolford and Gorman, 2010). However, both government attempts were unsuccessful. While the land reform program destroyed almost all agrarian structures in the Mekong Delta, the other was considered an expensive failure because of its social and environmental adverse consequences, such as increasing saltwater intrusion and reducing nutrient sedimentation leading to crop yield decreases.

From 2015 to 2017, agricultural drought occurred in the Mekong Delta (Fawthrop, 2019, Ho, 2016, Quang, 2017), which may be a consequence of climate change and anthropologic activities. These events shocked local farmers since they were not adequately prepared for this extreme weather phenomena. While the scientific community is looking for the appropriate response, farmers in the Mekong Delta continue to face challenges, such as lack of potable water, loss of agriculture-based income, and the need to migrate to alternative living sources. The Food and Agricultural Organization (FAO**)** (2016) pointed out that smallholder agriculture producers in developing countries could be very vulnerable to these changes; however, they can gain substantial benefits from applying resilience measures.

In efforts to cope with the drought disasters, the Vietnamese government spent approximately $2.7 million to upgrade dykes, construct sluices, and drill additional wells (Pham et al., 2017). Also, farmers living in these vulnerable areas have applied different adaptations to protect their livelihoods from these disasters. These farmer-led innovations vary from switching to more resilient crops to integrated rice-fish farming (Tran et al., 2018, Tran & Rodela, 2019).

The VMD covers 39,000 km^2, stretching from the Vietnam and Cambodia national borders to the south of Ho Chi Minh City, and finally to Ca Mau province at the southern tip of Vietnam (Figure 1). The VMD is located between latitude 8.5˚N - 11˚N and longitude 104.5˚E - 106.64˚E (Chen et al., 2011). As the Mekong River passes through Vietnam, it divides into two main branches, the Mekong River (*Tiền Giang* in Vietnamese) and the Bassac River (*Hậu Giang* in Vietnamese). These two main branches divide the VMD into three regions, including the Long Xuyen Quadrangle locating west of the *Hậu* River, the Plains of Reeds located east of the *Tien* River, and the area between the *Tiền* and *Hậu* rivers (Nguyen et al., 2015). Then, their waters drain into the East Sea. The VMD has a tropical monsoon climate, with two main seasons: rainy and dry. The rainy season is typically from July/August to December/January, while the dry season is typically from January/February to June/July. Therefore, the annual precipitation in the VMD varies from region to region. Figure 6 illustrates precipitation distribution in the VMD. The area between the *Tiền* River and *Hậu* River has the lowest annual mean precipitation rate of about 1,400 mm.

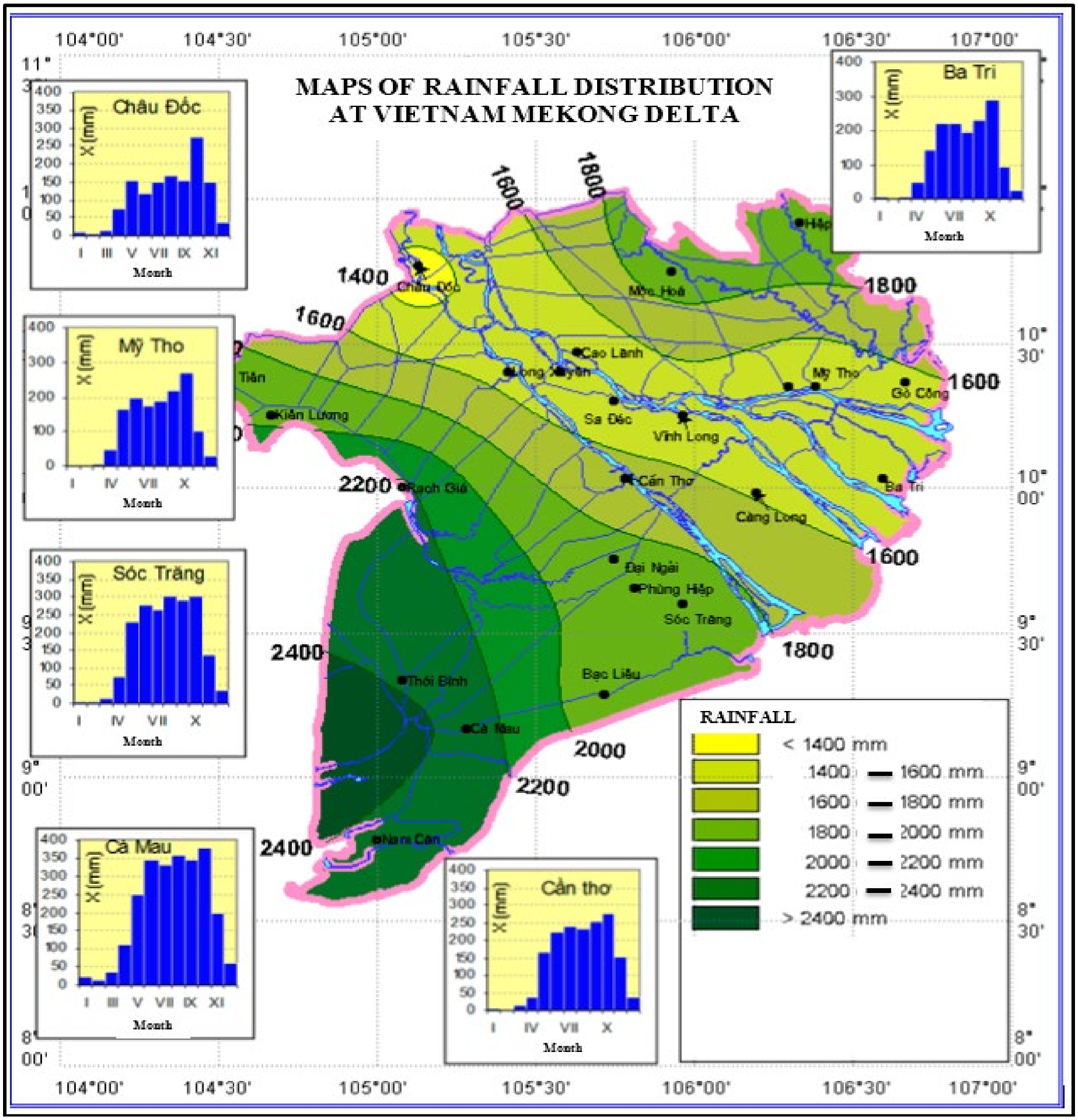

Figure 6. Map of precipitation distributions in the VMD (Modified from MONRE, 2010). Note: the black nodes represent mete orology stations.

The VMD population is about 18 million (General Statistics Office, (GSO)**,** 2014), which accounts for 20.63% of Vietnam's population. More than 82% of them are living in rural areas. On average, an individual farmer has around 0.87 hectares (ha) (MORNE, 2010). There are many different land-use-land-cover types in the VMD. Table 1 represents the most popular land uses in VMD since 2010. The VMD is named the “rice bowl” of Vietnam. Rice cultivation is the primary livelihood of about 60% of the population (Kakonen, 2008) and the region produces about half of the national food volume with 51% of total rice-paddy production, 55% of the domestic fisheries and fruit production, 60% of the exported aquaculture goods, and 61% of total export value.

Table 1. Summary of Land use classification in the VMD. Source: MONRE 2010

Land use classification		**Area (ha)**
1	Crop land	2,536,295
2	Orchard land	219
3	Aquaculture area	486,056
4	Forestry cultivation land	347,453
5	Developed area	496,992
6	Marginal land	941
7	Wetland	98,887
8	Opened area	580,350
9	Reforestation area	261,521
10	Salt production land	3,897

The VMD hydrology depends on the tropical monsoon climate with the two distinct seasons described above. Residents of Southern Vietnam are annually influenced by the floods, tidal regime, and saline intrusion from the coast. When the temperature is high and the rainfall is less during the dry season, water scarcity and saltwater intrusion from the East Sea threaten the region. In contrast, during the rainy season, floodwater brings alluvial-based nutrients to fertilize the land, driving seawater intrusion back to the ocean, and eliminating crop pests and diseases. In addition, climate change has resulted in sea level rise (SLR) and changes in precipitation patterns, which together increase the risk of freshwater depletion in the VMD.

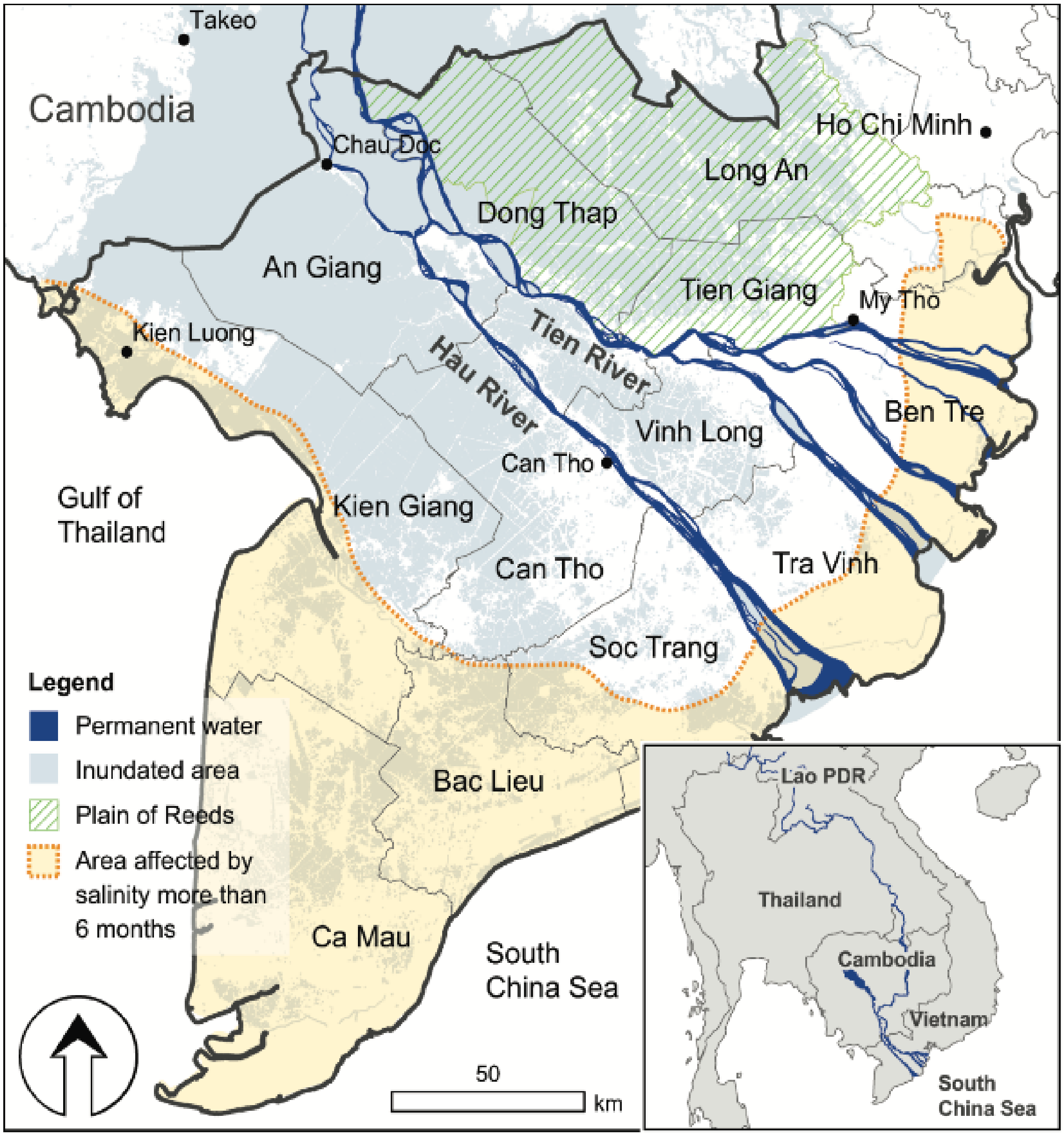

Figure 7. Map of the Vietnamese Mekong Delta with distributions of flood area and brackish area. Source: modified from Kakonen 2008)

Tanaka (2003) compared the flood regime in the Tonle Sap region of Cambodia and the VMD using specific sensor microwave/imager (SSM/I) data and national oceanic and atmospheric administration advanced very high-resolution radiometer (NOAA/AVHRR) to estimate the water coverage area from May 1997 to April 1999. He found that water coverage in VMD was greater than in Tonle Sap throughout the year. Similarly, Le (2011) used a hydrologic model approach to research climate-related phenomena on the Mekong Delta Basin flood regimes. In that study, the flood regimes in the Mekong River Delta were affected by regional flow variation, which is significantly influenced by climate change, especially the changes in annual precipitation, on the upper parts of the basin. Le applied the special-report-emissions-scenarios-A2-greenhouse-gas (SRES A2 GHG) scenario suggested by the Intergovernmental Panel on Climate Change (IPCC) for sea-level rise to project the regional climate model, regional hydrodynamic model, and the ocean circulation model. The data from the three models were then fed into the Environmental Impact Assessment 3D model. Le's model predicted that most of the flood water would be blocked in the upper part of the region instead of draining toward the East Sea. Figure 8 illustrates differences in the flood regimes in the 1980s and the predicted changes in the 2030s at the Mekong River (Le, 2011). The submerged area, in blue, was projected to be much more extensive in the 2030s than during the 1980s period.

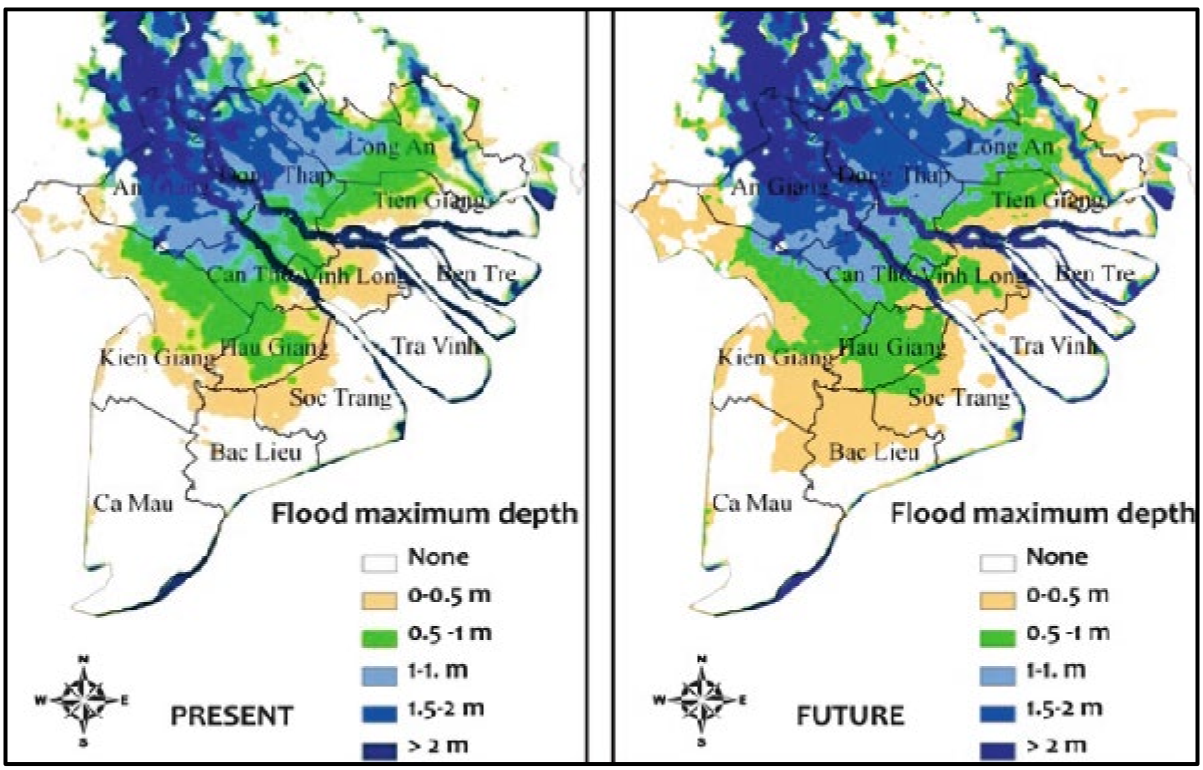

Figure 8. Flood water coverage in the Mekong Delta in the 1980s and 2030s (reproduced from Le, 2011).

Chen et al. (2011) used National Aeronautics and Space Administration's (NASA) Moderate Resolution Imaging Spectroradiometer (MODIS) data to estimate soil moisture with the temperature vegetation dryness index (TVDI) and rice crop system. Using crop pattern indices in two years, 2002 and 2006, the researchers derived the spatial soil moisture distribution using temperature vegetation dryness index and classified the drought area in the region. Figure 9 illustrates differences in TDVI between 2002 and 2006 monitoring soil moisture variability connected to rice cropping systems in the VMD using MODIS data (Chen et al., 2011). Son (2012) suggested that TDVI is a respectable indicator for evaluating drought-related climate change at the Mekong Delta. Similarly, Zhang et al. (2014) conducted a remote sensing-based model to calculate Net Primary Productivity (NPP) as a drought index using the following equation:

$$SAI_{NPP} = \frac{NPP_i - \overline{NPP}}{\sigma_{NPP}} \qquad \text{Eq. 1}$$

where SAI_{NPP} = the NPP anomalies, NPP(i) = the annual NPP in the i^{th} year, $\overline{NPP}$ = the value of mean NPP for the period 2000–2011, and σ_{NPP} = the standard deviation of the 12-year NPP. The investigators obtained data using the Palmer Drought Severity Index (PDSI) at 0.5^o x 0.5^o spatial resolution from the Numerical Terra Dynamic Simulation Group. The research concluded that the irrigation method applied in Vietnam could reduce the impact of drought in 2005 on croplands.

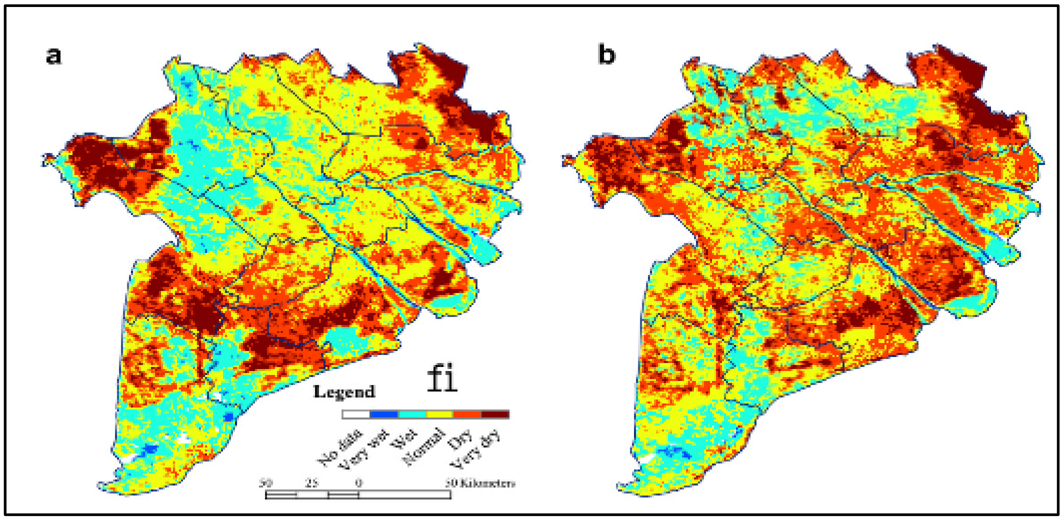

Figure 9. The spatial distribution of soil moisture in February in the year 2002 and 2006 at the Vietnamese Mekong Delta (modified from Chen, 2011).

Arias et al. (2014) evaluated the potential impact of dams on Mekong tributaries using the Soil Water Assessment Tools (SWAT) model to estimate daily runoff. The study used both the generic water quantity and quality simulation model (IQQM) and the Reservoir System Simulation (HEC-ResSim) models to compute daily discharge in the Mekong Kratie branch of the Mekong River. Next, the researchers set their scenarios, including Baseline, Definite Future, and 3S (Sesan, Srepok, and Sekong river) Dam Development, to run models based on these scenarios. Then, each model outcome was calibrated with observed data collected at Tonle Sap. The study concluded that the 3S dam development scenario introduced a high probability of altering the water levels and the dynamics of water level change rates along the Mekong River. Although the research site was located in LMB, the authors did not report the effect of the dam development on the VMD.

Although numerous publications are applying Artificial Neural Networks (ANNs) studies using deep learning-based methods on hydrology, predictions are limited. Agana et al. (2017) introduced research using a deep learning algorithms approach for long-term drought prediction. The authors suggested that, because drought variables are random and non-linear, it is difficult to find an accurate drought prediction. Hence, one should apply the ANNs method to extract hydrological features from past observed data. This research was implemented at the Upper

Colorado River Basin. In this study, the authors used Restricted Boltzmann Machine (RBM), a generative energy model, to define energy balance equations between visible and hidden layers**.** In this research, RBM was described as an activation function which is written as

$$E(v,h) = -\sum_{i=visible} a_i v_i - \sum_{j=hidden} b_j h_j - \sum_{ij} v_i h_j w_{ij} \qquad \text{Eq. 2}$$

where $v_i$and h_j are the binary level of visible unit i and hidden unit j, respectively. a_i and b_j are the bias, and w_{ij} is the weight between a and b.

The study compared observed data that were collected from 1912 – 2013 to a prediction model named deep belief network (DBN). The authors found that the output of the DBN drought prediction model had a higher correlation with the observed data than the traditional model.

Two surveys were conducted to access the farmers' perception in Maharashtra state, India, and the VMD. The research in India aimed to understand the farming community's perception of drought effects on household socio-activities, local environment, individual's adaption, and government opinion. This study carried out a face-to-face interviews with primary data collected from 223 samples. The questionnaire was divided into sections including general household characteristics, farmers' perception of drought and its impact on agriculture and livestock, environmental impacts, adaptation strategies, and mitigation measures. There were several sub-questions in each section using dichotomous**,** Likert scale, and multiple-choice types. The study found that Indian farmers needed mitigations to adapt to droughts, even though they had a good perception of the drought severity. Unfortunately, this research did not introduce a quantitative relationship between farmers' perception and the adaptations' success (Udmale et al., 2014).

Dang et al. (2014) investigated farmers' perceptions of, and adaptations to, climate change in the VMD. The study used a structural equation model to estimate interrelationships among constructs in the conceptual model. The investigators interviewed 685 farmers in total, with a refusal rate of 8.3%. The authors applied multi-stage probability sampling to identify twelve communes in the region. In this study, the questions constructed depended on specific variables. For example, to measure maladaptation to climate change, farmers were asked to rate to what extent they agreed with a given statement, based on a 7-point Likert scale. The investigators found that the farmers in VMD understood, and intended to adapt to, climate change.

RESEARCH OBJECTIVES

This study's objective was to assess the impact of climate change, anthropogenic activities, and water management interventions on environmental and socio-economic conditions in the Mekong Delta region. This was accomplished through the following studies:

1. Investigating the variation of soil moisture and agricultural drought in the Mekong Delta region using a macro-scale variable infiltration capacity (VIC) model with the Soil Moisture Anomaly Percentage Index (SMAPI) of drought.

2. Developing and validating a Multi-layer Perceptron Neural Networks (ANNs) to predict soil moisture in the Mekong Delta, comparing historical soil moisture data with the ANNs predicted model data.

3. Evaluating the willingness of the inhabitants of the VMD to engage in potential tradeoffs to avoid potential disaster risk in the region, and making this information available to the Vietnamese government, as it develops environmental policies in the VMD.

CHAPTER 2. INVESTIGATING VARIATION OF SOIL MOISTURE AND AGRICULTURAL DROUGHT IN THE MEKONG DELTA REGION USING A MACRO-SCALE VARIABLE INFILTRATION CAPACITY MODEL WITH THE SOIL MOISTURE ANOMALY PERCENTAGE INDEX OF DROUGHT

Abstract

The Mekong River Basin (MKB) is an economically and ecologically important region vulnerable to climate variability and land cover changes. To effectively develop long-term plans for these potential changes, potential results of climate variability and land cover change must be evaluated. This study predicted the impact of future land cover change on MKB spatial and temporal hydrologic parameters. The research goal was achieved by (1) using baseline land cover change to predict future land cover change and (2) feeding the predicted future land cover change as inputs into the Variable Infiltration Capacity (VIC) hydrologic model to predict future changes in soil moisture and drought in MKB. The VIC model outputs were analyzed against historical data on soil moisture and drought to understand to what degree land cover changes may affect the region's hydrology and where these changes would occur within the region. This study found that most land cover changes would occur in the Lower Mekong Basin (LMB), caused by increased use of land for agricultural purposes, but that the change in land cover would not affect soil moisture or drought. The results of this study may be used by policy makers to develop effective policies for land and water resources management in the LMB.

1. Introduction

The Mekong Delta watershed is a comprehensive ecosystem with complex stream systems. The whole system is supplied by the Mekong River and its millions of branches. The Mekong River is over 4,000 kilometers in length, with an annual mean discharge of approximately 475 km^3 (MRC, 2005). Its enriched alluvial water brings natural fertilizer to the Mekong Delta via sedimentation processes. Also, the Mekong River is the home to numerous native wild freshwater species, such as giant Mekong catfish, aquatic snail, and the rare river dolphin (Campbell, 2016). There are approximately 900 freshwater species in the Mekong River, making it the second most biodiverse river ecosystem on Earth (Campbell, 2016; Ziv et al., 2012). The watershed is a dynamic system that changes significantly under natural processes and anthropogenic activities.

Climate variability and land cover change have been identified as the main variables contributing to regional vulnerability within the Mekong Delta (Francisco, 2008). These changes have implications on crucial functions of the river such as aquatic ecosystem productivity (Kummu and Sarkkula, 2008, Lamberts, 2008), transport of sediment and nutrients (Kummu et al., 2006), freshwater supply, and disasters (i.e., flooding) (Lauri, et al., 2012). Given that the watershed itself covers almost 795,000 km^2, it is not feasible to implement field-based research covering all elements of the Mekong Delta. Hydrologic models have considerable advantages in watershed modeling with the innovation of computer science, Geographic Information System (GIS), and remote sensing technologies. Many studies to date have predicted how climate change will alter the discharge of the Mekong River (Keskinen et al., 2010; Lauri et al., 2012). Nijssen et al. (2001a, 2001b) evaluated climate effects on the streamflow of the MKB in the context of global warming and predicted that the MKB streamflow would decrease due to climate change.

Additionally, more targeted studies into the effects of climate change on the MKB (Eastham et al., 2008, Prathumratana et al., 2008, Kingston et al., 2011, Lauri et al., 2012), concluding that streamflow is highly dependent on changes in precipitation. Flow discharge reduction has also been estimated to have an impact on traditional agriculture, including irrigation (MRC, 2010). Therefore, it is important to understand the possible impact climate variability and land cover change have on the hydrology of the MKB system.

Soil moisture content (SMC) is a fundamental soil characteristic for understanding occurrences like erosion, flooding, groundwater recharge, and drought (Ahmad et al., 2009, Verstraeten et al., 2008). Spatio-temporal variation of soil moisture reflects a conjoint variability of climatic and spatial variables, such as the interactions among precipitation, land cover types, and evatransporation (Luong et al., 2020). Therefore, a better understanding of the spatio-temporal variation of soil moisture is of great importance for investigating the driving mechanisms and influencing factors for agricultural drought at the regional scale, which has important implications for water resource management as well as agriculture.

Recently, extreme droughts have occurred in the Mekong Delta (Fawthrop, 2019, Ho, 2016, Quang, 2017), which may be a consequence of climate change and anthropologic activities. These events shocked local farmers since they were not adequately prepared for this extreme weather phenomena. While the scientific community is looking for the appropriate response, farmers in the Mekong Delta continue to face challenges, such as lack of potable water, loss of agriculture-based income, and the need to migrate to alternative living sources.

It is essential to investigate the impact of mereological indicators, land cover changes, and topography on the spatial and temporal variation of drought in different regions in the MKB. However, the questions on how these variables influence the spatio-temporal variations of soil moisture in the regions remain unanswered. Therefore, the main objective of this study was to estimate the water budget of the region using the VIC model, a semi-distributed land surface hydrologic model. Then, the soil moisture and drought variation were derived from the VIC model results to:

1. Estimate agricultural drought variation in the MKB using the soil moisture anomaly percentage index (SMAPI).

2. Simulate soil moisture and drought variations for the different land cover change scenarios to determine effect of land cover on soil moisture and drought variation in the MKB.

2. Method and Materials

2.1. VIC Soil Moisture Simulation

The VIC model was first introduced by Liang et al. (1994) as a hydrological modelling effort implemented at the University of Washington, Seattle. The model operates by using both water balance and energy balance equations within a grid-cell. Each active grid-cell is apportioned into multiple vegetation and soil layers with variable infiltration rates and topography (Tatsumi & Yamashiki, 2015). The VIC model runs on the Linux/Unix platform. Several studies have applied the VIC model. Applications of the model to the continental U.S. have established reasonable estimates between predicted and observed measurements, between observed and simulated snow water equivalent, and between observed and simulated streamflow (Andreadis & Lettenmaier, 2006).

The VIC model estimates the hydrological features based on the water balance equation (Eq.3). While soil moisture, evapotranspiration, infiltration, and runoff are outputs, soil parameters, such as precipitation, land use land cover, and soil texture, are required as hydrologic inputs (Liang et al., 1994, 1996, Nijssen et al., 1997, Vigerstol et al., 2011). The water balance equation is written as

$$\frac{dS}{dt} = P - E - R \qquad \text{Eq. 3}$$

The dS/dt = the terrestrial water storage, P = precipitation, E = evapotranspiration, and R = the total runoff. In the long-term calculation, it is assumed that moisture in the atmosphere and soil are unchanged. Eq.3 can be simplified as

$$\bar{R} \approx \bar{P} - \bar{E} - \nabla\bar{Q} \quad \text{Eq. 4}$$

where $\nabla\bar{Q}$ = horizontal water vapor. Eq.4 can be interpreted as the system's horizontal water vapor, which approximately equals the total runoff out of the system.

The VIC model outcomes usually estimate hydrologic watershed elements, including daily surface runoff, baseflow, evaporation, soil moisture, and snow water equivalent for each grid-cell. With these outputs, the drought index can be characterized by the water balance equation (Ma et al., 2016). The VIC model's calibration and validation processes for this study were conducted from 2019 to 2020 using the streamflow data obtained from the stream gauges along the river. For calibration and validation procedures, the sensitivity parameters of the VIC model, including variable infiltration curve parameter ($b_{infiltration}$), maximum velocity of baseflow (D_{smax}), fraction of D_{smax} where non-linear baseflow occurs (Ds), and fraction of maximum soil moisture where non-linear baseflow occurs (W_s) were adjusted (Markert et al., 2018). The critical metrics for model performance evaluation showed that the VIC model could capture the hydrologic dynamic over the MKB with Pearson's correlation coefficient reaching 0.75 and the index of agreement approaching 0.85. Using the simulation outputs of the VIC model, the simulated soil moisture dataset for nine years (2010–2018) was extracted to analyze the agricultural droughts within the MKB in this study. The soil moisture datasets were calculated and presented for dry, wet, and transitional periods.

2.2. Soil Moisture Anomaly Percentage Index

The Soil Moisture Anomaly Percentage Index (SMAPI) indicator, suggested by the Copernicus European Drought Observatory (EDO), was applied for determining the start and duration of agricultural drought conditions relating to soil moisture variability, which adversely affects crop yield (Luong et al., 2021). The grid-cell based SMAPI is calculated using daily soil moisture content estimated by a hydrological model as follows

$$SMAPI = \frac{SMI_t - \overline{SMI}}{\overline{SMI}} \qquad \text{Eq. 5}$$

where SMI_t = soil moisture index (SMI), standardized daily soil moisture with mean between the wilting point and the field capacity in a t-day period. The $\overline{SMI}$ = mean of SMI, which are both calculated for the same period t (time) within a baseline period of the start-year. SMA can be used to estimate weekly or every ten-day agricultural drought (EDO, 2019).

The SMAPI is suitable to predict drought based on modelled SMC and the spatial extension of the regions impacted by or at risk of drought conditions (EDO, 2019). However, the SMAPI may produce large approximations of the actual SMC because of the hydrological models' impractical assumptions. Therefore, to avoid progressive divergence from actual conditions, model calibrations and validations were performed. Agricultural drought classification using SMAPI are presented in Table 2.

Table 2. Classification of drought conditions using the soil moisture anomaly percentage index (SMAPI).

Category	Description	SMAPI Range
D4	Extreme drought	≤− 0.50
D3	Severe drought	−0.50 to − 0.30
D2	Moderate drought	−0.30 to −0.15
D1	Mild drought	−0.15 to −0.05
N	Near normal	−0.05 to 0.05
W1	Slightly wet	0.05 to 0.15
W2	Moderately wet	0.15 to 0.30
W3	Very wet	0.30 to 0.50
W4	Extremely wet	0.50

2.3. Data Collection and Preparation

a) Land surface data

The land cover data applied in this study was extracted from National Aeronautics and Space Administration (NASA), Moderate Resolution Imaging Spectroradiometer (MODIS) combined land cover product version 6 (MCD12Q1v6) published May 14, 2018 (Friedl et al., 2019) and downloaded from the Goddard Earth Sciences Data and Information Services Center

(GES-DISC) database. The land cover legend of the dataset followed the International Geosphere-Biosphere Programme (IGBP) classification scheme which includes 16 land classes and is represented in Table 3.

Table 3. The IGBP legend and class descriptions used in MCD12Q1v6

Name	Value	Description
Evergreen Needleleaf Forests	1	Dominated by evergreen conifer trees (canopy >2m). Tree cover >60%
Evergreen Broadleaf Forests	2	Dominated by evergreen broadleaf and palmate trees (canopy >2m). Tree cover >60%.
Deciduous Needleleaf Forests	3	Dominated by deciduous needleleaf (larch) trees (canopy >2m). Tree cover >60%.
Deciduous Broadleaf Forests	4	Dominated by deciduous broadleaf trees (canopy >2m). Tree cover >60%.
Mixed Forests	5	Dominated by neither deciduous nor evergreen (40-60% of each) tree type (canopy >2m). Tree cover >60%.
Closed Shrublands	6	Dominated by woody perennials (1-2m height) >60% cover.
Open Shrublands	7	Dominated by woody perennials (1-2m height) 10-60% cover.
Woody Savannas	8	Tree cover 30-60% (canopy >2m).
Savannas	9	Tree cover 10-30% (canopy >2m)
Grasslands	10	Dominated by herbaceous annuals (<2m).
Permanent Wetlands	11	Permanently inundated lands with 30-60% water cover and >10% vegetated cover.
Croplands	12	At least 60% of area is cultivated cropland.
Urban and Built-up Lands	13	At least 30% impervious surface area including building materials, asphalt, and vehicles.
Cropland/Natural Vegetation Mosaics	14	Mosaics of small-scale cultivation 40-60% with natural tree, shrub, or herbaceous vegetation.
Permanent Snow and Ice	15	At least 60% of area is covered by snow and ice for at least 10 months of the year.
Barren	16	At least 60% of area is non-vegetated barren (sand, rock, soil) areas with less than 10% vegetation.
Water Bodies	17	At least 60% of area is covered by permanent water bodies
Unclassified	255	Has not received a map label because of missing inputs.

The monthly leaf area index and albedo were derived from the second Modern-Era Retrospective Analysis for Research and Applications (MERRA-2), which is a NASA atmospheric reanalysis using an upgraded version of the Goddard Earth Observing System Model, Version 5 (GEOS-5) data assimilation system.

b) Meteorological data

Forced meteorological data is an essential input variable for a hydrology model used in water balance through energy and mass balance equations. These data were extracted from the dataset freely available at Copernicus databases through the National Center for Atmospheric Research (NCAR) Research Data Archive from the European Centre for Medium-Range Weather Forecasts (ECMWF) ERA-Interim reanalysis dataset (ECMWF, 2009, Dee et al., 2011, Berrisford et al., 2011). The WorldClim version 1 observed climate dataset was used to study annual climatic averages of meteorological forcing variables such as annual precipitation and average temperature needed for parameterization into the hydrologic model (Hijmans et al., 2005).

The study accessed the precipitation products from the Precipitation Estimation from Remote Sensing Observation using Artificial Neural Networks Cloud Classification System (PERSIANN-CCS), which is designed and operated at the Center for Hydrometeorology and Remote Sensing (CHRS) at the University of California, Irvine.

2.4. Land Cover Change Prediction

Land cover projections were modeled using a multilayer perceptron neural network built-in the land change modeler (LCM) for ecological sustainability in TerrSet software, published by Clark Labs. The LCM, used for the assessment and prediction of land cover change and its application, are organized into major areas: change analysis, change prediction, and planning interventions. The LCM workflow included (1) Change Analysis, (2) Transition Potential, and (3) Change Prediction.

In the Change Analysis section, the LCM requires land cover images for earlier and later years in the period of study. In addition, the basic road and topographic layers are required for dynamic development predictions. Based on land cover change during the 2010-2018 period, the LCM estimated the main variables that drove changes in land cover. In this study, we chose distance to water, distance to urban area, distance to road, and distance to cropland as driven variables for disturbances in the MKB. These driven factors were tested for significance using p-values of Cramer's V for significance.

The change prediction deployed a Multi-layer Perceptron (MLP) neural network with one input, one output and one hidden layer. The input of MLP were cells that showed change during the period. Using a trial-and-error method, the hidden layer had six nodes using three Sigmoid functions and three linear functions. We set the learning rate at 0.01 as default.

The expected accuracy rate of the MLP was a function of the number potential transitions being modeled in a sub-model along with the number of persistence classes in the "source" land cover classes. The accuracy rate was calculated by equation:

$$\mathrm{E(A)} = \frac{1}{(\mathrm{T}+\mathrm{P})} \qquad \text{Eq. 6}$$

where

E(A) = expected accuracy, T = the number of transitions in the sub-model, P = the number of persistence classes = the number of "from" classes in the sub-model.

A measure of model skill is then expressed as:

$$S = \frac{A-E(A)}{1-E(A)} \qquad \text{Eq. 7}$$

where A = measured accuracy, this measure ranges from -1 to 1 with a skill of 0 indicating random chance (Atkinson et al., 1997, Chan et al., 2001, Civco et al, 1993).

3. Result and Discussion

3.1. Land Cover Change Prediction

Based on the number of changed cells of each land cover category (Figure 10), Forest, Savanna, Cropland, and Grassland had very dynamic changes from 2010-2018, while Urban and Wetland/Water were stable during the same period. In the beginning, Cropland and Savannas expanded gradually before decreasing substantially in 2016. The decrease in Cropland areas may have been caused by the negative impacts of climate change and drought in the regions (Markert et al., 2018). It is possible that the Cropland areas may have been replaced by Grassland and Savanna areas because the Grassland and Savanna areas increased after 2016. Unfortunately, the Forest area decreased from 2010 to 2014 and then again starting in 2016.

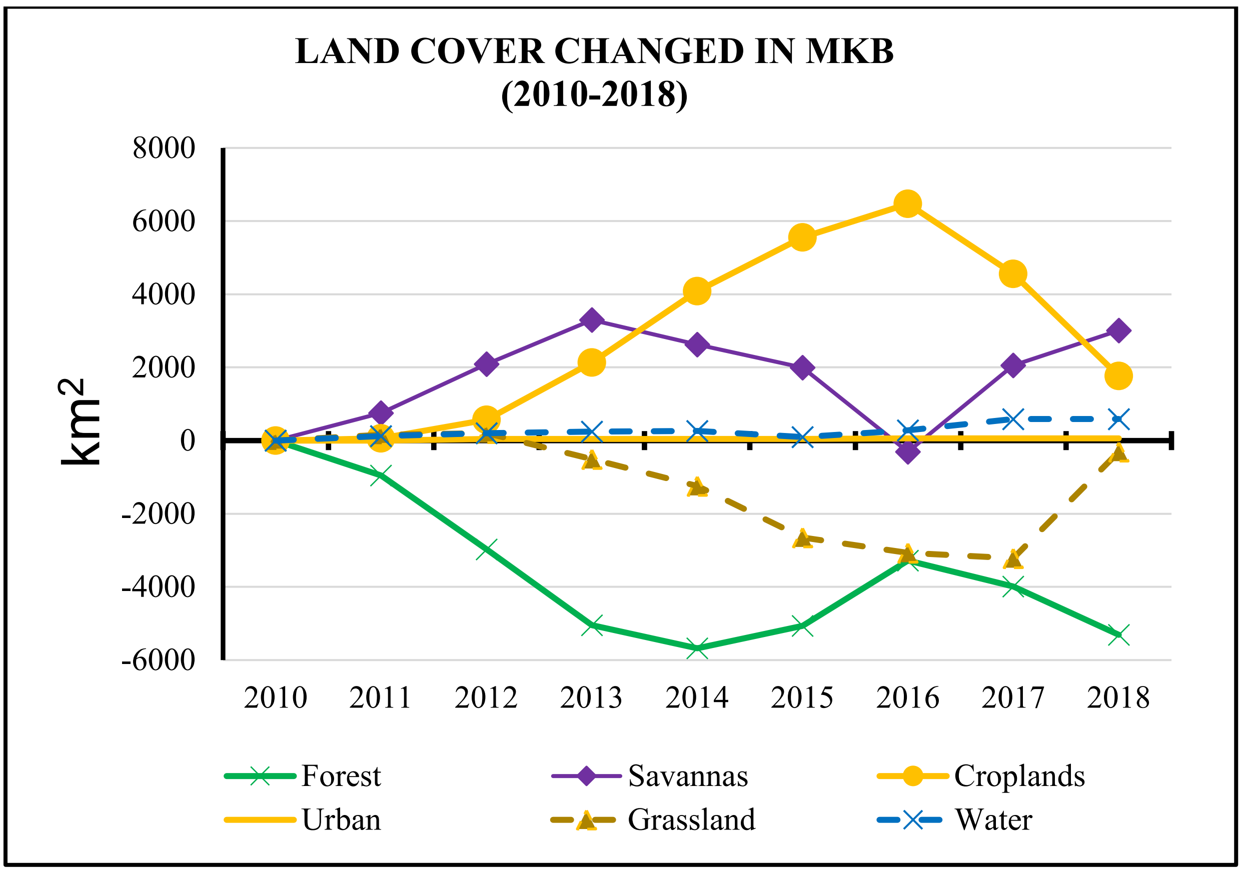

Figure 10. Land cover changed in MKB during 2010-2018

Table 4 shows contributions of different land types to Cropland changes during 2010-2018. Grassland was the most extensive area converted to Cropland with more than 1.2 million km^2. Next, Savannas and Evergreen Broadleaf Forest contributed to Cropland, about 420,750 km^2 and

7,254 km^2, respectively. In contrast, Cropland lost almost a million km^2 to Closed Shrublands, Permanent Wetlands, Woody Savannas, and Cropland/Natural Vegetation Mosaics.

Table 4. Contributions to net change in Croplands

Land Cover Types	**Area change (km^2)**
Grasslands	1,204,225
Savannas	420,753
Evergreen Broadleaf Forests	7,254
Closed Shrublands	-7,254
Permanent Wetlands	-21,763
Woody Savannas	-101,561
Cropland/Natural Vegetation Mosaics	-870,524

The present study applied the LCM model to project land cover change using TerrSet (Clark Lab, 2020) with the MLP neural network. We focused only on the transition from other land cover types to Cropland, Forest, Savannas and Grassland since they have shown the most dynamic trends in the region.

Results of LCM model showed that most of the contributions to cropland change were located at the lower part of the MKB (Figure 11). This finding is in agreement with that of Markert et al**.** (2018)

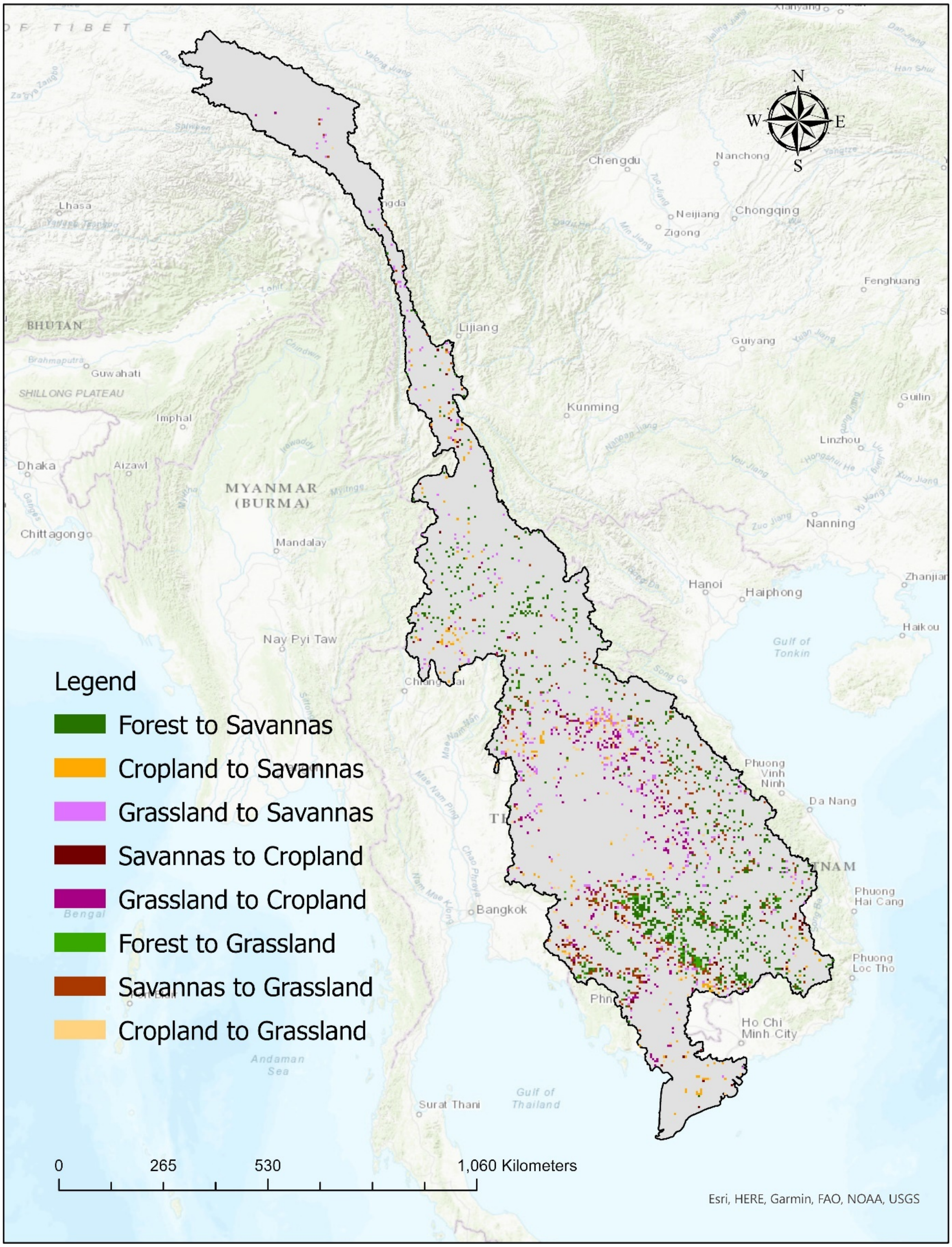

Figure 11. Distributions of land cover changes during the period 2010-2018

3.2. Land Cover Change Simulations

The predicted land cover simulations were run at five-year increments from 2018 to 2050 with multiple scenarios. This simulation used land use changes in period 2010-2018 as input for the MLP (Clark Lab, 2020), with the 2018 data as the baseline for predictions. The MLP model used three independent variables, including distance to water bodies, distance to urban areas, distance to main roads as input for the model. We also used one dummy variable, named Distance to All Cropland, to reduce the potential bias as suggested by LCM (Clark Lab, 2020).

The parameters and performance of the MLP are shown in Table 5. The model accuracy rate of 62.22% was acceptable, when considering that the MKB is a large geographic area with different ecoregions that have different suitability for different classes**.** As such, the model created for this study was optimized to capture the general trends, not specific regional trends within the basin. Also, the MLP showed a higher accuracy rate compared to previous research on MKB land cover change (Markert et al., 2018).

Table 5. Parameters and Performance

Parameters	**Values**
Input layer neurons	5
Hidden layer neurons	6
Output layer neurons	7
Requested samples per class	38
Final learning rate	0.001
Acceptable RMS	0.01
Iterations	100,000
Training RMS	0.26
Testing RMS	0.28
Accuracy rate	62.22%

The spatial distributions for each class under all scenarios for 2050 are presented in Figures 12, 13, 14. The maps of the predicted large-scale spatial patterns appear to show little change over time. However, the model shows that predicted decreases in Grassland and Natural Vegetation would be replaced by predicted agricultural land. This shift between the two classes was identified mainly in the Cambodian and Vietnamese regions of the MKB. These predicted changes make it essential to simulate the hydrologic response to these changes in order to understand the significance of shifts in land cover.

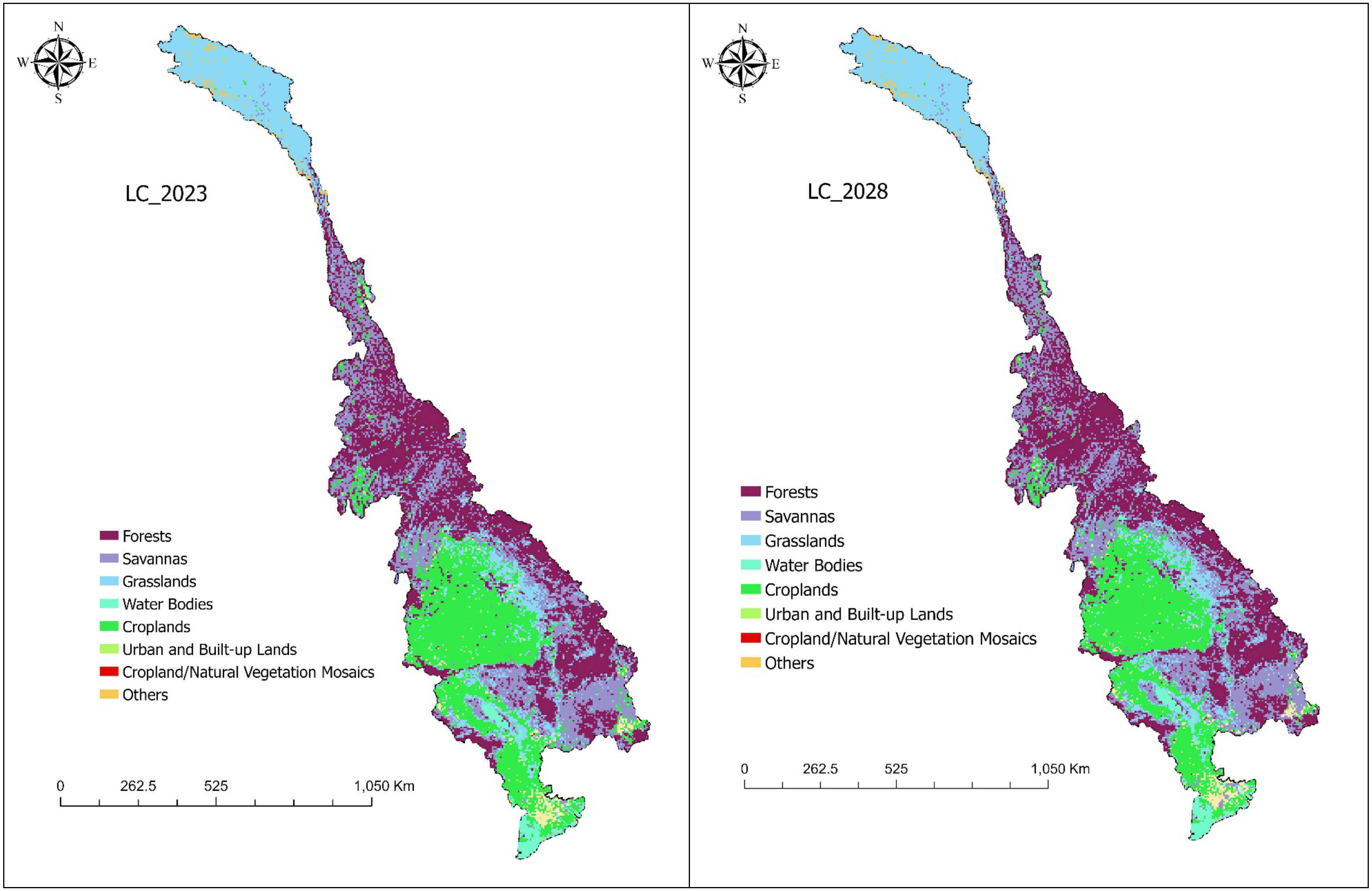

Figure 12. Predicted land cover for 2023 – 2028.

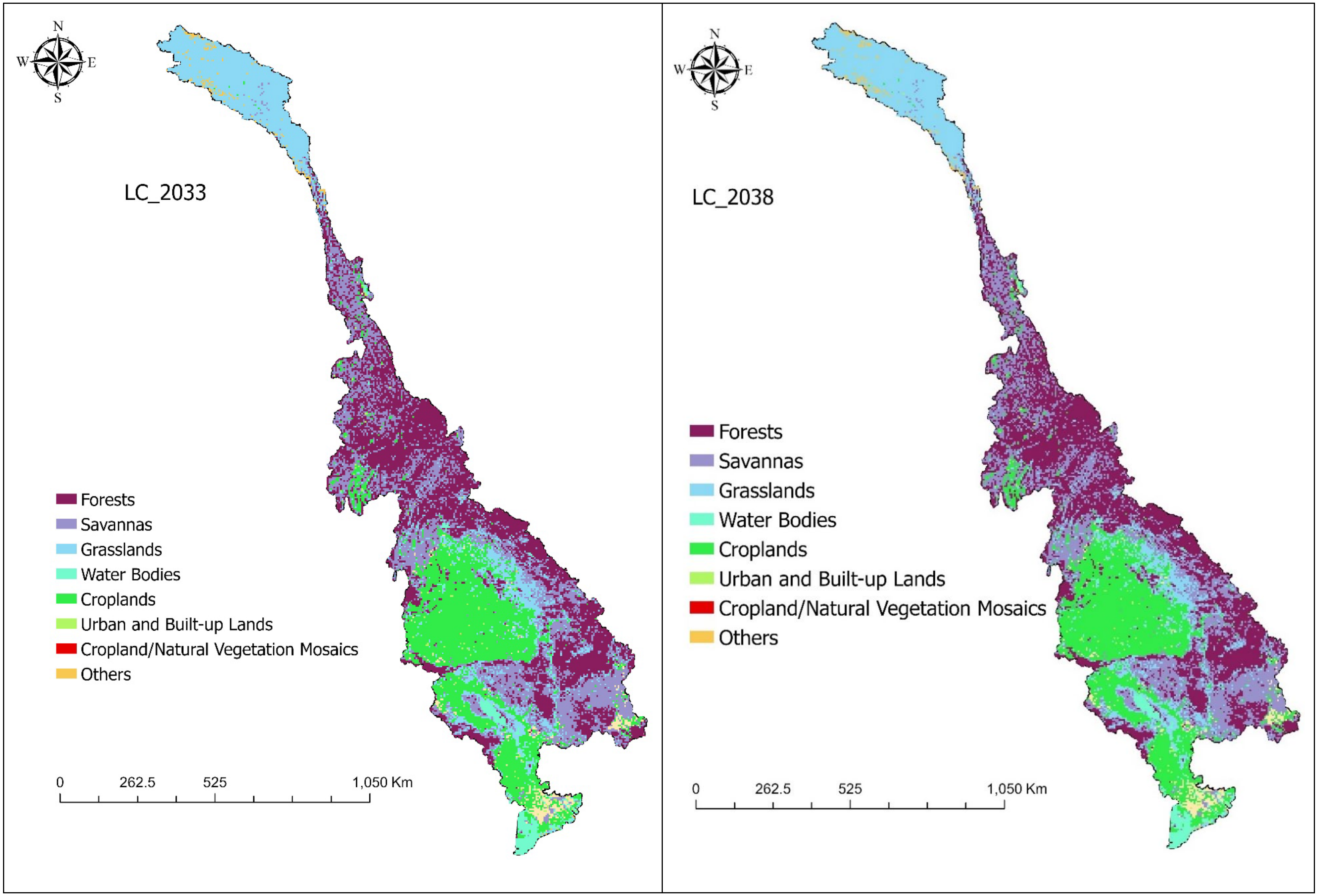

Figure 13. Predicted land cover for 2033 – 2038.

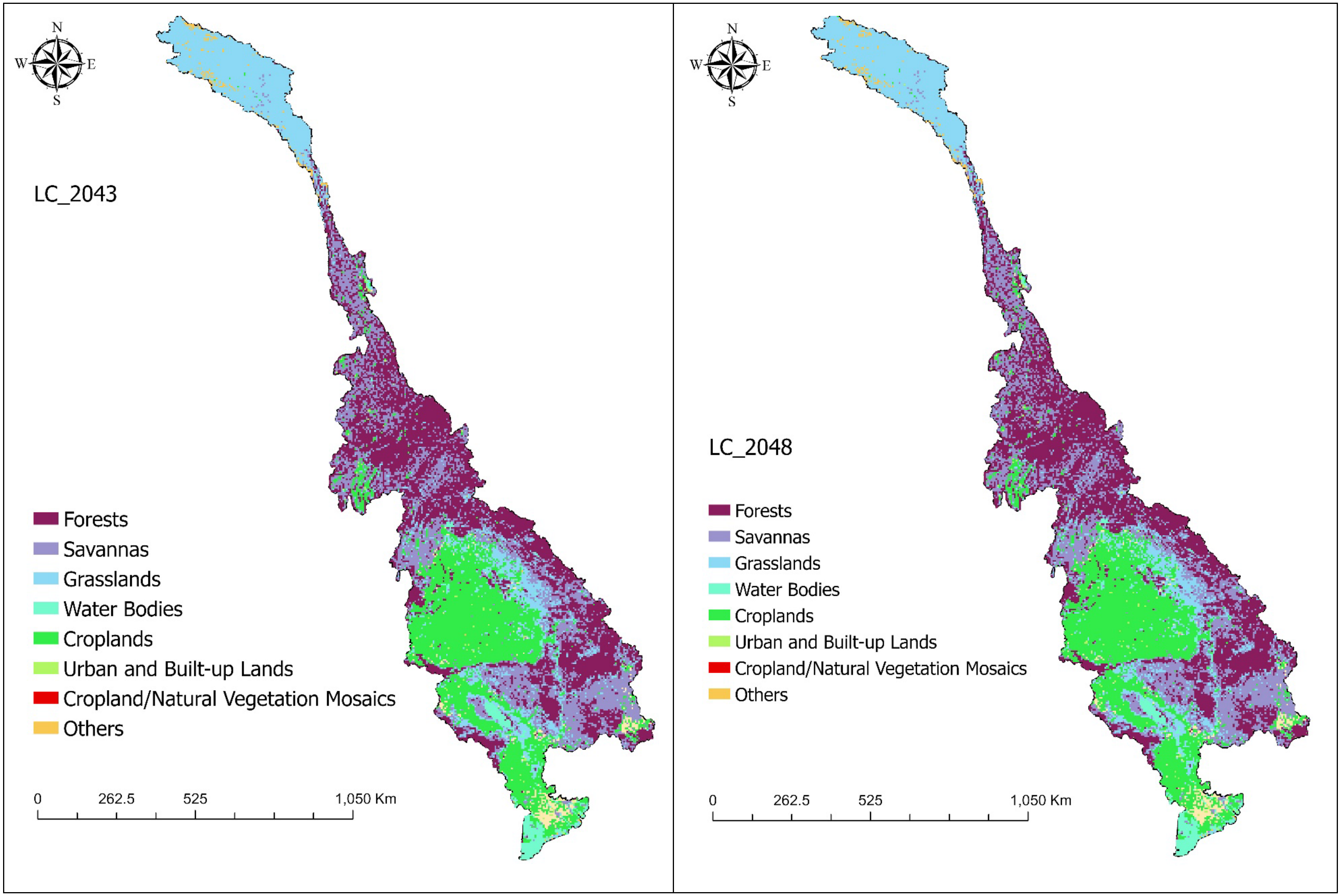

Figure 14. Predicted land cover for 2043 – 2048.

Figure 15 presents predicted changes in different land cover types for each five-year period from 2023 to 2048 in comparison to baseline (2018). The MLP model predicted a substantial increase in Cropland during this period, except for 2028. Savannas and Natural Vegetation were the two most prominent contributors to the change of Cropland. During this period, the regions are predicted to lose their Forest and Natural Vegetation areas due to conversion to Cropland. Wetlands/Water areas were projected to remain stable in the future. In addition, there was no predicted change in the Urban area.

The MLP model predicted a large increase in Cropland in year 2023, but a large decrease in Cropland in year 2028. This suggests that the MLP model was too aggressive in predicting the outcome for 2023. However, the MLP predictions improved in the succeeding predicted years.

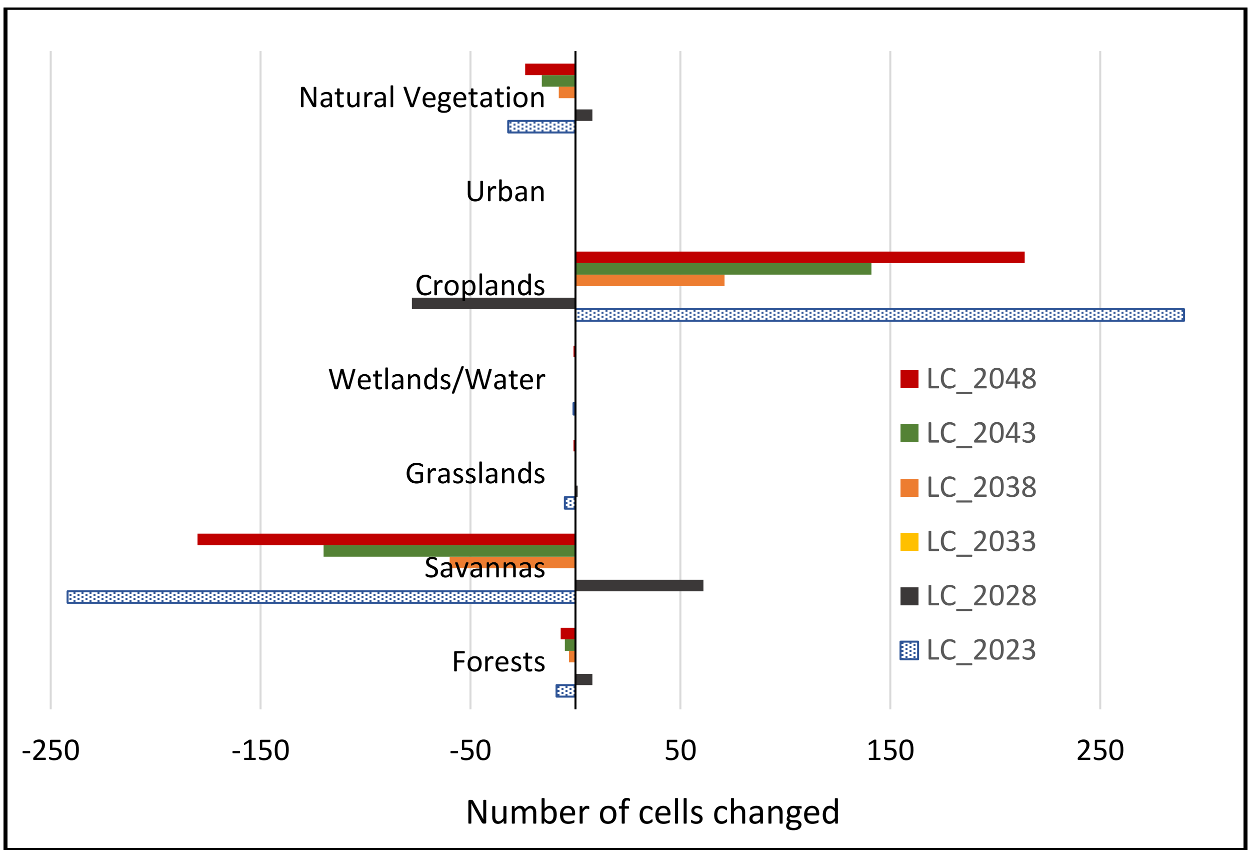

Figure 15. Predicted land cover trend from 2023 to 2048 in comparison to 2018.

3.3. Spatio-Temporal Variation of Soil Moisture

Soil moisture distribution in MKB during the period 2010-2018 is presented in Figure 16. The model predicted large variations in soil moisture at the LMB and stable soil moisture at the UMB. In 2015, soil moisture reduction occurred in the Vietnam and Cambodia regions of the MKB but increased slowly in 2017 and 2018.

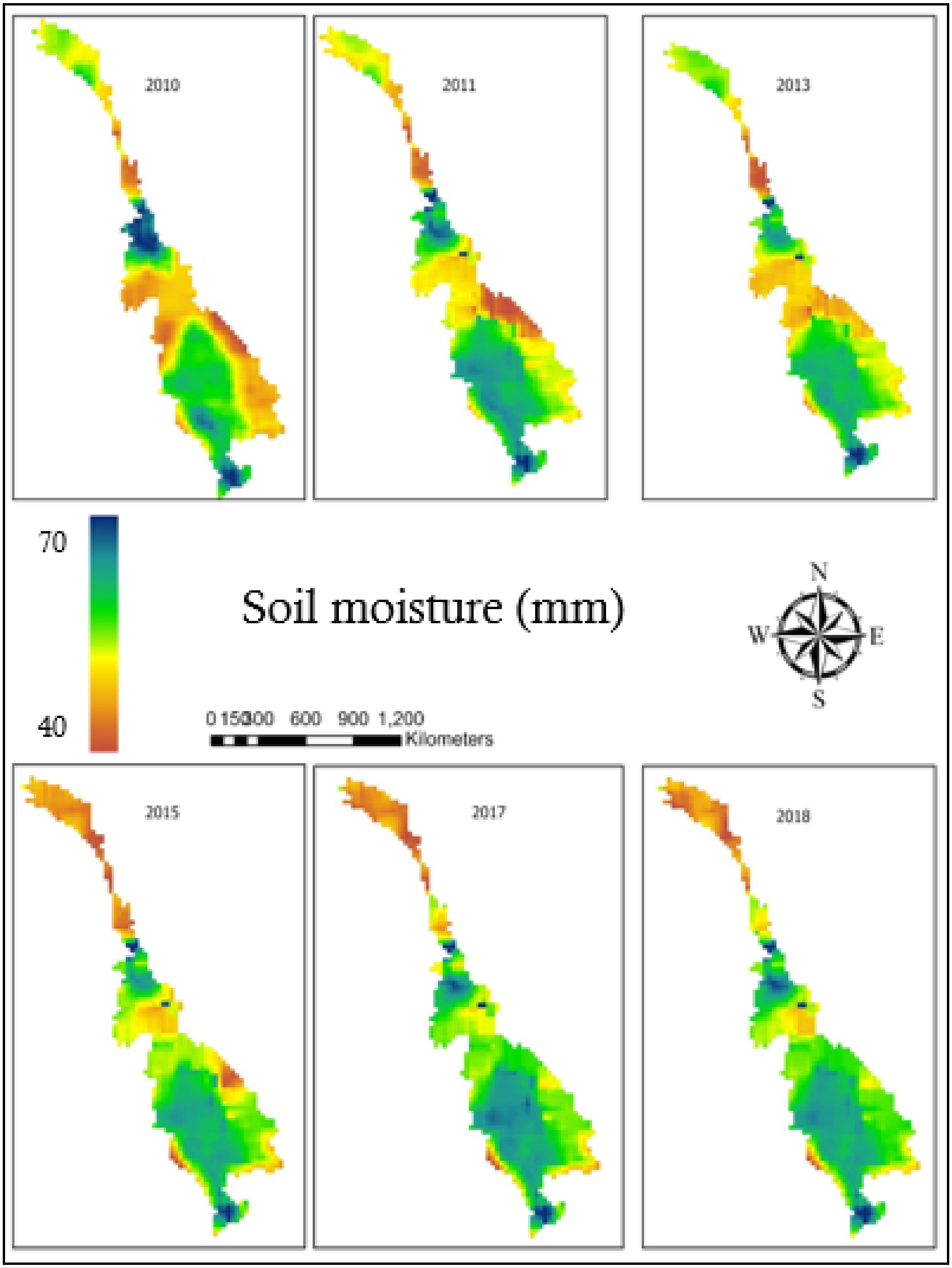

Figure 16. Soil moisture distribution at MKB during 2010-2018

3.4. Relationships among SMAPI, Land Cover, and Rainy Season

The seasonally averaged SMAPI maps for the MKB during the period 2010–2018 are displayed in Figure 17. The SMAPI maps captured the spatio-temporal variability of drought conditions in different regions of the MKB. In general, during the dry season and the transition season, there was severe drought throughout the MKB, especially in the LMB coastal areas. During the wet season, drought continued to occur in the UMB (China) and at several locations in the LMB. During the wet season, most areas in the southern region of MKB were classified as slightly wet.

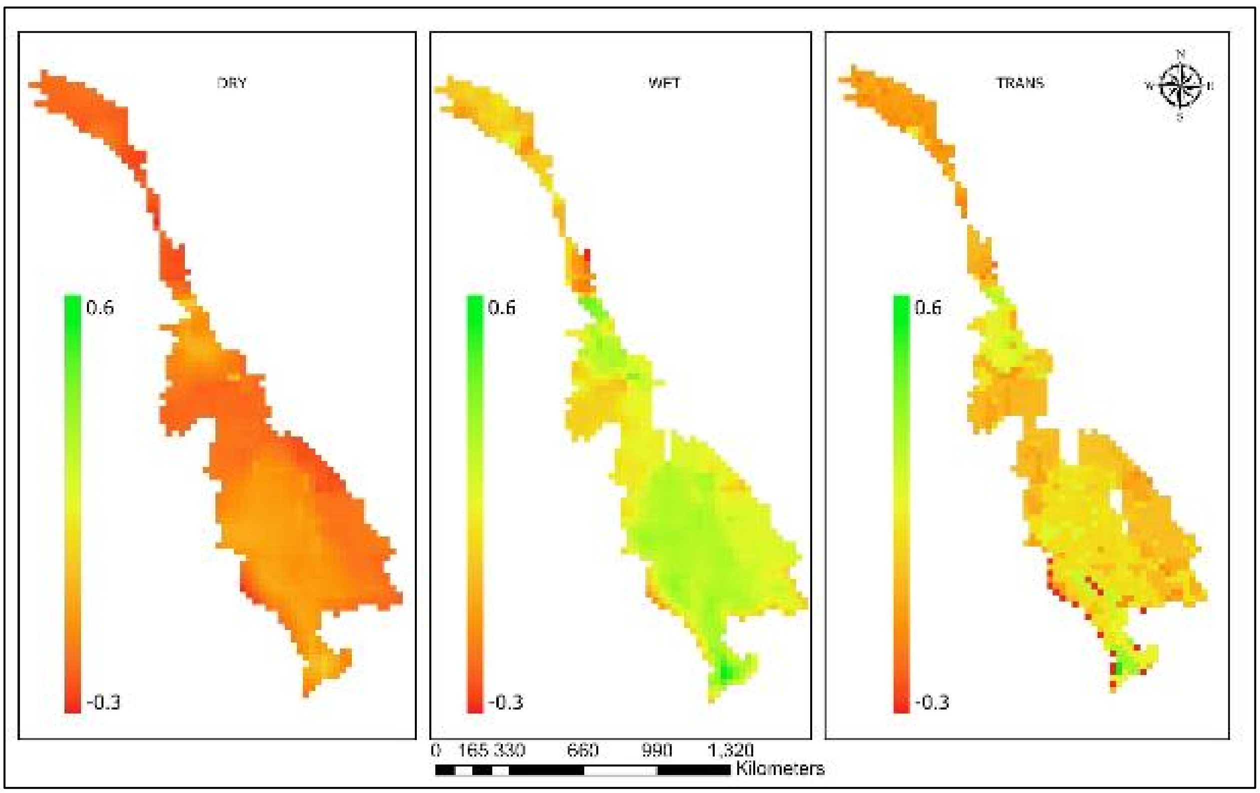

Figure 17. SMAPI maps for the dry (Dry-left) season, wet (Wet-center) season, and transitional (TRANS) months for the period of 2010–2018 win the MKB.

Drought versus wet conditions have important implications for agroforestry activities. The relationship between land cover type and drought/wet conditions are presented in Table 6. Land cover types were separated into two major categories. The first major category included Urban, and built-up land, water bodies, and herbaceous wetland. Even though some areas were affected by drought in 2015-2016, the VIC model was not able to capture these events. The second major category included cropland, grassland, forest, and savanna. For this category, the VIC model captured variations in drought versus wet conditions during the wet and dry season.

In the second category, there was little difference in projected drought conditions during the dry and wet seasons in the Forest areas, which suggests that forested areas are protected from drought. But for Cropland and Grassland, projected drought occurred at the beginning of the dry season almost immediately, while the reverse occurred almost immediately during the wet season. This different in projected drought would be due to the greater evatransporation in Cropland and Grassland than in Forest.

In the Savanna regions, there was little change in projected drought conditions between wet and dry season. However, in coastal areas of extreme drought (D4) Savannas in those areas were projected to suffer from drought during the wet season.

There was a substantial difference in projected drought conditions in Cropland areas during the dry and wet season. In areas of mild drought (D1), drought during dry season was projected to be 8.75 times higher than during the wet season.

Table 6. Drought/Wet conditions according to percentage of land cover types

Land Cover Type	**Area (%)**	**Dry season**								**Wet season**					
		D4	**D3**	**D2**	**D1**	**N**	**D4**	**D3**	**D2**	**D1**	**N**	**W1**	**W2**	**W3**	**W4**
Evergreen Needleleaf Forests	0.74	0.001	-	0.007	-	-	0.001	0.001	0.003	0.002	0.001	-	-	-	-
Evergreen Broadleaf Forests	25.4	0.011	-	0.201	0.045	0.002	0.008	-	0.014	0.062	0.136	0.027	0.002	-	-
Deciduous Broadleaf Forests	2.5	0.002	-	0.008	0.016	-	0.002	-	-	0.002	0.013	0.008	-	-	-
Mixed Forests	2.4	0.003	-	0.010	0.010	0.001	0.003	-	0.004	0.004	0.008	0.006	0.001	-	-
Woody Savannas	14.5	0.006	-	0.108	0.034	-	0.010	0.002	0.006	0.053	0.055	0.022	0.001	-	-
Savannas	11.8	0.004	-	0.065	0.050	0.002	0.004	-	0.007	0.025	0.046	0.034	0.006	-	-
Grasslands	17.3	0.002	-	0.129	0.046	-	0.003	-	0.028	0.076	0.041	0.028	-	-	-
Permanent Wetlands	0.3	-	-	0.004	0.008	-	-	-	0.001	0.001	0.003	0.008	-	-	-
Croplands	21.4	0.008	-	0.038	0.175	0.004	0.008	0.001	0.001	0.020	0.050	0.142	0.003	-	-
Urban and Built-up Lands	0.5	-	-	0.002	0.005	-	-	-	-	0.001	0.003	0.003	-	-	-
Cropland/Natural Vegetation Mosaics	0.3	-	-	0.002	0.006	0.007	-	-	-	0.002	-	0.006	0.005	0.002	-
Barren	0.4	-	-	0.004	-	-	-	-	0.002	0.002	-	-	-	-	-

4. Conclusion

This study investigated the historical spatial and temporal change to the MKB hydrologic system due to climate variability and land cover change and then predicted future changes using the VIC model. In this study, the VIC macroscale hydrological model was applied to simulate the daily soil moisture at a grid resolution of 0.25 × 0.25 degrees during the nine years of 2010–2018 for the MKB. The VIC simulation successfully captured the spatio-temporal variability of soil moisture in the MKB. The predicted land cover change had minimal impact on soil moisture. Although the MKB has a wet and dry season, this model predicted that some areas of the MKB would suffer drought year-round. This model predicted that forest and savanna areas would generally be protected from drought. However, soil moisture in cropland areas was predicted to fluctuate by season, creating drought during the dry season and increasing soil moisture during the rainy season.

The predicted drought conditions during the dry season in the cropland areas is of great concern for the agricultural production and socio-economic welfare of the inhabitants of the areas affected by drought. These findings imply that proper irrigation management in cropland areas should be considered during the dry season in the MKB. Also, the savanna areas may be potential sources of increased agroforestry because these areas are predicted to be protected from drought, except for coastal areas, as suggested by Luong et al. (2020). These findings support the critical need for water resource and forest protection management policies in response to droughts predicted to occur in the MKB.

Limitations

This study had several limitations. We used the VIC model that requires remote sensing data input. However, some data were not completely available for the MKB for the 2010-2018 period, which makes it difficult to predict future trends for the entire region. Also, different input data were extracted from different sources, which varied in resolution. Therefore, this study had to interpolate and resample several data points, leaving small areas of the MKB without results. This study used the Python package for the VIC model, which requires regular updating of the source code to compile the model without error.

CHAPTER 3. DEVELOPING AND VALIDATING AN ARTIFICIAL NEURAL NETWORKS TO PREDICT SOIL MOISTURE IN THE MEKONG DELTA, AND COMPARING HISTORICAL SOIL MOISTURE DATA WITH THE ARTIFICIAL NEURAL NETWORKS -PREDICTED MODEL DATA

Abstract

Soil moisture is a fundamental soil characteristic, which has played an essential role in plant growth, flood generation, land degradation, and drought responses. Climate change and anthropogenic activities impact soil moisture dynamics globally. Understanding the interactions among soil moisture, climate data, and land surface information in climate change conditions is essential to preserving vulnerable regions from drought risk caused by soil moisture decrease. This study aimed to identify the relationship between SMC and the drought risk at the Mekong River Basin (MKB) to climatic variables and human impacts by using artificial intelligence to create simplified hydrological models. A multi-layer perceptron Neural Networks (ANNs) architecture was applied to estimate daily soil moisture and predict agricultural drought risk using Soil Moisture Deficit Index (SMDI). An ANNs architecture was built with one input layer, one output layer, and two hidden layers on the JMP Pro platforms. Then, the ANNs architecture was applied to 1105 grid-cells to predict daily soil moisture at the top layer of soil from 2010-2018 in MKB. Our model used climate data, land surface data, and river discharge data to predict soil moisture. This study also used the observed daily soil moisture datasets extracted from the Copernicus Global platform regions to train and validate the ANNs models. We tested our models' performance against the observed soil moisture using the coefficient of determination (R^2), root mean square (RMSE) indicators. We also tested the impact of topography and land cover on our models' performance using pairwise correlation tests. We found that the best predictive model architecture included two hidden layers with nine nodes. The R^2 value for both training and validation of these models ranged from 0.44 to 0.99 for predicting soil moisture and drought. The RMSE for both training and validation achieved 0.08 for predicting soil moisture and drought. Both land cover and topography in the region had weak positive correlations with the R^2 and the RMSE in predicting soil moisture and drought. In conclusion, the developed ANNs models had strong ability to predict soil moisture and drought in the MKB.

1. Introduction

1.1 Spatial Soil Moisture Issues

The SMC is affected by precipitation in surface runoff, infiltration, and groundwater recharge, and has played an essential role in plant growth, flood generation, land degradation, and drought responses (Luong et al., 2021, Myeni et al., 2019). (Ahmad et al., 2009, Verstraeten et al., 2008). SMC has recently been affected by an increasing number of complex water resources management issues, which are often exacerbated by impacts of climate change (Berg & Sheffield, 2018). Because SMC is essential for agricultural planning, there is a need to monitor and predict SMC in order to support policymakers, farmers, and other stakeholders who rely on flood predictions, drought forecasts, and water quality information for their livelihoods (Adeyemi et al., 2018, Verstraeten et al., 2008).

SMC is most accurately determined by a direct application of field measurement techniques (Millán et al., 2020). However, due to some constraints related to limited financial, technical, and human resources, in situ measurements are often only carried out at specific times and locations. Thus, the measured data is not enough for large-scale SMC measurement (Luong et al., 2021). Over the past few decades, there have been efforts to develop spatial soil moisture measurement products from active and passive microwave sensors, via remote sensing technologies. For instance, the ECMWF C3S has provided global surface soil moisture datasets to the community since 1991. These datasets include the Active, the Passive, and the Combine. The Active and Passive are derived from the scatter meter and radiometer product respectively, while the Combine is a blended product of the two (Kidd, 2018a, 2018b). Another popular database, Global Land Data Assimilation System (GLDAS), has provided daily surface soil moisture in different layers since 1948 at 0.25-degree resolution, and supports current water resources and water cycle investigations (Kidd, 2018b). However, since many factors, such as land cover, precipitation, and vegetation impact the sensitivity of the signal, SMC cannot be entirely observed in many areas of the world (Dorigo et al., 2010, Llamas et al., 2020).

1.2 Artificial Neural Networks to Predict Soil Moisture Content

The ANNs have been found to accurately predict SMC and other soil water variables such as field capacity and permanent wilting point (Ali et al., 2010, Keshavarz & Karami, 2013). An advantage of using the ANNs technique compared to regression models is that no priority model structure requires assumed relationships between input and output data (Merdun et al., 2006, Mohanty, 2015).

The ANNs are machine learning models that define potential relationships from a training data set, with a learning algorithm similar to that of human-learning ability (Ahmad et al., 2009). Since there can be robust to noisy data and approximate multivariate non-linear relationships between variables, neural networks have been used to conduct analyses in a variety of scientific scenarios (Ahmad et al., 2009, Twarakavi et al., 2006, Widrow et al., 1994). The ANNs have been used to study hydrological features such as streamflow modeling, soil moisture, and drought predictions (Adeyemi et al., 2018, Capraro et al., 2008, Tsang & Jim, 2016). This method has been recognized as appropriate for complex time-series predictions as an alternative method to traditional numerical predicting models, which may be limited in time-series projections due to the complexity of the systems. The term "complexity" also illustrates potential difficulties that rapid climate change in recent decades has added to predicting extreme climate events (Agana & Homaifar, 2017, Zhang et al., 1998).

The novelty of this study lies in employing ANNs, which not only derives soil moisture information at the regional scale but also fills missing data from geospatial databases for the MKB. This study employed a neural network model to explore the spatio-temporal dynamics and characteristics of SMC in the MKB to address these knowledge gaps. The soil moisture dataset was simulated for nine years (2010–2018) and then utilized to establish the SMDI, as was established by Martinez-Fernandez et al. (2015) in order to assess the intensity of agricultural drought**.** Furthermore, this study investigated the impacts of meteorological variables (precipitation and temperature) and land cover properties, topography, and soil types on the spatial and temporal variation of soil moisture and drought in different regions in the MKB. Our study is the comprehensive estimation of soil moisture and agricultural drought over the MKB using the deep learning ANNs model. The key objectives of this study were to (1) develop a ANNs model to investigate the sensitivity of soil moisture to meteorological conditions, land cover properties, and topography in different regions in the MKB; and (2) analyze the intensity of agricultural drought concerning land uses in the MKB.

2. Methodology

2.1 Study Area

The Mekong River originates in China at the Tibetan Plateau and flows downstream through Myanmar, Laos, Thailand, and Cambodia before draining into the East Sea in Vietnam. The Mekong River is over 4,000 kilometers long, with an annual mean discharge of approximately 475 km^3 (MRC, 2005). The hydrologic characteristics of the Mekong River are complicated due to extensive watershed areas covering various geographic features. The MKB supports approximately 70 million people, a population projected to increase to 90 million in 2050 (Markert et al., 2018, UN, 2020). The Basin supports a substantial human population, over 900 freshwater species, and many more land vertebrates, making it the second most biodiverse river ecosystem on Earth (Campbell, 2016, Ziv et al., 2012) The MRB is divided into two parts: the Upper MKB and the Lower MKB (Thompson et al., 2014, Tanaka, 2003, MRC, 2010). In the LMB, over three-quarters of the population depends directly or indirectly on agriculture (Kityuttachai et al., 2016) and other economic activities, including tourism, agriculture, forestry, fishing, manufacturing, and energy production (Costenbader et al., 2015a). Vietnam and Thailand, both of which are partially situated in the MKB, are the primary and secondary exporters of paddy production in the world United States Department of Agriculture, 2021, with total exports valued at an estimated US$ 703.68 million from 2000 to 2004 (Thanh and Singh, 2006).

2.2. Artificial Neural Networks Model in the JMP Pro Platform

Theoretically, an ANNs model learns the structure of a sample dataset to understand it. In this study, we used a MLP algorithm for the ANNs because MLP is the most common ANNs classifier applied for time series forecasting (Kaynar et al., 2010). The MLP requires at least three layers of neuron nodes, including an input layer, a hidden layer, and an output layer. Each node in the hidden layer has an activation function that weighted and accumulated the values of the inputs to the output nodes. The weighted sum is then transferred from node to node by transfer functions (Kaynar et al., 2010, Zhang et al., 1998). Eq. 8 presents a non-linear relationship between input and output in a multi-layer perceptron with a hidden layer:

$$y = f_2.\left[\sum_{j=0}^{h}\left[w_j f_1\left(\sum_{j=0}^{n} w_{ji}.x_i\right)\right]\right] \qquad \text{Eq. 8}$$

where f_1 and f_2 = transfer functions for the hidden layer and the output layer, respectively. x_i = the past data set as an input layer, and y = the output layer. The weights w_j and w_{ji} = the weight and biases which connect the neurons between input and hidden layers and between the invisible and the output layers, respectively (Agana & Homaifar, 2017).

This study used a multi-layer perceptron network in the JMP Pro platform to apply the ANNs in such a way that they benefited from using built-in statistical tools to analyze the model results. The network's structure consisted of an input layer where input data was fed into the network, two hidden layers, and an output layer. We offered two hidden layers to avoid potential errors from correlated input variables, as suggested in earlier studies (Patterson & Gibson, 2017). There are three transfer functions built-in the JMP platform, including Linear (2), TanH (3), and Gaussian (4) (Klimberg & McCullogh, 2018)

$$f(x) = (0, x) \qquad \text{Eq. 9}$$

$$f(x) = \frac{e^x - e^{-x}}{e^x + e^{-x}} \qquad \text{Eq. 10}$$

$$f(x) = e^{-x^2} \qquad \text{Eq. 11}$$

For input data, we acquired 13 datasets, including one dependent and twelve independent variables. Based on the number of datasets, the number of nodes was calculated using the equation suggested by Kurt (2020):

$$N = Round(\frac{2}{3} \times N_i + N_o) \qquad \text{Eq. 12}$$

where N = the number of hidden nodes, N_i = the number of input variables, and N_o = the output variable. Then, N is rounded up to the nearest integer.

There were two main processes involved in the ANNs model, namely forward and backward processes. During the forward process, the training data point was propagated through the hidden layers. The output value obtained was compared with the actual target values to calculate the error between nodes (Azid et al., 2014). In the backward procedure, the calculated error was propagated back towards the hidden layers. The output weightings of the node were adjusted to reduce the errors, with each interaction resulting in improved models (Azid et al., 2014). These processes guided the directions of data analyses.

Although it is an essential step in using ANNs, there is no specific method to define the structure of nodes and functions to form the model, save for the trial and error method (Zhang & Govindaraju, 2000, Zhang et al., 1998). We selected two sub-datasets and tested all possible combinations of three activation functions and the number of nodes in two layers to determine the ANNs structure. We used R^2 and RMSE indicators to test the trial results.

The ANNs model can be very flexible, and is likely to overfit the data (JMP**,** 2019). Therefore, a penalty was applied on model parameters along with the use of an independent data set to assess the model's predictive power to avoid these issues. Validation was performed using a portion of input datasets to estimate model variables and evaluate the model's predictive ability. We deployed K-fold cross validations to test the model’s performance (JMP, 2019, Klimberg & McCullogh, 2018). JMP divided the original dataset into seven groups or folds containing approximately the same number of observations as a K-fold technic. The model used six folds to form the training subset and used the seventh fold as a validation data set (Klimberg & McCullogh, 2018).

A script using JMP scripting language (JSL) was created to run multiple ANNs models automatically (JMP, 2019). The script conducted three main tasks: creating a subset of datasets based on the cell’s identification, running the ANNs model in each subset, and recording predicted values, R^2, RMSE, and hidden nodes formulas.

Table 7. Input Dataset used in ANNs

Dataset	Unit	Spatial resolution	Temporal resolution	Database source	Accessed at
Landcover (LC)	unitless	300m x 300m	yearly	C3S	https://cds.climate.copernicus.eu/cdsapp#!/home
LAI (hv, lv)	m^2 m^{-2}	0.1 x 0.1 degree	monthly	C3S	https://cds.climate.copernicus.eu/cdsapp#!/home
Forecast Albedo	unitless	0.1 x 0.1 degree	monthly	C3S	https://cds.climate.copernicus.eu/cdsapp#!/home
Evapotranspiration	m water equivalent	0.25 x 0.25 degree	daily	GLDAS CLSM L4 V2.0	GES DISC
Windspeed (at 10m height)	m/s	0.25 x 0.25 degree	daily	GLDAS CLSM L4 V2.1	GES DISC
Tmax, Tmin	K	0.5 x 0.625 degree	daily	MERRA2	GES DISC
Total precipitation	mm	0.25 x 0.25 degree	daily	TRMM	GES DISC
Soil moisture	%	0.25 x 0.25 degree	daily	LPRM Surface Soil Moisture Data	GES DISC
USDA Soil class	unitless	1km x 1km	-	HWSD	FAO
DEM	m	90 m x 90 m	-	STRM	CGIAR

2.3 Data Collection

To develop our ANNs for the MKB soil moisture prediction, we derived datasets, including daily air temperature maximum and minimum (Tmax, Tmin), daily precipitation (Precip) including solid and liquid stages, daily leaf area indices for low (LAI_lv) and high (LAI_hv) vegetation types, daily wind speed, daily evapotranspiration (Evapotrans), annual land cover (LC), soil classification (SC), daily forecasted albedo (ALB), daily discharges (RD), and daily observed SMC. Amongst the 13 inputs, two datasets, LC and SC, were nominal; the rest were continuous. The datasets covered nine years from 2010 to 2018.

The LC, LAI, and ALB were extracted from the Copernicus Climate Change Services (C3S). The Evapotrans and windspeed were derived from Global Land Data Assimilation System (GLDAS) Catchment Land Surface Model L4 V2.0 at 0.25 x 0.25-degree at Goddard Earth Sciences Data and Information Services Center (GES DISC) (Chen et al., 2013, Rui et al., 2019). Daily climate data, including daily total precipitation Precip (mm), Tmin (K), and Tmax (K), were extracted from the daily MERRA-2 product at 0.5 x 0.625-degree resolution at GES DISC (Ostrenga, 2017). Annual LC and monthly LAI were converted into daily values.

Soil characteristics were extracted from the Harmonized World Soil Database of Food and Agriculture Organization (HWSD) V1.2 database (Batjes et al., 2012). This product combines multisource soil information worldwide at a 30 arc-second spatial scale with over 16,000 different soil mapping elements. The digital elevation model (DEM) from NASA's shuttle radar topographic mission 90 m digital elevation database version 1.4 with raster format was collected to obtain topographical data (Farr & Kobrick, 2000). Table 7 presents input datasets characteristics, including sources, temporal and spatial resolutions, and units.

We tested multicollinearity diagnostics to avoid the presence of multicollinearity in the ANNs model inputs. There was no collinearity among selected input variables (Figure 18). Hence, the ANNs models would reduce unstable and high standard errors due to inputs.

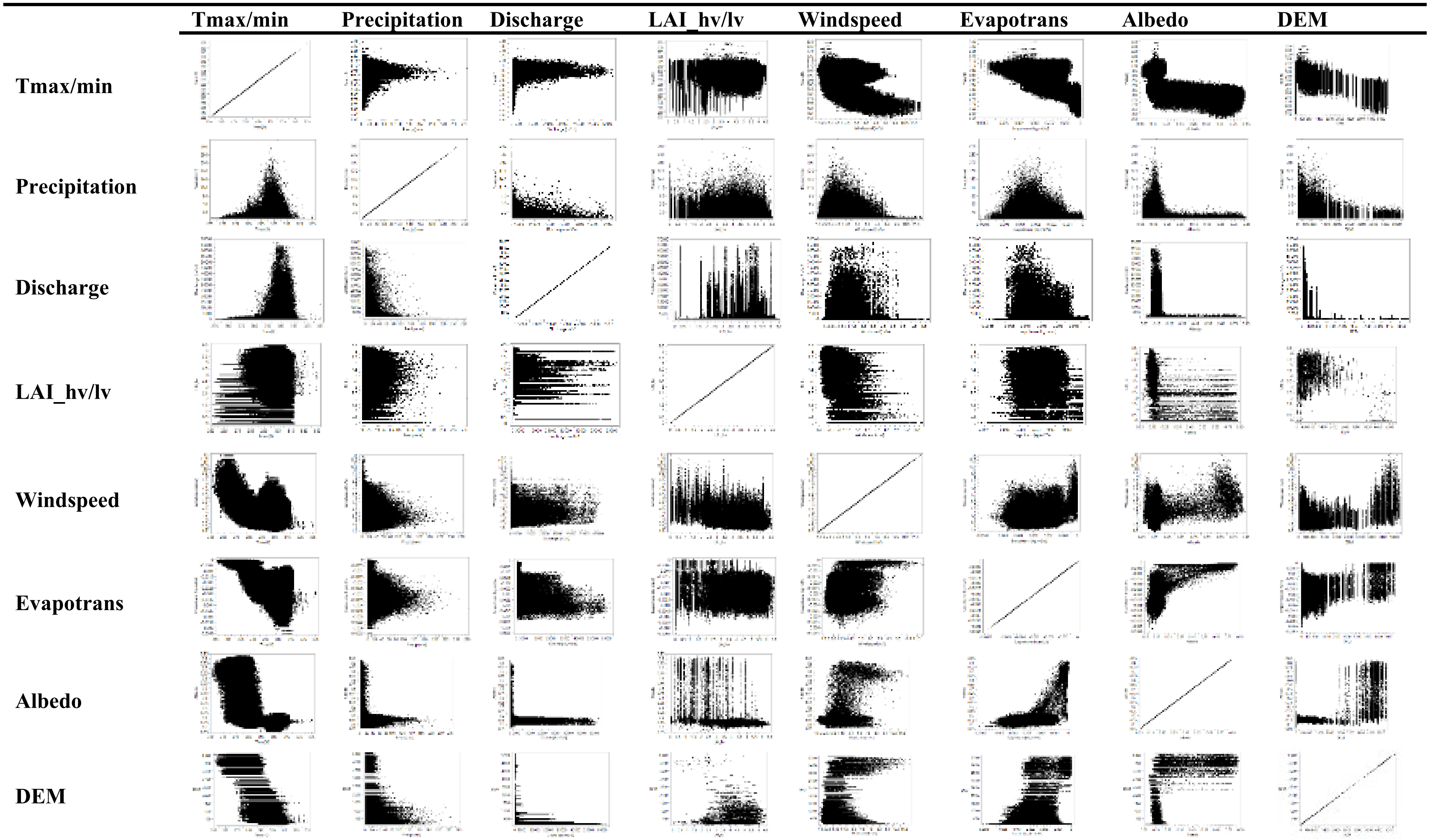

Figure 18. Collinearities among input variables for (LAI _hv/lv = Leaf area index for high vegetation /low vegetation, DEM = Digital elevation model, Tmax/min = Temperature (K) max/min)

2.4 Data Preparation

Since datasets differ in their resolution, format, and spatial reference, it is necessary to convert them into a unique data frame. First, all datasets were projected to the geographic coordinate system, GCS-WGS-1984 (World Geodetic System 1984), Prime Median – Greenwich. Then, the datasets were converted into GeoTIFF format using ArcGIS geospatial tools. To extract the value of each dataset to the grid-cells, first, we created a fishnet shapefile that contained multiple cells based on the Mekong basin boundary using the fishnet tool in ArcGIS to grid the MKB area into 0.25 x 0.25-degree grid-cells. There were 1105 cells in total, with cell size set at 0.25x0.25-degree. Each cell had a unique longitude and latitude. We used the ArcGIS sample tool to extract the values of datasets into the fishnet attribute (ArcGIS, 2021). Since the data contained different grids, they required refitting to adhere to a typical grid resolution. This study used classic bilinear and nearest neighborhood interpolation methods to re-grid the datasets. For the monthly LAI dataset, we assumed that LAI values did not change during months.

We assumed that each cell to be homogeneous and simulated independently of the other. Hence, there was no communication between grid-cells (Lohmann et al., 1996, Lohmann et al., 1998, Markert, 2018). This assumes that the water can only move between soil layers vertically in each grid-cell. This assumption was similar to one applied in semi-distributed hydrologic models, such as the VIC model (Markert et al., 2018, Luong et al., 2021). After this step, all input datasets were stored into cells according to their unique coordinates. Each cell contained 42,731 data points (3,287 days x 13 datasets). Finally, we exported the fishnet attribute tables to a CSV file. The final CSV file contained columns storing the cell identifications (CELL_ID), longitude (X), latitude (Y), twelve input variable columns, and an observed soil moisture column. The final CSV file was input to the ANNs model on the JMP14.2 Pro platform (JMP, 2019).

2.5 Model Performance Criteria

The performance of the ANNs models is assessed based on statistical performance criteria like R^2 and RMSE).

$$R^2 = 1 - \frac{\sum_i \left(y_{obs} - y_{pred}\right)^2}{\sum_i (y_{obs} - \bar{y})^2} \qquad \text{Eq. 13}$$

$$RMSE = \sqrt{\frac{\sum_i^N \left(y_{obs} - y_{pred}\right)^2}{N}} \qquad \text{Eq. 14}$$

where, y_{obs} and y_{pred} = the observed and predicted values, respectively, $\bar{y}$ = the mean of observed values, and N = the total of predictions (Agana & Homaifar, 2017, Adeyemi et al., 2018, Klimberg & McCullogh, 2018).

3. Results and Discussion

3.1 Data Quality

There was a total of 13 variables x 3287 days for the period from 2010 to 2018. The total missing data in the datasets was minimal (~3%) compared to the overall data. Figure 19 demonstrates statistical summaries of meteorology data inputs, including Tmax (K), Tmin (K), Precip (mm), Albedo, and Windspeed (m/s). While others were relatively uniform, Precip and Albedo datasets showed significant variations in the MKB. The daily precip ranged from 0 to 283.29 mm, while daily ALB ranged from 0.06 to 0.83.

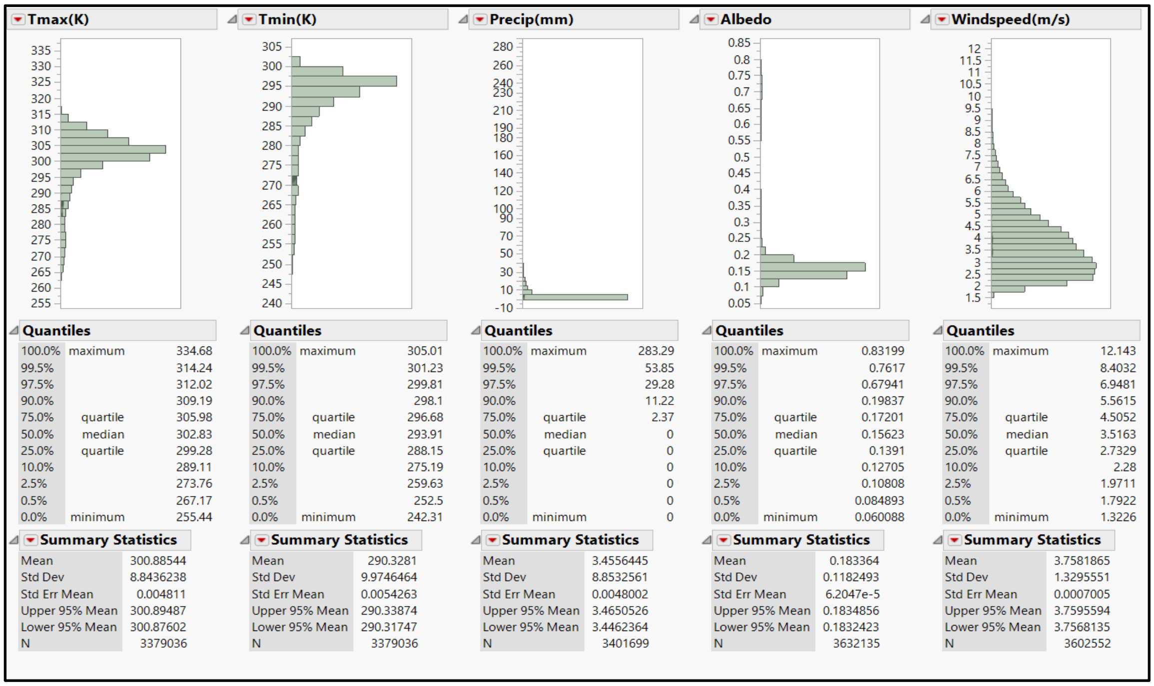

Figure 19. Meteorological Dataset Input Statistic Summary

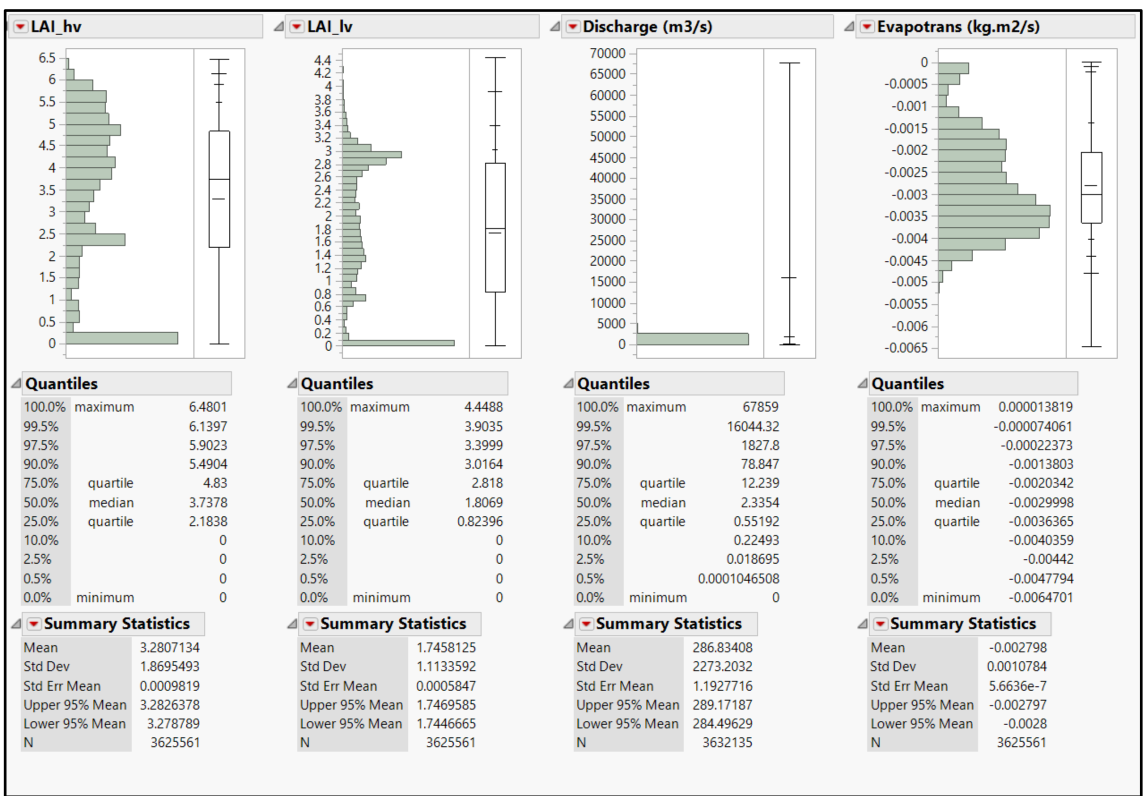

Figure 20. Surface and Vegetation Input Statistics Summary

Figure 20 shows statistic summaries of vegetation and surface datasets, which were input in the ANNs model. The LAI_hv and LAI_lv were daily high-level and low-level leaf area indices, respectively. While LAI_hv ranged from 0 to around 6.5 with a mean of 3.28, the LAI_lv was from 0 to about 4.4 with a mean of 1.75. Like precip, the range of river discharge (RD) (m^3/s) was large but captured the characteristics of the Mekong River and its tributary features. There are millions of river tributaries with various discharges dominating the MKB.

3.2 Neural Network Structure Selection

Figure 21 presents the result of the trial-and-error test on a sub-dataset, which was used to select the ANNs structure. The highest R^2 of the trail models was 0.73, while the lowest RMSE was 0.46. Hence, we selected an ANNs structure that included six nodes using three TanH and three Gaussian active functions in the first hidden layer and three nodes using a TanH, a Linear, and a Gaussian function in the second hidden layer. Figure 22 presents the ANNs structure that was used to predict the soil moisture in the MKB.

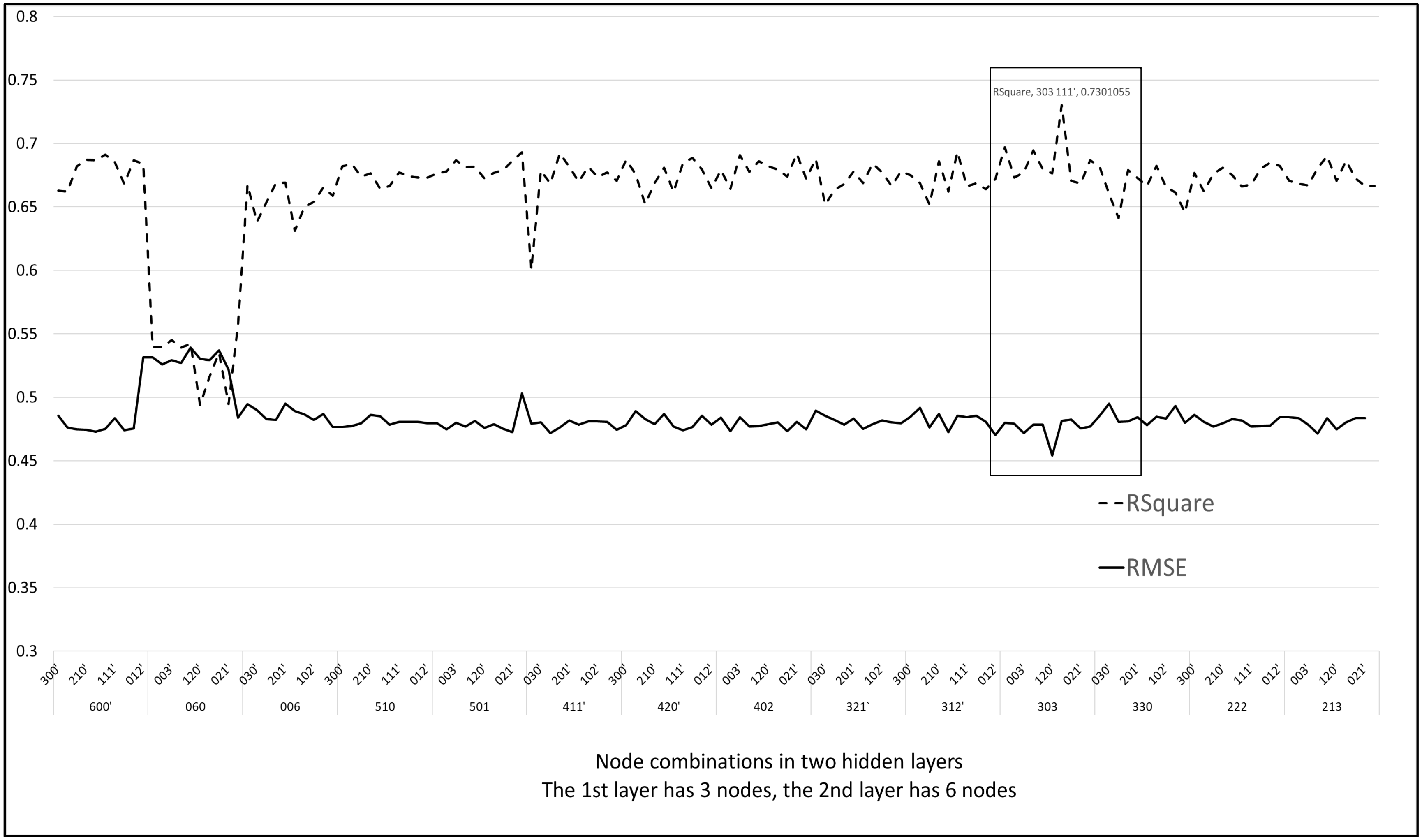

Figure 21. R-square and RMSE of Models with Different Activate Functions Combination

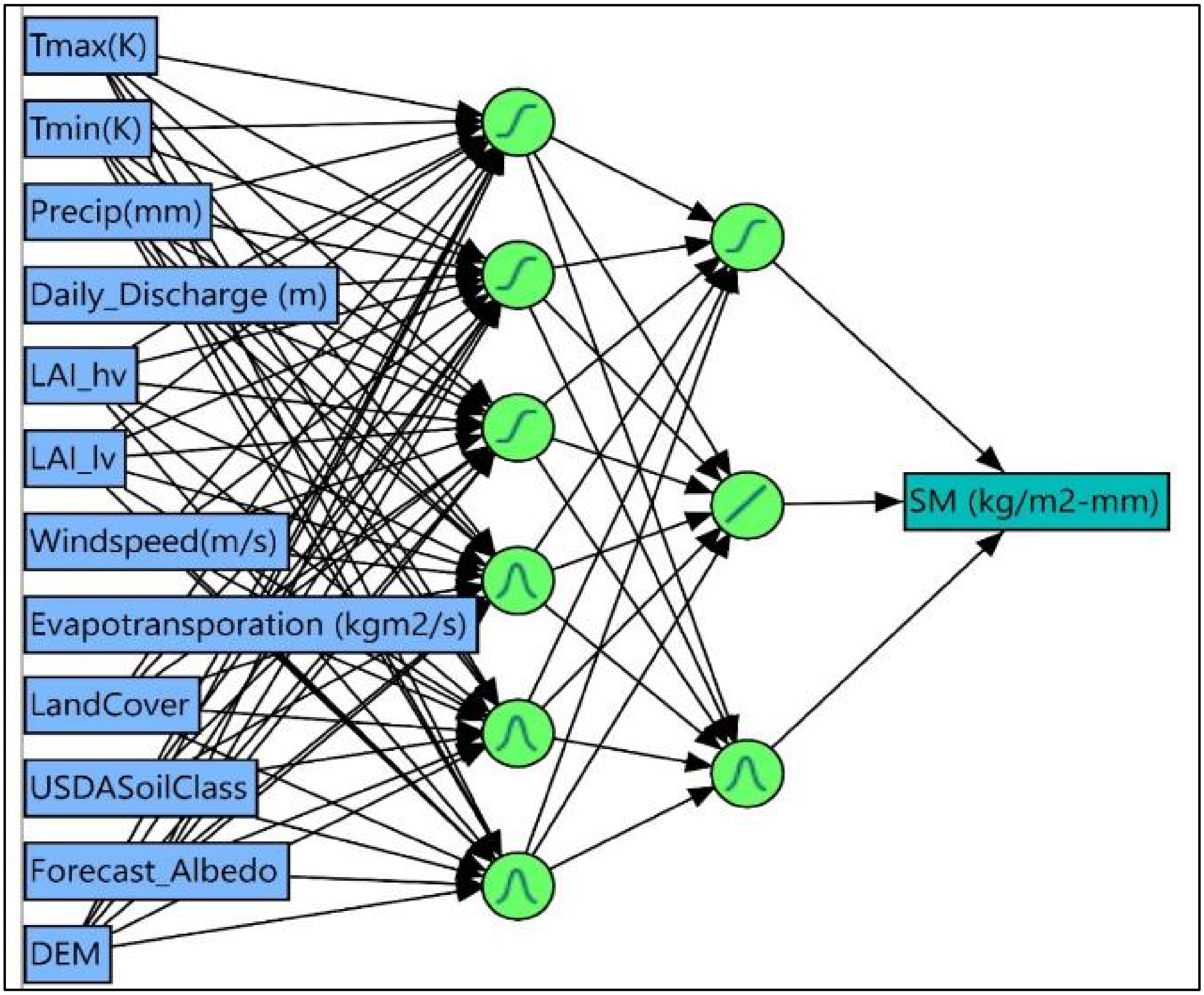

Figure 22. Diagram of Neural Network Structure with an Input Layer, Two Hidden Layers, and an Output Layer

3.3 Model Performance

We used each grid-cell as a dataset of all input variables to train the model framework. Hence, there were a total of 1105 models being tested. All the prediction results presented are based on the test data sets. We used R^2 and RMSE in training and validation processes to examine the model's performance, as suggested by Klimberg et al. (2018). In general, the models performed relatively well for SMC prediction since the R^2 values were relatively high (mean = 0.89), and the RMSE values were relatively small (mean = 6.3) (Table 8).

Table 8 described statistical summaries of R^2 and RMSE of models at 1105 cells. High R^2 and low RMSE results confirmed that ANN models could predict SMC well based on input variables. However, the models showed deficient performances at some grid-cells. These unexpected results may be errors related to missing data in datasets and/or impacts of elevation and land cover at those cells.

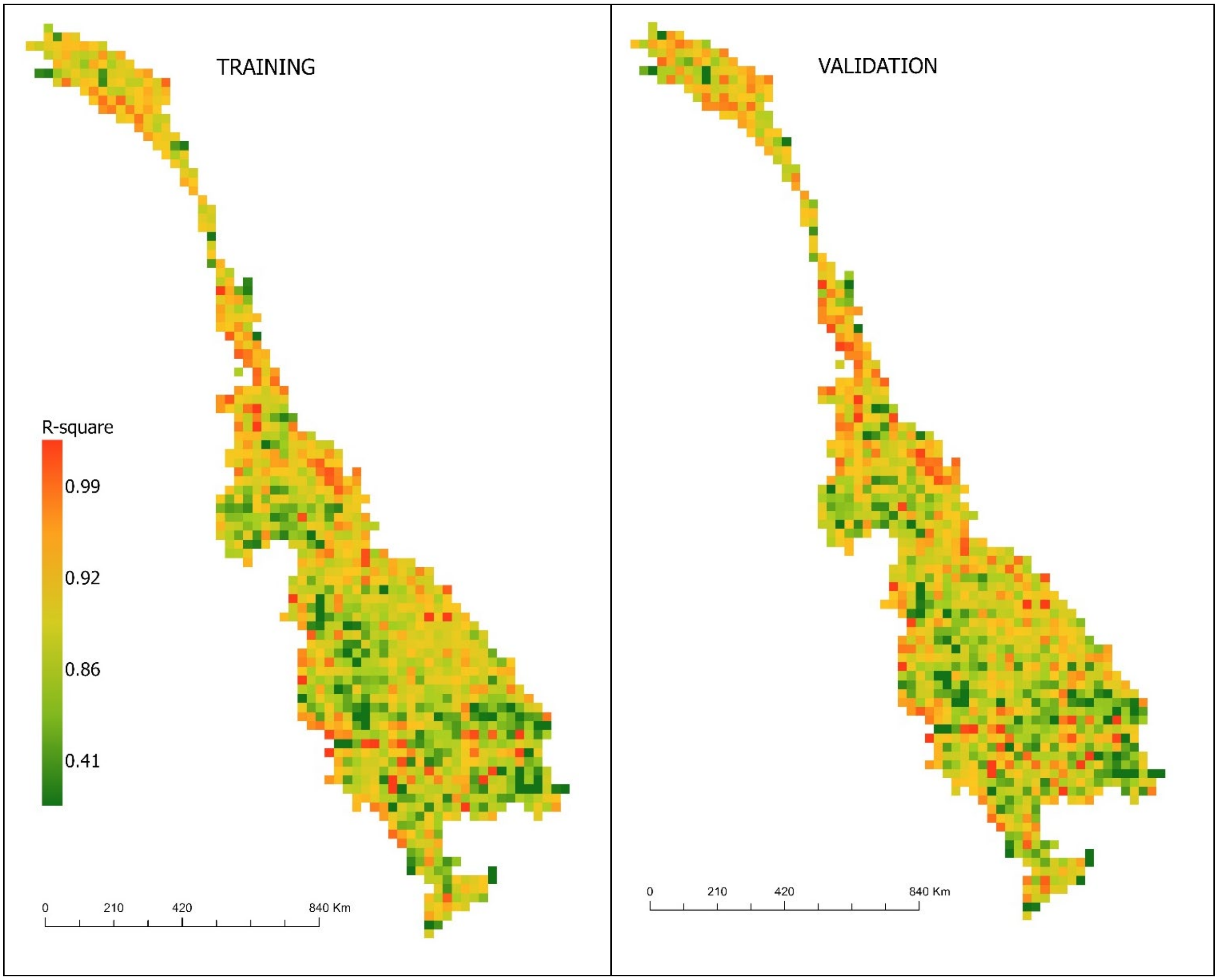

Figure 23. Training and Validation R-square of 1105 models

Figure 23 presents training and validation R^2 of soil moisture prediction using the ANNs models. The R^2 ranged from 0.44 to 0.99 and were distributed without any pattern. Figure 24 presents training and validation RMSE of soil moisture prediction, using the ANNs models. The RMSE of soil moisture prediction was 0.08, also distributed without any pattern.

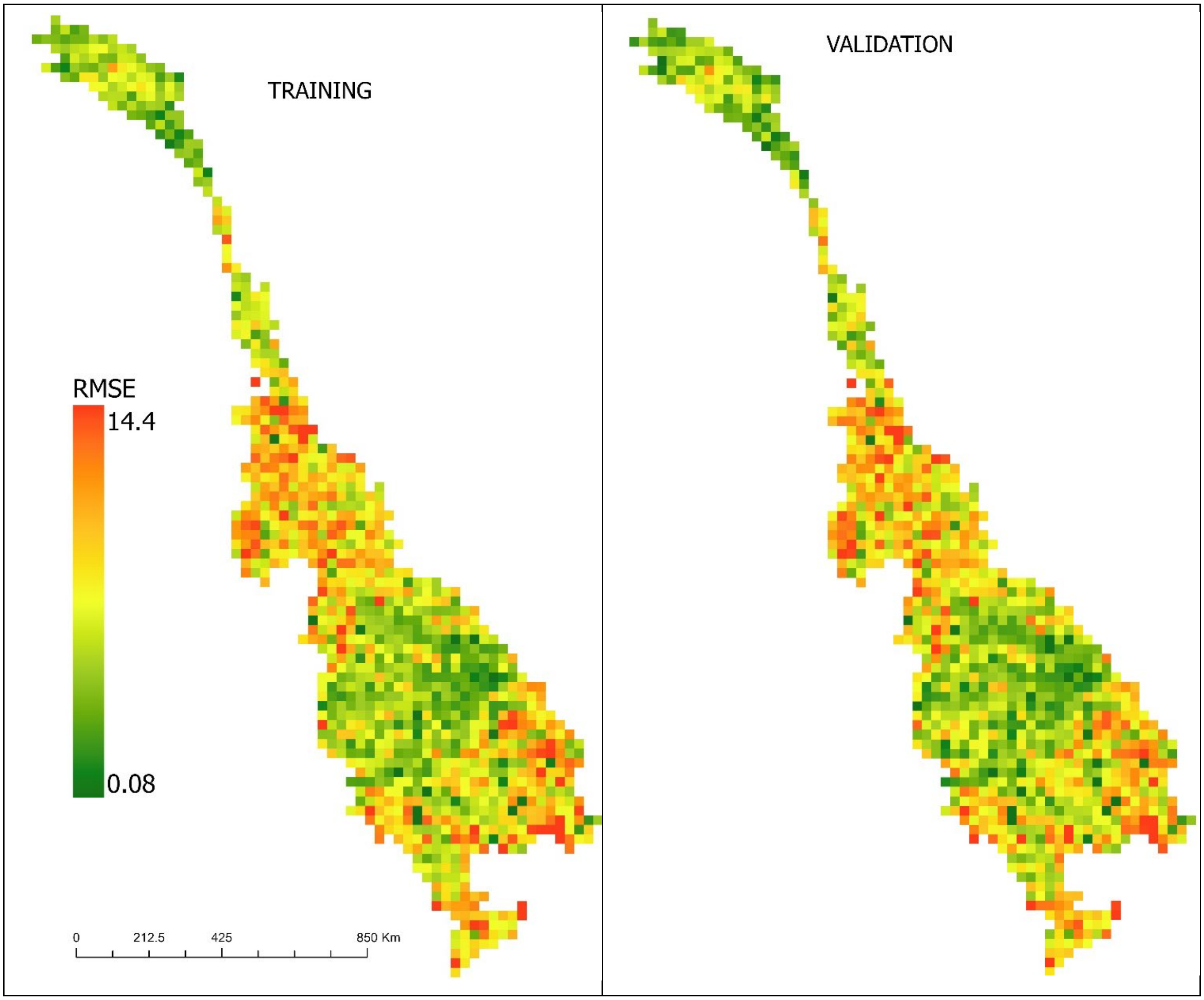

Figure 24. Training and Validation RMSE of 1105 models

Table 8. Distribution of R-square and RMSE for Both Training and Validating Processes

	R-square		**RMSE**	
	Training	**Validation**	**Training**	**Validation**
Max	0.99	0.99	14.36	13.13
Min	0.41	0.49	0.08	0.08
Mean	0.89	0.89	6.3	6.2
Std Dev	0.043	0.045	1.63	1.68
Std Err Mean	0.001	0.001	0.05	0.05
Upper 95% Mean	0.897	0.89	6.39	6.32
Lower 95% Mean	0.885	0.887	6.2	6.12
DF	1104	1104	1104	1104

We also tested the impacts of DEM and LC on model performance using a pairwise correlation test. In general, both LC and DEM showed positive correlations with both R^2 training and RMSE training. However, as the test results indicate, DEM and LC do not substantially impact the R^2 and RMSE of the models. Figure 25 shows the pairwise correlation test between DEM and model R-square. R-square and DEM have a weak correlation since the correlation value was 0.19.

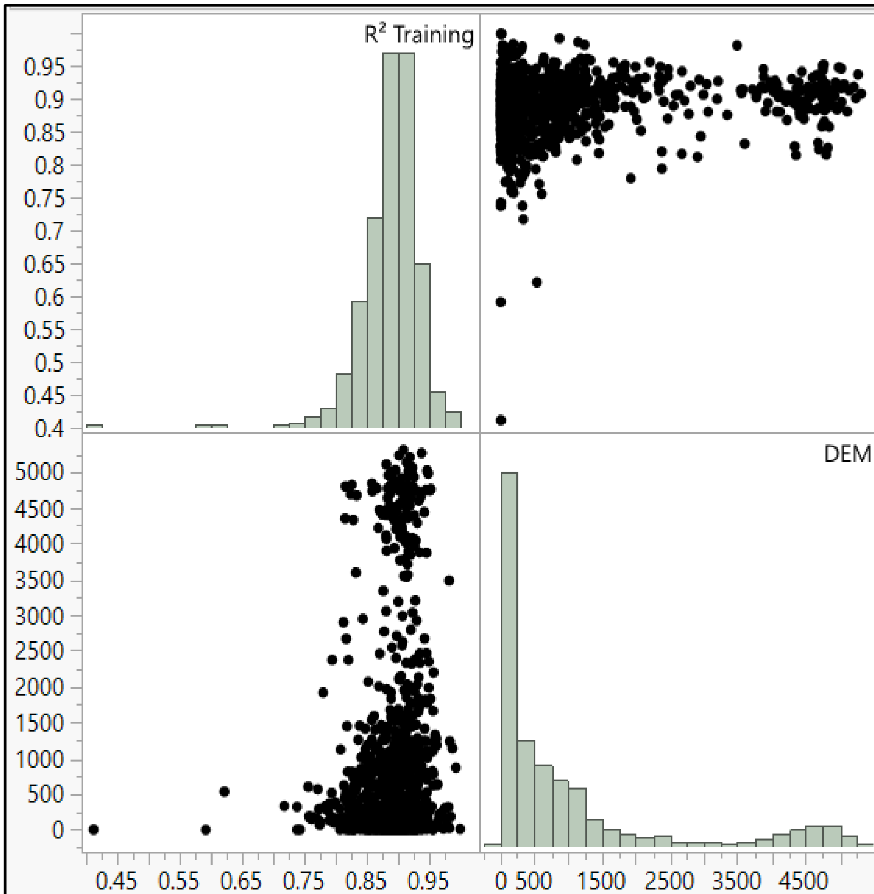

Pairwise Correlations

Variable	by Variable	Correlation	Count	Lower 95%	Upper 95%	Signif Prob	-.8 -.6 -.4 -.2 0 .2 .4 .6 .8
DEM	R^2 Training	0.1860	1105	0.1284	0.2423	<.0001*	

Figure 25. Pairwise Correlations between DEM and R-square Values

In addition, we applied Newman-Keuls as suggested by Keuls (1952), to compare the mean of the R^2 of the model in different land cover types. Table 9 shows the result of the comparison test. In general, there is little difference in the mean of R^2 between land cover types.

Table 9. Newman-Keuls Test for R-square Comparison between Land Cover Types

Level		Mean R^2
Bare land	A	0.906
Grassland	A	0.900
Forest	A	0.893
Shrubland	A	0.893
Wetland	A	0.893
Vegetation	A	0.888
Water bodies	A	0.886
Cropland	A	0.878
Urban areas	A	0.861
Levels not connected by same letter are significantly different		

The scatter plots (1:1) of the observed against predicted SMC and SWDI show the dataset's goodness of fit at different R^2 levels, presented in Figure 26 and Figure 27, respectively. In these figures, we presented SMC and SWDI in three R^2 levels including small R^2 (< 0.7), medium R^2 (0.7 - 0.85) and high R^2 (> 0.85). There were strong correlations between observed and predicted results, which confirms a stable performance of the ANNs models.

Figure 28 illustrates the observed and predicted SWDI at two different grid-cells. Overall, the model at different accuracy levels shows their ability to predict the drought index in the area. The model at cell ID = 63 presented a better performance than at cell ID = 32. At cell ID = 63, the model reflected the drought event happening during at years 2016, 2017, and 2018 at the Mekong Delta in Vietnam (Ho, 2016, Tran, 2018). In contrast, the model at ID = 32, where R^2 and RMSE were modest, did not reflect the drought events due to a lack of data input information. It may be necessary to have a missing filling data step in data preparation to achieve better results.

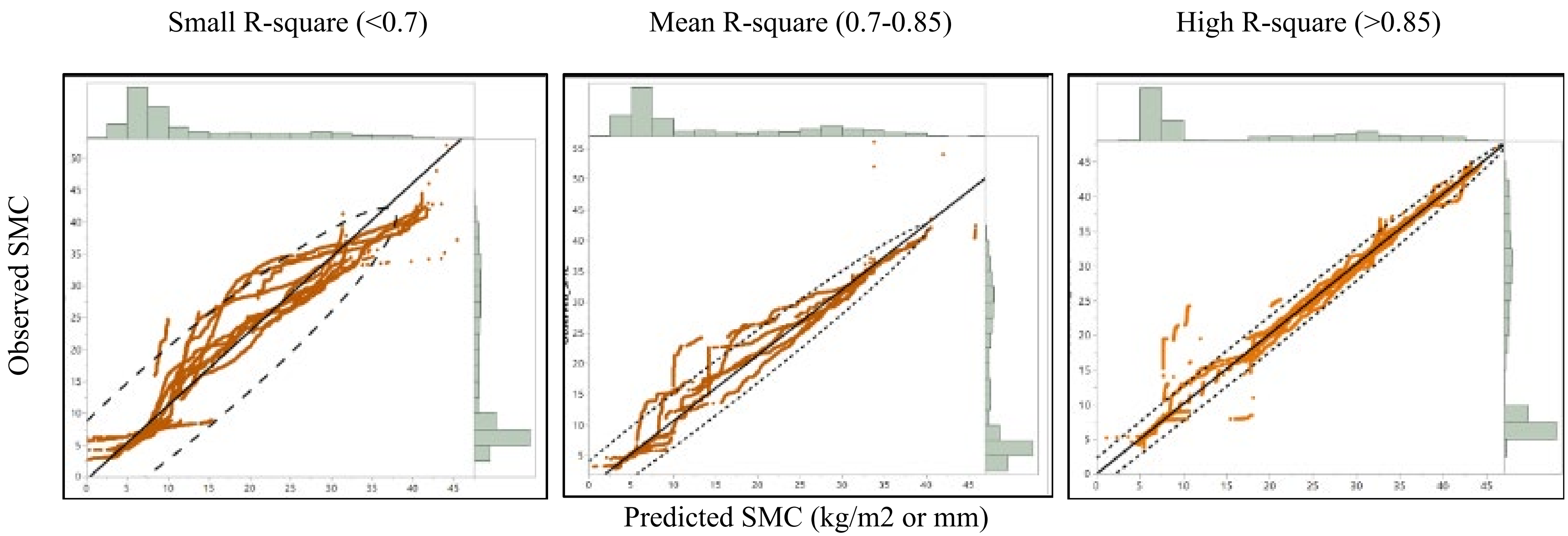

Figure 26. Scatter plot of observed against predicted SMC at different levels of the R-square.

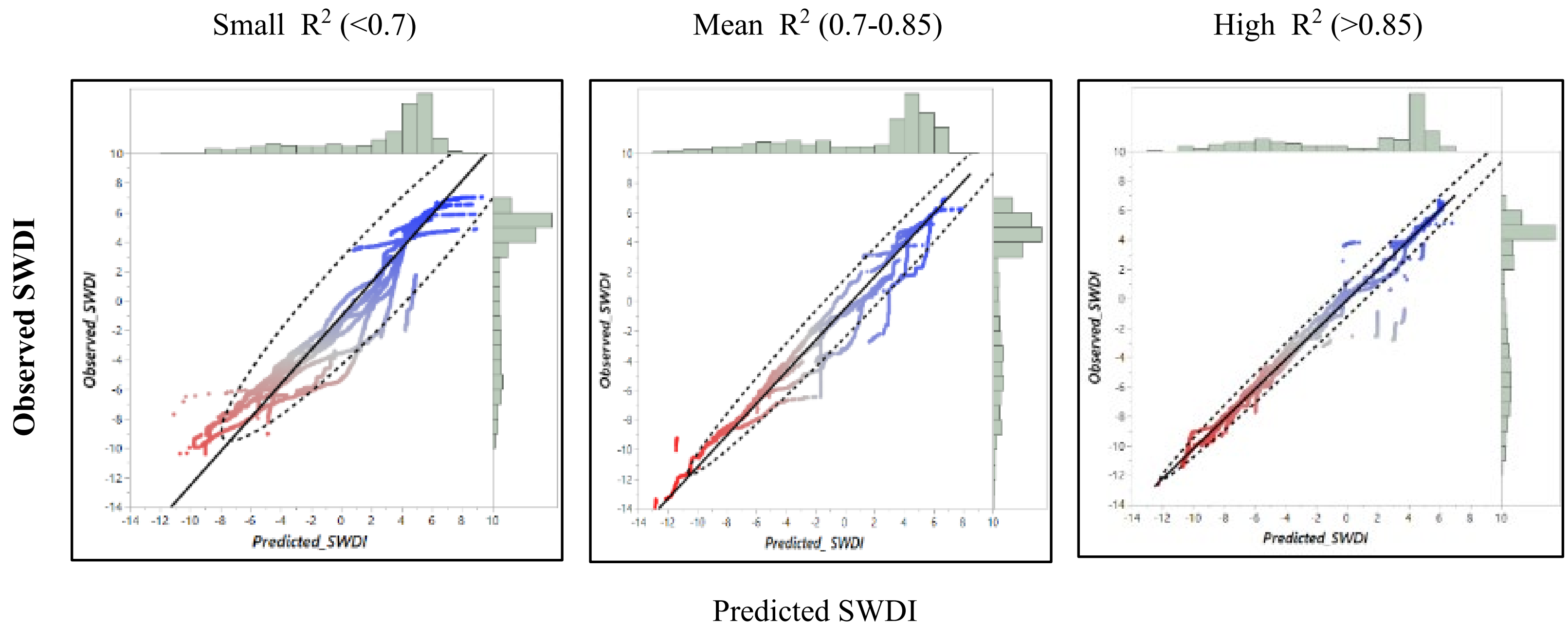

Figure 27. Scatter plot of observed against predicted SWDI at different levels of the R-square

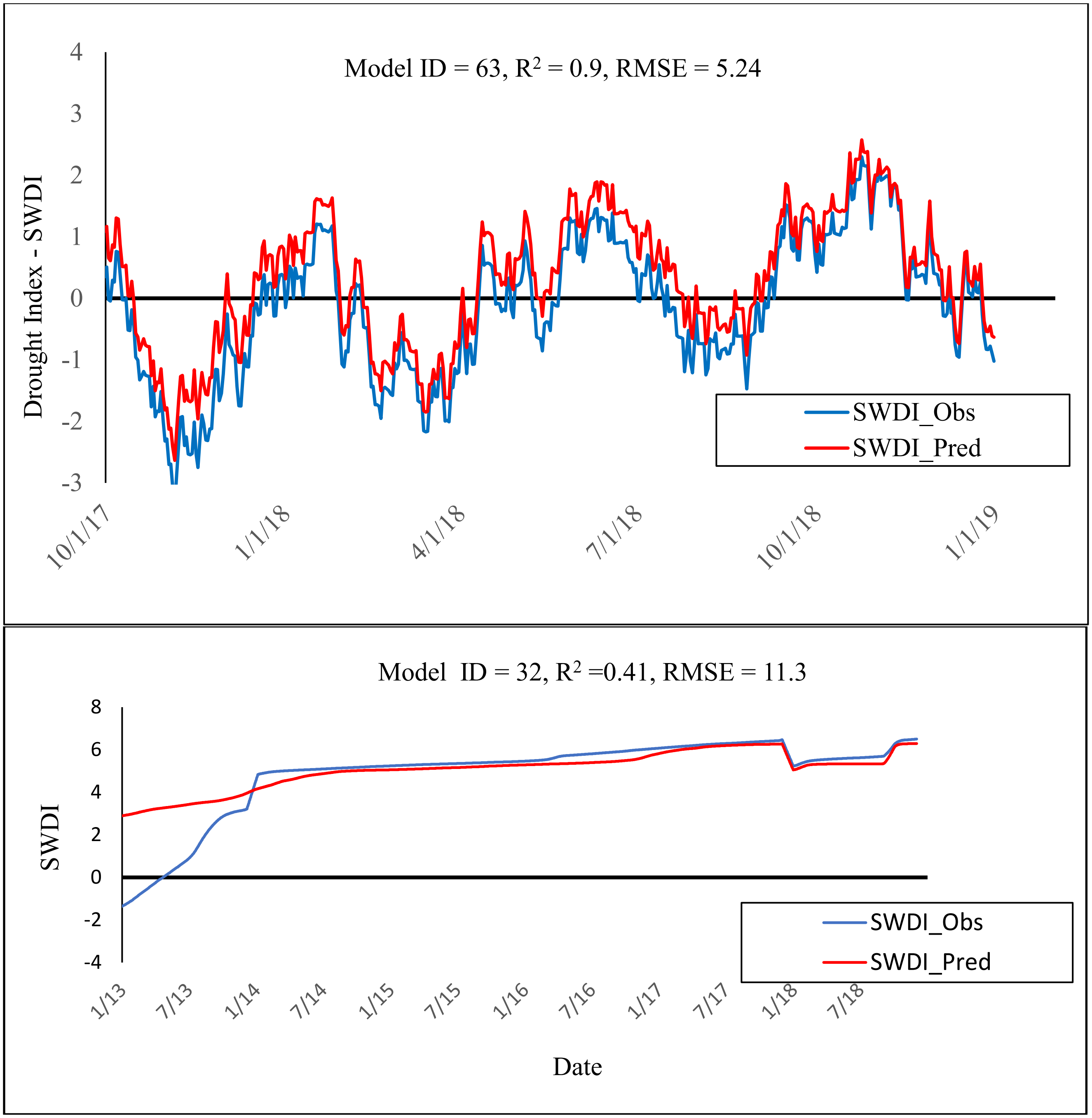

Figure 28. Observed and predicted SWDI of models

4. Conclusion

This study, investigated the SMC and agricultural drought problem using a deep learning-based approach to identify interactions among soil moisture, climate data, and land surface information in climate change conditions, is essential to preserving vulnerable regions from drought risk caused by soil moisture decrease. We designed a multi-layer perceptron ANNs architecture was applied to estimate daily soil moisture and predict agricultural drought risk from 2010 to 2018 with the SMDI index. The ANNs architecture had one input layer, one output layer, and two hidden layers on the JMP Pro platforms. We trained and validated the ANNs with 1105 grid-cells within the MKB using observed soil moisture derived from the Copernicus Global platform and twelve independent spatial datasets covered to train 1105 models. The models' performance against the observed soil moisture was tested using the coefficient of determination (R^2), the root mean square (RMSE) indicators. In general, the models had a solid predictive ability to estimate SMC and agricultural drought using SWDI in the research area. In addition, as a data-driven model type, the model's performance strongly correlated with missing data problems. The R^2 value for training and validation of these models ranged from 0.44 to 0.99 for predicting soil moisture and drought. The RMSE for both training and validation achieved 0.08 for predicting soil moisture and agricultural drought. Both land cover and topography in the region had weak positive correlations in predicting soil moisture and drought. In conclusion, the developed ANNs models had a solid ability to predict soil moisture and drought in the MKB.

Future work should involve comparing the ANNs model and traditional hydrologic model, including the VIC model, in soil moisture and drought prediction within the MKB. Further studies could investigate the model's performance for different input series in different climatic, geographical and hydrological conditions for enhancing the applicability of models.

Limitations

This study showed limitations during data preparation and model training processes. First, since the datasets used to train the models were varied in spatio-temporal resolutions, we applied interpolations which may have caused errors during data preparations. In addition, although we applied informative missing methods during the training and validation processes, missing data still impacted model performance. Hence, data filling should be conducted before inputting data for training the model.

CHAPTER 4. IDENTIFYING POTENTIAL TRADE-OFFS OF SHORT-TERM BENEFITS FOR LONG-TERM SOCIOECONOMIC STABILITY AMONG INHABITANTS OF THE VIETNAM'S MEKONG DELTA REGION ASSOCIATED WITH THE GOVERNMENT'S FLOOD CONTROL PROGRAM

Abstract

The VMD has played an essential role in Vietnam's socio-economic development. Residents of southern Vietnam have been annually influenced by coastal flooding, tidal regime, and saline intrusion for centuries. However, recent hydropower development, climate change, and the combined effects of sea-level rise and deltaic subsidence have become the main drivers impacting people's livelihoods in the region. In response to these problems, Vietnamese governmental flood control measures have had both positive and negative effects on the VMD population's livelihoods. These flood management strategies have been reported to reduce alluvial sediment load and water flow, intensifying saltwater intrusion from the South China Sea/East Sea into the VMD. We surveyed 615 VMD residents using a Best-Worst choice design to quantify the socio-economic trade-offs between the advantages and disadvantages of the government's flood management measures in the VMD. The best worst scaling results showed that subjects most highly valued long-term sediment replenishment and reduced salinity, and in the short-term, the amount of fish caught and crop yield. The willingness to accept analysis showed that people living within upstream VMD were willing to accept compensation of US $39.41 each season to receive more sediment and accept US $13.18 each season to shift their crop yield from high to medium level. But, the willingness to accept figures for those living downstream were only US $1.40 and US $11.46, respectively. The greater motivation to accept a lower subsidy by those downstream is most probably due to two factors (1) the greater intrusion of sea water and greater incidence of drought in the downstream region compared to the upstream region and (2) less sedimentation deposits downstream compared to upstream. These findings could be applied to quantify the tradeoffs between long-term and short-term benefits in flood water management in VMD.

1. Introduction

1.1. Agricultural Production in Vietnam's Mekong Delta

Vietnam's Mekong Delta region in southern Vietnam plays an essential role in the country's agricultural development (Khong et al., 2018). About 17 million people (GSO, 2020) live in the VMD, most of whom are largely dependent on the Mekong River and its tributaries for transportation, commerce, irrigation, aquaculture, fishing, and domestic and industrial use. Moreover, the VMD is known as the "rice bowl" of Vietnam since rice cultivation is the primary livelihood of about 60% of the population (Kakonen, 2008). This region produces about half of the national food volume with 51% of total rice-paddy production, 55% of the domestic fisheries and fruit production, 60% of the exported aquaculture goods, and 61% of total export value (Khong et al., 2018, Käkönen, 2008, Tran et al., 2011). The VMD's primary source of water is the Mekong River, which originates at the Tibetan Plateau in China and passes through Myanmar, Laos, Thailand, and Cambodia before flowing through the heart of the VMD and finally emptying into the East Sea.

Global warming has substantially impacted the VMD's agricultural development through shifting rainfall patterns and rising temperatures, which has resulted in water shortages and drought throughout the region. Also, because of sea level rise in the East Sea, saltwater has infiltrated the Mekong River and its tributary system, increasing the salinity of the water used for agriculture (Nguyen et al., 2021, UN, 2020). In addition, there has been a marked increase in the construction of upstream hydroelectric dams in China, Laos, and Cambodia since 1992, disrupting the Mekong River's streamflow (Orr et al., 2012, Soukhaphon et al., 2021). Lu et al. (2014) compared pre-dam (1960-1991) and post-dam (1992-2010) discharge flow along the river and found a strong correlation between dam construction and decreased discharge. Others have found that the damming process has resulted in a decrease in downstream sedimentation as well as substantial ecological damage (Orr et al., 2012, Tran et al., 2019).

As extreme weather events have intensified, there has been a decrease in agricultural production in the VMD (Hoang et al., 2018, Sebastian et al., 2016, UN, 2020). For example, because of drought and salinity infiltration, in 2016 almost 400,000 ha of cropland were affected, including 26,000 ha suffering complete crop failure (Sebastian et al., 2016). In addition, alluvial sediment, which provides natural fertilizer, decreased more than 75% due to upstream dam development, with an estimated annual loss of $24 million due to crop yield reduction (Chapman et al., 2016). Also, crop failure directly affected household income. In that same year, more than 208,395 VMD households faced insufficient freshwater for domestic use (Sebastian et al., 2016).

1.2. Vietnam's flood management systems

In addition to the problems described above, internal Vietnamese policies have affected agricultural production and the livelihoods of Vietnamese in the VMD. In 1986, the Vietnamese government instituted an economic reform policy known as *Đổi Mới* (restoration, reformation) to shift from a centrally planned economy to a market-oriented economy (Kingdom of the Netherlands, 2011, Toan et al., 2011). The main objective of this reform was to increase rice production in the VMD (Sebesvari et al., 2012). To protect cropland areas, mostly paddy fields, the government installed various water management systems. During the 1990s, the government installed low dikes, drainage canals, and irrigation systems. This process allowed the production of two crops per year, one during the regular rice-growing season and one in the off-season (Nguyen & James, 2013, Tran et al., 2018).

During the land reclamation and flood protection program that started in 1996, a large-scale high dike system was installed at the upstream region of the VMD with the intention to produce three rice crops annually (Kien, 2014). To accomplish this goal, many residents were relocated to flood-protected villages (Danh & Mushtaq, 2011). Over the next period, in addition to the high dikes, the government-built sluices and other flood control infrastructures to produce rice cultivation compartments. However, in the attempt to produce three crops per year, the agricultural fields have been cut off from the natural flooding process, with high floods spilling over low dikes, inundating cultivation areas. In addition, the flood control infrastructure has interrupted the natural resources replenished by floodwaters, such as wild fish stocks and fertile sediments (Tran, 2018).

The flood control measures instituted by the government have had both positive and negative effects on the VMD population's livelihood. For example, the sluice system allows three rice crops per year in An Giang and Dong Thap provinces, the two provinces immediately downriver from the sluices (Tran et al., 2019). However, the sluice system has stopped the normal process of flooding that farmers in the entire VMD had adapted to over generations. Before the introduction of the sluices, the upper part of the Mekong River deposited approximately 475 tons of fish, of which there were more than 1,200 species, into the VMD annually (Manh et al., 2015, Van et al., 2013, Arias et al. 2013, Chapman et al. 2016). However, today the fish yield has been significantly reduced, with a concomitant reduction in the ability to make a livelihood from fishing in the VMD (Tran et al., 2019). This has especially negatively affected fishers' livelihoods in An Giang and Dong Thap, two provinces (Danh & Mushtaq, 2011) previously known for fish production. Also, before the introduction of the new flood control system, 160 million tons of sediment were deposited each year in this region. However, the sluice system has reduced natural sedimentation in the VMD region, reducing soil nutrition and negatively affecting crop production. This reduction in natural sedimentation has resulted in a significant increase in the use of artificial fertilizer by farmers in this region (Tran et al., 2018b). Also, in addition to the reduction of water flow into the VMD due to the dam systems in the upriver countries described above, the sluice system has exacerbated the intrusion of saltwater from the East Sea into the VMD due to the rise of sea level caused by global warming (Tran et al., 2019).

The sluice system is essential to the triple rice crop each year in An Giang and Dong Thap provinces, which was the government's main objective when installing the sluices (Nguyen et al., 2014). While there is a wealth of research on the negative and positive impacts of flooding in the Mekong Delta (Hoang et al., 2018), very little work has been published examining the priorities of the people of the VMD in resolving this crisis. From the perspective of most farmers in the VMD, the flood management system is a hindrance to their livelihoods (Tran et al., 2018, Howie, 2011). Therefore, the purpose of this study was to identify the variables that are important to upstream and downstream farmers in the VMD to better inform government policies on controlling the flood infrastructure. We hypothesized that the residents of the VMD would be willing to accept the disadvantages of the opening of the upstream sluice gates in the VMD during flood season in exchange for certain benefits.

1.3. Best-Worst Choice Tool

This paper used a novel social survey, best-worst choice, to quantify the socio-economic trade-offs of the physical relationship between benefits and constraints of flood management in the VMD. This experiment used the Best-worst choice (BWC) method, which combines best-worst scaling (BWS) and discrete choice experiment (DCE). BWS, developed by Finn and Louviere (1992), is a discrete choice method that asks a person to select the "best" or "most preferred" and the "worst" or "least preferred" item in each choice set. BWS is usually applied to provide more choice data than traditional methods (e.g., Likert Scale) and recognizes choice processes through a random utility framework, allowing one to estimate the value of a specific item or attribute within a choice set (Finn & Louviere, 1992). Due to the nature of this framework, BWS is frequently perceived as having greater discriminatory power than other scale measures, providing greater insight into importance scaling, and is less cognitively demanding for the survey taker to generate valid data (Louviere et al., 2015, Burton et al., 2019, Parvin et al., 2016). DCE is a quantitative method that evaluates preferences by accessing respondents' willingness to accept (WTA) or willingness to pay (WTP) in a given scenario based on the entire profile (Finn & Louviere, 1992, Flynn & Marley, 2014). Integrating BWS inherent value with DCE monetary value allows invaluable insight by measuring individuals' WTP/WTA estimates for a given product based on traditional demand theory (Soto et al., 2016, Soto et al., 2018, Oluoch et al., 2021).

2. Materials and Methods

2.1. Subjects

Subjects' demographic data are presented in Table 10. The subjects were adult male and female farmers living in four different provinces in the VMD (n = 605). Almost half of the subjects lived upstream in An Giang or Dong Thap province (n = 280), located just below the sluices. A little more than half of the subjects lived in Ben Tre or Vinh Long province, located further downstream in the Mekong River (n = 335), where water salinity is greater, and sediment deposition is less than the upriver provinces (Figure 29). Each subject signed an informed consent approved by the Montclair State University's Institutional Review Board, IRB-FY20-21-1950.

Table 10. Best-worst scaling attributes and levels.

Attributes	Definition	Levels
Amount of fish caught (AFC)	Flood water brings aquatic species (e.g., fish, crab, and snail) to the VMD. People living in flood zones can catch these species as a benefit from the floods. Since the amount of capture fish per household per day in VMD were reported ranged from about 2 kg to 22 kg (Hortle, 2007; Lem, A & Nghia, N, 2003), we selected three levels of AFC attribute as described in the right column.	0-10 kg*(F010) 11-20 kg (F1120) 21-30 kg (F2130)
Sediment rate (SR)	The enriched alluvial water brings natural fertilizer to the VMD via sediment processes. The increase in sediment rate is one of the benefits of opening the sluice gates.	Low* (SL) Medium (SM) High (SH)
Reduce salinity rate (RSR)	As an extreme water-related event, saltwater intrusion has occurred annually during dry seasons in the VMD. It has caused adverse impacts on people's livelihood due to the increase of salinity in surface water. The floodwater can push seawater back to the ocean resulting in salinity reduction. According to the expert interview and literature review, the salinity rate rages from 0.4 g. l^{-1} to 30 g.l^{-1}.	25%*(RSR25) 50% (RSR50) 75% (RSR75) 100% (RSR100)
Crop Yield (CY)	Floodwater provides freshwater and nutrient sediment and wipes out pets and diseases. This benefit helps, implicitly, to increase crop productivity. Most of the land in production is dedicated to paddy; we used the annual yield of paddy by the province to represent the crop yield. The average yield at the VMD was 5,970 kg per hectare (597 kg per 1000 m^2) (GSO 2020).	Low* (YL) Medium (YM) High (YH)
Tax subsidy (TS)	Although floods bring many advantages to the VMD, they also cause losses, such as decreasing yield, creating difficulties in daily activities, and affecting people's livelihood. Therefore, the government will provide a subsidy in tax reduction to those who are getting influence.	25% reduction* (T25) 50% reduction (T50) 75% reduction (T75) 100% reduction (T100)

Asterisks (*) indicate the baseline variable for each attribute used for level-scale coding.

2.2. Survey Design

We developed a questionnaire using ArcGIS Survey123 software, introduced by ESRI (2018), where respondents answered the questions using a mobile device (e.g., a tablet). One of the main benefits of using this software is that response data is automatically recorded and preprocessed instantaneously, thus avoiding the loss of information. Participants were required to be at least 18 years old and to be living at the site when the survey was conducted. The first part of the survey included sociodemographic questions, including sex, age, education, farming experience, and household income. The second part of the survey explored farmers' perceptions and beliefs surrounding extreme weather events that may impact their lives. The third part of the survey, which was the key focus of this study, was designed to explore the importance that farmers attached to the characteristics of floodwater as they affect their livelihoods. We also conducted an in-person expert interview to gather information about recent situations relating to changes in the water regime in local areas in order to identify the attributes and their levels (Table 10). Seventeen experts, all long-term employees of local agricultural extensions with extensive knowledge of agricultural activities and water regimes in their local regions were identified in An Giang, Ben Tre, and Can Tho provinces.

Although researchers have estimated the amount of sediment transported by flooding to the VMD (Piman & Shrestha, 2017), very few studies have reported the actual amount of alluvial sediment trapped in a given unit of land field area in the VMD (Manh et al., 2015, Nguyen et al., 2014). The experts reported that, in their experience, sediment deposition rate ranged from 2 – 8 $kg.m^{-2}$ annually. These figures agree with those of Hung et al. (2013). Therefore, we set the low level of sediment at 2 $kg.m^{-2}$, medium level of sediment at 5 $kg.m^{-2}$, and high level of sediment at 8 $kg.m^{-2}$.

The data from the literature suggest that salinity rates at the Mekong delta varies according to season and year. Ho (2015) reported that the salinity rate in the Mekong River (*Tiền Giang* River) ranged from 7.4 $g.l^{-1}$ – 21.6 $g.l^{-1}$. However, our experts reported that, the salinity rates ranged from 0.4 $g.\ l^{-1}$ – 30 $g.l^{-1}$ in Ben Tre, Can Tho, and An Giang provinces.

Based on experts' opinions and literature reviews (Manh et al., 2015, Nguyen et al., 2014; Piman & Shrestha, 2017, Tran et al., 2019), five attributes and 17 attribute levels were selected for this study, slightly modified to reflect the benefits of floodwater to local farmers' livelihood. Table 10 describes the attributes and their levels used in this study.

For this study, we used the sediment loads and salinity rates reported in the literature and the data reported from the experts to arrange levels of these attributes, which are presented in Table 10. It should be noted that we created the ranges of levels to assist survey participants in selecting responses. These levels were not used as quantitative values in this study.

The hypothetical agricultural tax subsidy was calculated using Decision 74-CP, issued by the Ministry of Agriculture and Rural Development of Vietnam on October 25, 1993, which assigns the annual agricultural tax based on a unit of 1000 m^2 of paddy field.

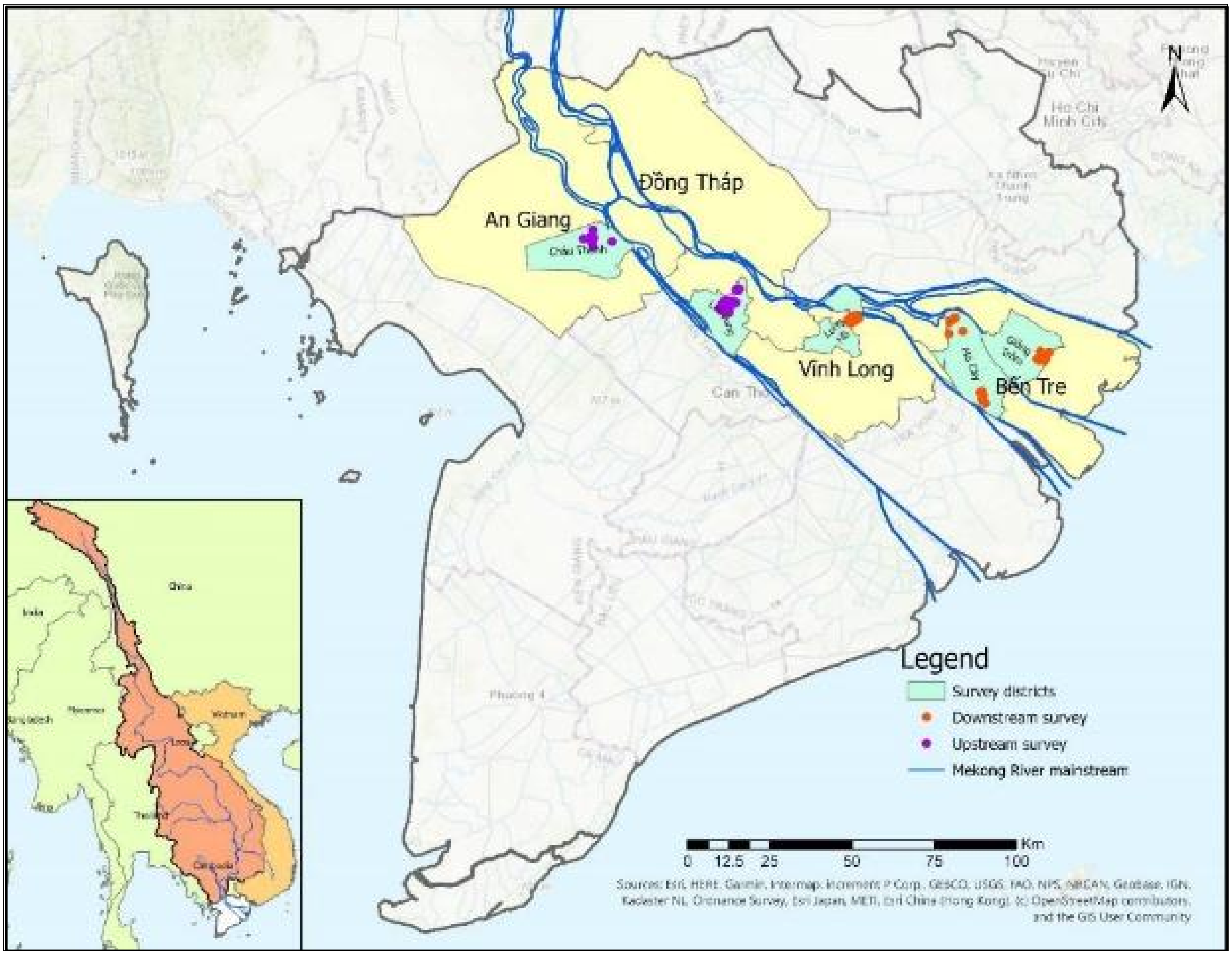

Figure 29. Upstream versus downstream interview locations in the VMD

The associated levels of attributes in Table 10 allow the possible number of combinations equal to the multiplication of the number of attribute levels. That is, 432 (3*3*4*3*4) potential profiles existed, which is an unfeasible number to employ in the survey. Therefore, we generated the MaxDiff Design Platform, which follows a balanced incomplete block design, through JMP Pro 14.2, to select a set of optimal choice profiles and created choice sets used in the main part of the survey (Olouch et al., 2021, Smith et al., 2020). The choice sets allowed for orthogonality, balance, and minimal overlap. We obtained 36 choice set profiles, divided into six questionnaire blocks forming the respondent's choice options. The respondents were randomly assigned one of six blocks, reducing potential bias caused by correlation among these choices in responses. Each respondent completed two tasks in each set of questions, (1) to choose the "Best" and the "Worst" attribute level, and (2) to agree or not agree with the hypothetical tax subsidy program. These two tasks allowed the researchers to both compare the utility of all attribute levels and to estimate farmers' willingness to accept introduced attribute levels. A sample questionnaire is presented in Figure 30 below.

(Check one option as the BEST and one option as the WORST)
Program 1 _ Mekong Flood subsidy program

	BEST	**WORST**
Result in **Fish** caught up-to **11-20kg** per day	●	○
Provide **Medium** sedimentation	○	○
Reduce **salinity** by **75%**	○	●
Result in **Medium** crop **yield**	○	○
25% reduction in **household tax**	○	○

Would you support for this Mekong Flood subsidy program?
(Choose Yes or No)

● YES
○ NO

(Hãy chọn một lợi điểm mà ông/bà cho là TỐT NHẤT và một lợi điểm mà ông/bà cho là KÉM NHẤT của dự án)
Dự án 1 – Dự án hỗ trợ lũ lụt Đồng bằng sông Cửu Long

	TỐT NHẤT	**KÉM NHẤT**
Lượng **thuỷ sản** bắt được **11-20 kg** mỗi ngày	●	○
Cung cấp lượng **phù sa** mức **Trung Bình**	○	○
Độ mặn nước sông giảm **75%**	○	●
Năng suất nông sản đạt mức **Trung Bình**	○	○
Dự án hỗ trợ giảm **25% thuế nông hộ**	○	○

Ông/bà có ủng hỗ dự án hỗ trợ lũ lụt ĐBSCL này không?
(Chọn Có hoặc Không)

● CÓ
○ KHÔNG

Figure 30. Sample best-worst choice question

2.3. Sampling Method and Survey Administration

The questionnaire was translated from English into Vietnamese before the data collection process was started. The primary survey was administered in December 2020 in-person, using face-to-face interviews to reduce participant bias (Udmale et al., 2014). However, in November 2020, the survey was subjected to a small pre-test (n=20) to assess the clarity and usefulness of the information contained in the questionnaire. The pre-test also helped to avoid potential misunderstandings between the subjects and the interviewers, as the interviewers had more formal education and were from different cultural regions of the country. The feedback of the pre-test was used to improve the questionnaire before the start of data collection of this study. Those who participated in the pretest trial were excluded from the subject pool of the primary survey.

Although face–to–face interviews may result in the most expected outcome, the questionnaire may be biased by unanticipated communications between the subject and the interviewer (Udmale et al. 2014). Hence, while designing and administering the questionnaire, the study followed several steps to reduce bias. First, the language of the questions was simplified so that target subject population could easily understand the questions from the interviewer (UN, 2008). Second, various topics were categorized into sections to keep a uniform flow during the interview. Third, the questions were administered with care to avoid responses beyond the immediate question asked (Udmale et al., 2014). Fourth, the differences in local subculture terminology among target groups were considered.

Each province's local District People’s Committee office providing a list of households in their community. The interviewers then recruited respondents by either going from house to house or gathering farmers at central points to conduct the survey (Thi et al., 2017). For those subjects who were interviewed at home, the oldest adult was interviewed. For households where no adult was present when the interviewer arrived, the subject later came to a central point for the interview (Oluoch et al., 2021).

2.4. Econometric Analysis

We used two different econometric models to analyze each choice task. First, a paired estimation approach (conditional logit) suggested by Flynn et al. (2007) and Louviere et al. (2015) was used to analyze at the sample- or respondent-level in the BWS part. Then, a multinomial condition logit (MNL) model was utilized to estimate the DCE for the second task, “supporting” or “not supporting” the hypothetical Mekong Flood subsidy program that we had constructed. In this study, we chose the best-worst paired estimation for the BWS to avoid the potential for large standard errors (Soto et al., 2016).

a) First task of BWC: Best worst scaling

As presented in Figure 30, the profile of attribute levels (items) that respondents evaluated before selecting the item maximized the difference of their preference. The possible best-worst combination of each profile may be calculated as

$$J * (J - 1) = 20 \qquad \text{Eq. 15}$$

where J = the number of attributes per choice set (J = 5 in our model). The chosen best-worst pair is coded as 1. Those pairs not chosen are coded as 0.

If individual *i* chooses item *j* as best and item *k* as worst in the *M* choices, then the level of importance or utility *U* of item *j* and item *k* is calculated by

$$U_{ij} = \mathrm{X}_j + \varepsilon_{ij};\ U_{ik} = \mathrm{X}_k + \varepsilon_{ik} \qquad \text{Eq. 16}$$

where, X_j; X_k = the locations of value *j* and *k*, and ε_{ij}; ε_{ik} represent random error terms.

The different utility or importance, *U*, with respondent *i's* selection of item X_{ij} as best and X_{tk} as worst (j, k ∈ M; j ≠ k) in the choice set *t* is calculated by

$$U^i_{jkt} = \beta_j . X^i_{tj} - \beta_k . X^i_{tk} + \varepsilon^i_{tj} - \varepsilon^i_{tk} \qquad \text{Eq. 17}$$

(Soto et al., 2016, 2018)

where β and $\mathcal{E}$ = the coefficients and errors, respectively, of the regression model. Hence, the probability of individual, i, to choose j as best and k as worst in assigned set t, is expressed as a multinomial logit (MNL)

$$P_{BW}(X) = \frac{e^{\beta_j.X_{tj}^i - \beta_k.X_{tk}^i}}{\sum_{l,m \in M; l \neq m} e^{\beta_l.X_{tl}^i - \beta_m.X_{tm}^i}} \quad \text{Eq. 18}$$

The β_j parameters in the equation above are estimated using the MNL command (clogit) in STATA/SE 15.1, as Flynn (2007, 2008) suggested.

Therefore, each attribute's difference in importance (utility) is represented by the BWS equation adapted from Soto et al., 2016.

$$U_{diff}^i = \beta_{A1}^i + \cdots + \beta_{An}^i + \cdots + \beta_{A1L1}^i.D_{A1L1}^i + \cdots + \beta_{AnLn}^i.D_{AnLn}^i + \in^i \quad \text{Eq. 19}$$

where the importance of each best-worst pair for individual i (i = 1, … n) and the level values are such that the attribute that is chosen as best (β_{AnLn}^i) has an impact value (D_{AnLn}^i) of 1, the attribute chosen as worst having a value of -1, and the remaining having a value of 0 (Smith et al., 2021, Soto et al., 2016, Flynn & Marley, 2014).

b) Second task of BWC: binary choice model and willingness to pay (WTP) or willingness to accept (WTA)

For the DCE choice task, subjects were asked to make a discrete choice (YES or NO) to support or not support the hypothetical subsidy program. The dependent variable was coded as 1 if respondents were likely to support the program (YES) and coded as 0 if the respondent did not support the program. These data were analyzed using an MNL, which assumes that potentially unobserved heterogeneity is a part of the error term structure (Oluoch et al., 2021, Soto et al., 2016). We applied logit command in STATA/SE using a logit model to estimate binary responses by maximum likelihood for each variable and the model constant.

The modified random utility for individual i and binary choice task t is calculated by the below equation

$$U_{it} = \beta\chi_{it} + \alpha_i + \varepsilon_{it} \quad \text{Eq. 20}$$

where β = the coefficient of marginal utilities, χ_{it} represents attributes of choice, α_i = a specific individual error, and ε_{it}= the overall error term (Smith et al., 2021; Soto et al., 2016)

We also estimated WTA/WTP using the WTP command in STATA/SE, which estimated confidence for willingness to pay to calculate for dichotomous data using the calculated cost coefficient and the attribute coefficient from the model based on the tax subsidy variable (COST). When COST was selected as best/worst choice, we applied the following equation to estimate an implicit price (a) expressed as willingness to pay to achieve a given quality or quantity of an attribute.

$$a = -\left(\frac{\beta_a}{\beta_{cost}}\right) \qquad \text{Eq. 21}$$

where β_{cost} , is the cost/price of an attribute and β_a is utility of an attribute (Brennan & Van Rensburg, 2016). Then the implicit price may be used as a marginal WTP/WTA for discrete change in attribute level, which estimates the relative importance that the respondent placed on attributes (Oluoch et al., 2021).

3. Result and Discussion

3.1. Subject's sociodemographic data

Interviews were conducted with 615 subjects, with 605 (98.37%) completing the Best-worst choice questionnaire. The subjects' demographic data are presented in Table 11 along with the equivalent population distribution of the VMD as reported by the Vietnamese government (GSO, 2019). Some variables, including education level and sex, were somewhat reflective of government census data (Pearson test), but age was not. This may be explained by our method of choosing the oldest person in the household when conducting the survey.

Table 11. Demographic distribution of survey respondents compared to the Mekong Delta population (GSO, 2020)

Subjects	Percent of the subject pool	Percent of VMD population
Province Residence		NA
An Giang	19.3	
Dong Thap	26.2	
Vinh Long	21.3	
BenTre	33.2	
Sex		
Female	39.8	50.55
Male	60.2	49.45
Age		
18-24	1.1	11.2
25-29	2.0	10.4
30-34	3.3	11.9
35-39	7.2	12.1
40-44	12.4	10.9
45-49	10.4	10.2
50-54	16.4	9.7
55-59	14.0	7.9
60-64	14.0	6.2
65+	19.3	9.4
Education level		
Primary	44.6	51.2
Secondary	38.2	34.2
High	14.0	14.6
Vocational	1.5	2.3
University	1.8	4.3
Number of household members		
<3	10.1	NA
3-4	50.2	
5-6	33.8	
7-8	5.5	
>8	0.3	
Household incomes (monthly)		
< 3 million VND	21.8	NA
3 – 6 million VND	29.8	
6 – 9 million VND	18.2	
9 – 12 million VND	13	
12 – 15 million VND	7.3	

15 – 18 million VND	3.3	
> 18 million VND	6.7	
Cultivated area (1000 m^2)		
0 (No-farm)	7.3%	NA
< 5	42.9	
5-10	23.9	
10-15	11.4	
15-20	6.2	
20-25	3.3	
> 25	5.0	

The population data is taken from the Statistical Yearbook of Vietnam 2019. Figures in underline fail the Pearson χ^2 test.

Table 11 illustrates the socio-demographic characteristics of the survey pool. The null hypothesis for equality of means at 10%, significance level was rejected for age groups 18 to 24, 25-29 and 30-34. Perhaps these differences could be attributed to the older demographic of our subject pool, who were farmers. Number of household members, median household income, and cultivated area were not reported in the national census. In all the other socio-demographic characteristics, there was no statistically significant difference reported. Overall, the chi-square tests show that the VMD sample and VMD population had a goodness of fit for most of the socio-demographic factors.

The household income was found to be representative of the region, where more than 50 % of respondents earn less than six million VND per month, while higher incomes (above 12 million VND) accounted for only 17.3% of the subjects. The low income (less than 6 million VND) accounted for a large portion of respondents (more than 50%) and was likely due to more than 50% of subjects owning less than 5,000 m^2 cultivated area.

3.2. Best-worst scaling analysis

The conditional fixed-effects logistic regression (clogit) performed on the attribute impacts groups showed significance at 1% for each attribute (Table 12). Following the BWS convention, it was necessary to omit one attribute to avoid a saturated model. For this reason, we omitted the tax subsidy

(TS) attribute, as this attribute is objective while the others are subjective and based on the respondents' opinions. Removing this group also serves as a reference point for the underlying scale of importance for other groups (Oluoch et al., 2021, Smith et al., 2021).

Reducing the salinity rate (RSR) was found to be the most important, followed by sediment rate (SR). Interestingly, crop yield (CY) and the amount of fish caught (AFC) were significant but negative, implying that while these factors are important to respondents, they have a negative effect on overall perception of the hypothetical flood management program (Table 12). These results suggest that the respondents felt that long-term ecosystem benefits of floodwater, including sedimentation and reducing saltwater intrusion, were more important than the short-term benefits of annual CY and annual AFC. From a government policy perspective this is a very important finding, and decision makers should consider these findings when building programs that address these concerns.

Table 12. Estimation Conditional Logistic Regression Analysis

Attribute Impacts	**Coefficient**	**z**	**95% CI**	
Amount of fish caught (AFC)	-.467 (.0342) *	-13.63	-.535	-.400
Sediment rate (SR)	.095 (.0341) *	2.8	.028	.162
Reducing the salinity rate (RSR)	.298 (.0338) *	8.83	.232	.365
Crop Yield (CY)	-.459 (.0343) *	-13.37	-.526	-.391
Tax subsidy (TS)	omitted			
Level Scales	**Coefficient**	**z**	**95% CI**	
F1120	-.256 (.045) **	-7.69	-.348	-.163
F2130	-.165 (.067) *	-3.71	-.298	-.032
SM	.196 (.043) **	4.54	.111	.281
SH	.609 (.053) **	7.02	.506	.714
RSR25	.405 (.068) **	5.92	.271	.539
RSR50	.643 (.054) **	11.82	.536	.749
RSR75	.487 (.052) **	9.35	.384	.588

YM	-.438 (.045) **	-9.76	-.525	-.350
YH	.510 (.064) **	8.03	.385	.634
T50	.206 (.057) **	3.63	.095	.317
T75	.283 (.051) **	5.51	.182	.383
T100	.307 (.084) **	3.66	.143	.472
Number of observations	72,540			
LR Chi[2]	729.48			
Log likelihood	-10530.049			

a. One (*) and two (**) asterisks represent 0.05, 0.01 levels of statistical significance, respectively.
b. The number in parentheses are standard errors.
c. F1120 = Fish caught up to 11-20kg/da; F2130: Fish caught up to 21-30kg/day, SM: Sediment increase at Medium level, SH: Sediment at High level, RSR75: Reduce 75% salinity, RSR50: Reduce 50% salinity, RSR25: Reduce 25% salinity, YM: Crop yield at Medium level, YH: Crop yield at High level, T50: Subsidy 50% household tax, T75: Subsidy 75% household tax, and T100: Subsidy 100% household tax.

On closer observation of the level scale values, all attribute levels were found significant (at either 5% or 1%) in respect to their baselines. For the AFC level scales, we found both level scales (F1120 and F2130) to be negative. However, F1120 had a higher negative coefficient than F2130, which can be translated to mean that respondents find high fish yield more important than moderate fish yield, when given the option (Table 13). This result may indicate that the lowest yield (F010) was more valued than F1120 and F2130. That is, it may be that a yield of up to 10kg/day was considered by local fishermen as the maximum sustainable yield, which is the highest catch that a body of water can support long-term via the Gordon-Schaefer bioeconomic model (Zhang & Smith, 2006).

The SR attribute level results suggest that respondents thought that sedimentation management should be a key component of flood management strategies. It can be observed that the coefficient was positive, with respondents finding higher levels of sediments (SH) more important than medium (SM) and low (SL) levels of sediments (Table 12). Hong et al. (2016) suggested that sediment deposition provides several services to the VMD socio-ecological wellbeing. This result challenges the practice of Upstream infrastructure, e.g., the extensive damming systems, which starves the VMD of the much-needed sediment deposition critical for agricultural productivity and economic growth (Tran et al., 2016, Weger, 2019).

Extreme salinity conditions have inherent disadvantages by negatively impacting crop yields (Dam et al., 2019, Alam et al., 2017). For the RSR level scales, all the coefficients were positive with RSR50 being valued the highest, followed by RSR75 and RSR25. Evidence suggests that farmers in Ben Tre province switched from rice production to other agricultural products (e.g., shrimp, prawns) more conducive to growth in a higher salinity environment as salinity rates increased over time (Loc et al., 2021), which may explain why RSR50 was most valued.

Crop yield level scale coefficient exhibited surprising results, where medium yield (YM) had a negative coefficient whereas high yield (YH) was positive. This finding suggests that while CY overall is less important than environmental factors like SR and RSR, respondents still hold value in high yield which in turn would lead to increased income potential. As Mr. Hanh, from Can Thanh commune, Chau Thanh district, An Giang province, stated: "*Even though farmers know it's not profitable to grow a third rice crop each year, they continue to do so because rice production is their only income. They don't know what else to plant and don't know how to do anything else".* This statement suggests that the government should have education and training for these farmers to adapt to the new environmental reality.

The TS attribute, which in our study was the hypothetical tax reduction, showed consistent trends according to economic theory. Results showed that the 100% household TS (T100) was the most highly valued, implying that the respondents preferred a greater TS than lower TS. However, we observed that monetary payment was not the most important aspect of the hypothetical management plan. Rather, respondents valued long-term ecosystem benefits like salinity reduction and alluvial sedimentation deposition as providing much higher utility.

The key finding in this study was that respondents, in general, seemed to more highly value the attributes that have more long-term ecosystem impacts. Therefore, we deemed it important to further explore data by dividing the responses into two regions: the upstream region, including the An Giang and Dong Thap provinces, and the downstream region, including Vinh Long and Ben Tre provinces. Table 13 presents a comparison of BWS results between these two sub-regions.

Table 13. Best-Worst Scaling for Upstream and Downstream Survey Respondents

Attribute level	**Upstream**		**Downstream**	
	Coefficient	**z**	**Coefficient**	**z**
F1120	- .138 (.072)	-1.92	-.402 (.065) **	-6.14
F2130	- .149 (.102)	-1.46	-.205 (.096) *	-2.12
SM	.297 (.066) **	4.56	.114 (.061)	1.88
SH	.578 (.079) **	7.24	.719 (.076) **	9.51
RSR25	- .294 (.079) *	-1.90	1.017 (.074) **	13.84
RSR50	- .031 (.079)	-.39	1.346 (.081) **	16.67
RSR75	- .151 (.104)	-2.83	1.036 (.097) **	10.62
YM	- .364 (.067) **	-5.39	-.507 (.063) **	-7.99
YH	.336 (.095) **	3.55	.754 (.092) **	8.19
T50	.377 (.087) **	4.35	.141 (.079)	1.77
T75	.528 (.079) **	6.69	.071 (.071)	1.91
T100	.345 (.127) **	2.71	.391 (.119) **	3.27
Number of observations	31,300		39.320	
LR Chi^2	250,04		966.89	
Log likelihood	-4,583.562		-5,412.920	

a. One (*) and two (**) asterisks represent 0.05, 0.01 levels of statistical significance, respectively.
b. The number in parentheses are standard errors.
c. F1120 = Fish caught up to 11-20kg/da; F2130: Fish caught up to 21-30kg/day, SM: Sediment increase at Medium level, SH: Sediment at High level, RSR75: Reduce 75% salinity, RSR50: Reduce 50% salinity, RSR25: Reduce 25% salinity, YM: Crop yield at Medium level, YH: Crop yield at High level, T50: Subsidy 50% household tax, T75: Subsidy 75% household tax, and T100: Subsidy 100% household tax.

This analysis showed a marked difference in attribute utility among upstream and downstream respondents. One of the starkest differences can be seen when viewing the RSR attribute levels, where upstream respondents held negative utility with minimal to no significance, and downstream respondents held positive, significant utility. For downstream respondents, moderate salinity (RSR50) was in fact the most highly valued attribute, followed by RSR25 and RSR75 respectively. This result suggests that those living downstream are most impacted by unmanaged salinity intrusion and therefore most in need of an adaptive management system. According to Mr. Lach, who lives in Can Thuan commune, Chau Thanh district, An Giang province, mentioned: "*According to media reports, the Ben Tre region does not have enough water for irrigation due to drought and salinity. If possible, I would accept the release of floodwater our region in order to have enough freshwater for the downstream region. If I'm happy here upstream and people downstream are miserable, I don't want to....*".

While the trend in the SR attribute were the same among both groups, we observed that SH was more important to the downstream group (Table 13) than the upstream group. This may be due to the difference in SR between upstream and downstream, with upstream locations having a higher SR. Again, this supports the argument that greater water management system intervention is more important for the downstream provinces in order to satisfy the needs of those who live and farm there (Duong et al. 2018).

While CY was important for both groups, we observed that the downstream group more highly valued YH than the upstream group (Table 13). This can be explained by the fact that rice production is almost twice as high upstream compared to downstream according to the Vietnamese government annual statistical report (GSO, 2021).

The AFC levels were insignificant for the upstream group, but negatively significant for the downstream group. These results can be explained as follows: during the recent period, in the upstream area, the water in the canals below the sluice system has been low, resulting in a low rate of fish capture. Consequently, people in that region no longer rely on fishing as their primary source of income. According to Mr. Lach, "*In the past, this canal flooded both sides of the road. However, because no water discharges from upstream, now there is very little water arriving here. In February* *or March, the canal is so dry that boats cannot even travel; how can I catch fish here? Now I wish for more water to come back like it did before so that I can catch fish and eel to live through the day...*". Loc et al. (2021) reported that this problem does not exist to the same extent above the sluice system. For the downstream group, where the amount of fish caught per day has been historically low, the water management system has not affected this area as much as the upstream area (GSO, 2019).

For the hypothetical TS proposal, the upstream group found utility for the T50 and T75 level, but the downstream group found no utility in T50 or T75. However, both groups found utility for T100. These findings suggest that the TS was more important for the upstream group than the downstream group, because residents downstream are more concerned about the salinity attributes than other attributes since salinity has affected this group more than the upstream group (Thuy & Anh, 2015).

3.3. Willingness to accept analysis

In this section, we utilized the MNL regression model to quantify the WTA/WTP of local communities for potential externalities of floodwater. It is important to note that the cost attribute is not divided into levels, as depicted in the BWS analysis, but rather is a continuous variable that was calculated using the agricultural tax for 1000 m^2. Table 14 reports the impact of attribute levels on respondents' decisions and WTA/WTP compensation, and Figure 31 depicts the findings comparing the upstream and downstream group results. The negative monetary results represent WTA (i.e., receive tax subsidy), whereas the positive results represent WTP (i.e., give payment).

For AFC, the downstream group found that the F2130 attribute level provided utility. No other AFC attribute levels were considered important for either group. It should be noted that F2130 would be quite unrealistic for the downstream region.

For CY, both YM and YH attribute levels were considered important for both groups. The upstream respondents were WTA a much higher amount ($46.81) than the downstream respondents ($19.66) for YH. The same trend was seen for YM with a WTA of $33.63 and $8.20 for each group, respectively.

This finding suggests that the upstream residents would require a much higher tax subsidy than downstream residents if the hypothetical management intervention focused on crop yield.

The SR attribute levels show that both groups are WTA a higher amount for SH compared to SM. However, the difference between these two attribute levels is substantially different. The upstream group results show a WTA $60.71 for SH versus $21.30 for SM, while the downstream group shows a small difference of only $1.40 between these levels, $15.27 versus $13,87, respectively. Tran et al. (2019) reported that costs of sediment loss per hectare ranged from $145 to $370, indicating that loss of sedimentation is a major problem in the VMD region (Tran et al., 2019).

For RSR, RSR50 was the only attribute level found to have opposed views between the upstream and downstream group. The upstream group was WTP $24.58 compared to the downstream group who was WTA $5.36. These results suggest that the upstream group is quite concerned about the potential negative impact of salinity in the future and is willing to pay to reduce salinity. These results are supported by earlier findings which suggest VMD farmers do not want salinity impacting their cropland (Nhan et al., 2012). In contrast, the downstream group has already adapted to a high salinity rate and is willing to accept the RSR50 attribute level.

Table 14. Willingness to Accept/Pay MNL Model Estimations for the Upstream and Downstream Regions in VMD

Attribute level	**Upstream**		**Downstream**	
	Coefficient	**WTA ($US)**	**Coefficient**	**WTA ($US)**
F1120	-.183 (.148)	7.79	.110 (.123)	-2.90
F2130	.164 (.172)	-6.95	.573 (.172) *	-15.05
SM	.501 (.142) **	-21.30	.528 (.126) **	-13.87
SH	1.430 (.202) **	-60.71	.582 (.158) **	-15.27
RSR25	.243 (.213)	6.37	-.039 (.174)	-1.83
RSR50	-.578 (.177) **	24.58	.204 (.161) *	-5.36

RSR75	-.150 (.175)	-10.35	.069 (.174)	1.01
YM	.791 (.139) **	-33.63	.312 (.124) *	-8.20
YH	1.101 (.193) **	-46.81	.749 (.171) **	-19.66
Number of observations	3,120		3,946	
LR Chi[2]	540.92		663.85	
Log likelihood	-810.85		-1,038.10	

a. One (*) and two (**) asterisks represent 0.05, 0.01 levels of statistical significance, respectively.
b. The number in parentheses are standard errors.
c. Negative signs in WTA present willingness to accept. Positive signs of WTA present willingness to pay.

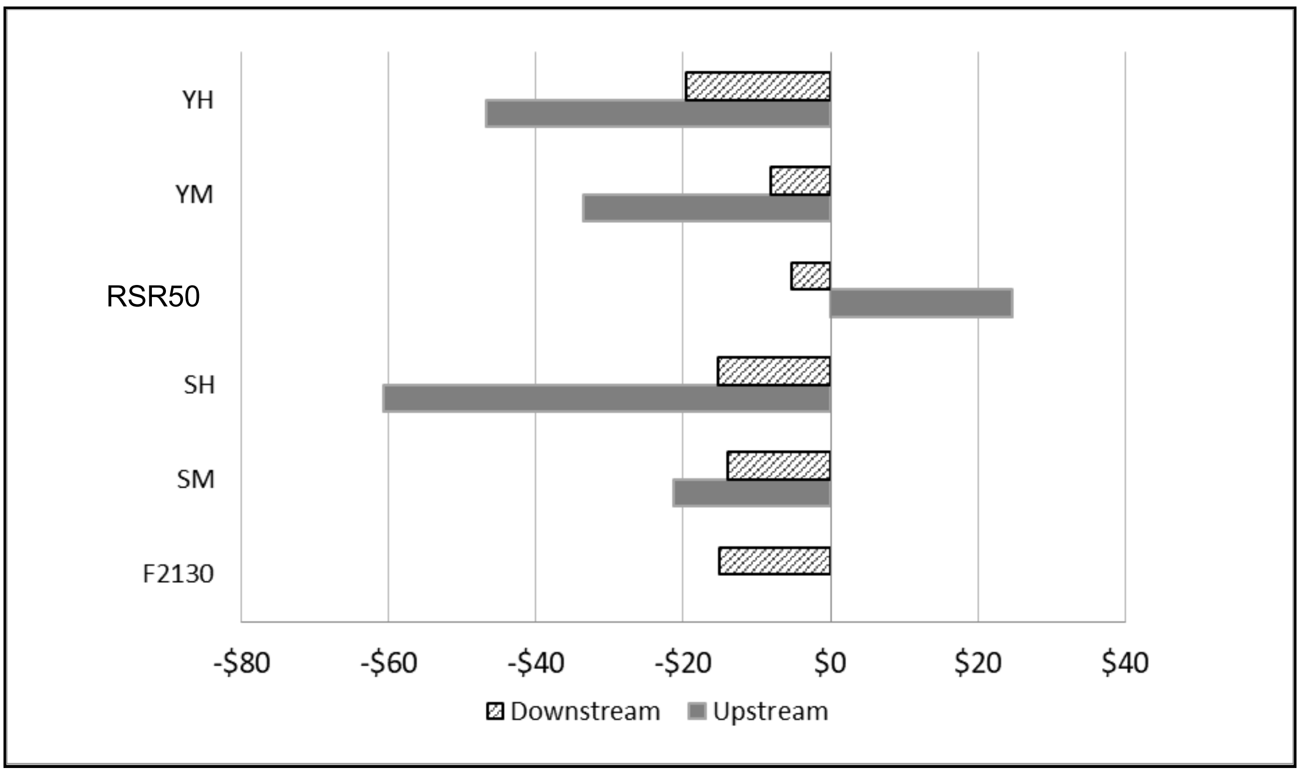

Figure 31. A Comparison between Upstream and Downstream Participants' Willingness to Accept/Willingness to Pay

The findings of the WTA/WTP analyses suggest that several aspects of a potential water management program in the VMD are important to residents, and that these aspects are valued very differently depending on where people reside. Overall, a management program for downstream residents would be much less costly, as respondents are WTA significantly less money than those upstream to see a change in the environment and therefore their livelihood. While a management program may be more costly to enact for upstream residents, the residents were actual WTP for moderate salinity levels, suggesting government intervention could indeed lead to government income.

4. Conclusion

The purpose of this study was to identify the important variables to upstream and downstream farmers in the VMD, using BWS, to better inform government policies on controlling the flood infrastructure. We found that there was not necessarily a one-size-fits-all approach to effective water management or intervention programs.

The BWS results suggest that respondents showed a higher preference for long-term floodwater ecosystem services, including sediment deposit and salinity reductions, compared to short-term benefits, including the amount of fish caught and crop yield. In addition, when choosing the attributes offered in the survey, the respondents did not necessarily choose the maximum attribute level. These results suggest that it is possible to convince residents of the VMD to agree to allow water from upstream to flood their land in order to bring resources downstream (e.g., sedimentation, fresh water) if their expectations are satisfied.

When dividing the respondents into an upstream or downstream group, the BWS results highlighting critical differences between these groups. While both groups valued high sedimentation and devalued amount of fish caught, the downstream farmers viewed salinity reduction in any amount as a positive attribute compared to upstream farmers who viewed it as a negative attribute. This demonstrates that the impact of flooding caused different results in the two regions. That is, those living downstream were more severely impacted by the present flooding control system.

We also proposed a hypothetical tax subsidy in this survey. Much like the BWS results, however, the WTP/WTA analyses showed differences in preferences among attributes between upstream and downstream residents. The downstream group was willing to accept a low mount of tax subsidy for each attribute, but the upstream group was only willing to accept a higher tax subsidy for most attributes. For the reduction in salinity attribute, the upstream group was willing to pay for a moderate reduction. These results suggest that a tax subsidy may be a viable form of compensation to help residents accept the destructive impacts of floodwaters. These fundamental differences in choices between the upstream and downstream group present an opportunity for the Vietnamese government to create multiple intervention programs, depending on the geographic location.

The findings of this study support the hypothesis the residents of the VMD would be willing to accept the disadvantages of the opening of the upstream sluice gates in the VMD during flood season in exchange for certain benefits. Also, these findings suggest that the Vietnamese government should offer appropriate education and training to farmers in the VMD to help them to adapt to the present and evolving environmental conditions.

Limitations

While the results of this study provide insight into potential water management programs, there were several limitations of this study. This study offered only five choices in the BWS, which may not represent the entire needs of the population of the two regions. There were 605 respondents to this survey in two different regions of the VMD, which makes it difficult to generalize the results to the population of the entire VMD. This study used a hypothetical agricultural tax subsidy for WTA/WTP. However, both the upstream and downstream group reported that they were currently receiving agricultural tax exemptions for extreme environmental events (e.g., drought, saltwater intrusion, flooding) during the survey process, which may confound the results of this attribute.

CHAPTER 5. SUMMARY AND CONCLUSION

1. Summary and Conclusion

Freshwater is a non-renewable resource that is vital to ecosystems and human society. The Mekong River flows through China, Myanmar, Laos, Thailand, Cambodia, and Vietnam, which raises political and economic issues among riparian countries. As in many other transboundary river basins globally, the MKB has faced issues relating to the sustainability of water supply when the region experience population increases, droughts, water quality, and water competition. These nations have exploited the benefits of the Mekong River, which has resulted in many conflicts among the countries. Because the VMD region is located at the mouth of the Mekong River, recent hydroelectric dam construction and increased agricultural use of water by upstream nations, in addition to climate change, has caused a substantial decrease in river flow to the VMD region. The Vietnamese government, through the MRC, has repeatedly requested that upstream countries adjust water management in order to increase the water flow to the VMD region. Thus, the objectives of this dissertation were to predict the surface water budget in the MKB by use of the VIC model, to develop an ANNs model for the prediction of soil moisture and drought risk, and to determine the willingness of residents of the VMD to accept short-term disadvantages for long-term water management interventions.

The VIC model predicted that land cover change would have a small impact on soil moisture and drought risk. This model also predicted that an increase in cropland would cause a decrease in soil moisture and an increase in drought risk. This model predicted that severe drought would occur along the coastal areas of the VMD year-round. However, our experience was such that the VIC model required much effort to prepare and compile the data into the model.

We developed an ANNs model using neural network architecture with two hidden layers to predict soil moisture and drought risk. This model's data calculated historical soil moisture distribution that had a high correlation with historical soil moisture data from remote sensing platforms. This suggests that the ANNs model may be used as an additional tool to predict soil moisture and drought risk in future studies.

We conducted a survey of inhabitants of the VMD to identify variables that the residents were willing to trade off short-term water management benefits for long-term floodwater benefits. The residents chose increased sediment deposits and salinity reduction as the most important long-term benefits in exchange for a short-term higher annual crop yield. However, there was a difference between the upstream and downstream farmers in the importance of salinity reduction. That is, the downstream farmers indicated that salinity reduction was of upmost importance, which reflects the greater sea water intrusion downstream compared to upstream. We also proposed a hypothetical tax subsidy to compensate farmers adversely affected by flood water. The downstream farmers were willing to accept a lower tax subsidy than the upstream farmers, most probably because the downstream residents are more severely affected by the existing flood control system. Many studies, such as Kakonen (2008), Tran (2018a, 2018b), Hoang et al. (2018), and Tran et al. (2019), have confirmed that using flood control measures at upstream regions for triple-rice cultivation resulted negative impacts to both ecological and socioeconomic aspects in VMD. Our research introduced a quantitative approach to estimate tradeoff between long term benefits, e.g., alluvial sedimentation, salinity reduction versus short term benefits, e.g. annual crop yield in flood control managements of Vietnamese government.

While this study identified attributes that residents of the VMD would be willing to trade, the bigger challenge is to convince the Vietnamese government to consider these data a call to reorganize its flood control policies in an equitable and sustainable manner. While scientists embrace the scientific process, government bureaucrats have their own agendas. Therefore, the next challenge would be to develop an approach to convince the government to consider a reorganization of the flood control policy such the application of a sluice-gated management schedule that would allow more floodwater flowing downstream during flood seasons.

This study estimated soil moisture and drought risk in the MKB based on the SLR and the digital elevation model obtained from the spaceborne platform SRTM DEM. However, recent studies have proposed that relative SLR is a combination of both SLR and land subsidence (Minderhoud et al., 2019, Tessler et al., 2015). However, the SRTM DEM does not consider land subsidence as a variable in SLR, which results in an underestimation of SLR compared to the relative SLR model. Therefore, future studies using the VIC and ANNs models to predict soil moisture and drought risk should consider using relative SLR (including land subsidence) as an input variable rather than using only SLR.

In summary, the present environmental conditions in the VMD, the attitudes of the residents of the VMD, and the data from the predicted model of the future of sea water intrusion, drought risk, and decreased freshwater flow in the VMD together suggest that the Vietnamese government should aggressively develop a more informed flood management system in the VMD.

2. Potential Application

Climate change has affected every river delta region globally. Predictions of the future of these bodies of water suggest that sea water intrusion and drought will only increase in these areas. Global population growth would certainly accelerate this process. The use of prediction models for soil moisture and drought risk are important tools to inform public policy. From our experience, the ANNs model is more user friendly than the VIC model for predicting soil moisture and drought. Therefore, future studies may consider using the ANNs model for predicting soil moisture and drought in similar large river deltaic systems (e.g., Nile River Basin, Mississippi River Basin).

The Best-worst scaling survey provided important information on VMD residents attitudes on tradeoffs of short-term benefits for long-term ecosystem services. This method may be used in other troubled river delta regions to define attributes that are important to residents to assist policy makers in developing policies to achieve sustainable and equitable socioeconomic development in the region. Thus, future studies of deltaic regions should consider using high-level techniques to predict change in soil moisture, drought, and seawater intrusion over time, how changes in these variables may affect the socioeconomic conditions of the residents of these deltaic regions, and how to influence government responses to these changing conditions that result in an equitable and sustainable future for the residents and the land.

REFERENCES

Agana, N., & Homaifar, A. (2017). A deep learning-based approach for long-term drought prediction. IEEE Xplore.

Andreadis, M.K., and P. D. Lettenmaier. (2006). “Trends in 20th-century drought over the continental United States.” Hydrology and Land Surface studies 1-4.

Assem, H., Ghariba, S., Makrai, G., Johnston, P., Gill, L., & Pilla, F. (2017). Urban water flow and water level prediction based on deep learning. Retrieved from ecmlpkdd2017: http://ecmlpkdd2017.ijs.si/papers/paperID343.pdf

Burke, Eleneanor J. (2006). “Modeling the Recent Evolution of Global Drought and Projections for the Twenty-First Century with the Hadley Centre Climate Model.” Journal of Hydrometeorology- Volume 7, 1113 - 1125.

Campbell, Ian C. (2016). “Integrated management in the Mekong River Basin.” Ecohydrology & Hydrobiology 16 255-262.

Chapman, Alexander. (2016). “Evaluating sustainable adaptation strategies for vulnerable mega-deltas using system dynamics modelling: Rice agriculture in the Mekong Delta’s An Giang Province, Vietnam.” The science of the Total Environment 326-338.

Chen, Chi-Farn, T.S. Nguyen, L.Y. Chang, and C.C. Chen. (2011). “Monitoring of soil moisture variability in relation to rice cropping systems in the Vietnamese Mekong Delta using MODIS data.” Applied Geography 463-475.

Daiss, T. (2016). Forbes. May. https://www.forbes.com/sites/timdaiss/2016/05/25/why-vietnam-is-running-dry-worst-drought-in-nearly-100-years/#2ab178e074b3.

Dang, Hoa L., Elton Li, Ian Nuberg, and Johan Bruwer. (2014). “Understanding farmers’ adaptation intention to climate change: A structural equation modelling study in the Mekong Delta, Vietnam.” Environmental Science & Policy 11-22.

Danh, V. T., & Mushtaq, S. (2011). Living with Floods: An Evaluation of the Resettlement Program of the Mekong Delta of Vietnam. In M. A. Stewart & P. A. Coclanis (Eds.), Environmental Change and Agricultural Sustainability in the Mekong Delta (pp. 181–204). Springer Netherlands. https://doi.org/10.1007/978-94-007-0934-8_11

Duc Tran, D., van Halsema, G., Hellegers, P. J. G. J., Phi Hoang, L., Quang Tran, T., Kummu, M., & Ludwig, F. (2018). Assessing impacts of dike construction on the flood dynamics of the Mekong Delta. Hydrology and Earth System Sciences, 22(3), 1875–1896. https://doi.org/10.5194/hess-22-1875-2018

Dung Duc Tran. (2018). Agricultural Land-Use Dynamics in The Floodplains of The Vietnamese Mekong Delta Hydrodynamic implications on flood regimes and adaptation options.

Eslami, S., Hoekstra, P., Nguyen Trung, N., Ahmed Kantoush, S., Van Binh, D., Duc Dung, D., Tran Quang, T., & van der Vegt, M. (2019). Tidal amplification and salt intrusion in the Mekong Delta driven by anthropogenic sediment starvation. Scientific Reports, 9(1), 18746. https://doi.org/10.1038/s41598-019-55018-9

FAO. (2016). The state of food and agriculture. Rome: FAO.

Flynn, T.N., Louviere, J.J., Peters, T.J., Coast, J., 2007. Best–worst scaling: what it can do for health care research and how to do it. J. Health Econ. 26, 171–189.

Friedl, M., Sulla-Menashe, D. (2019). MCD12Q1 MODIS/Terra +Aqua Land Cover Type Yearly L3 Global 500m SIN Grid V006

GSO. (2020). Statistical Yearbook of Vietnam_2019 (Vol. 2019). General Statistics Office. https://www.gso.gov.vn/wp-content/uploads/2020/09/Nien-giam-thong-ke-day-du-2019.pdf

Habiba, U., R. Shaw, and Y. Takeuchi. 2012. "Farmer's perception and adaptation practices to cope with drought: Perspectives from Northwestern Bangladesh." International Journal of Disaster Risk Reduction (Volume 1, 2012,) 1: 72-84.

Hang, N. T., & Wehn, U. (2016). Data sharing in international transboundary contexts: The Vietnamese perspective on data sharing in the Lower Mekong Basin. Journal of Hydrology, 351-364.

Heikkila, T., Gerlak K, A., Bell, A. R., & Schmeier, S. (2013). Adaptation in a transboundary river basin: Linking stressors and adaptive capacity within the Mekong River Commission. SciVerse ScienceDirect, 73-82.

Ho, B. M. (2016). "Vietnam's 2016 drought-hit rice output to fall 1.5 percent: government official." Reuters, May 30.

Hoang, L. P., Biesbroek, R., Tri, V. P. D., Kummu, M., van Vliet, M. T. H., Leemans, R., Kabat, P., & Ludwig, F. (2018). Managing flood risks in the Mekong Delta: How to address emerging challenges under climate change and socioeconomic developments. Ambio, 47(6), 635–649. https://doi.org/10.1007/s13280-017-1009-4

Holzman. (2014). "Estimating soil moisture and the relationship with crop yield using surface temperature and vegetation index." International Journal of Applied Earth Observations and Geoinformation (Elsevier B.V.) 181-192.

Hortle, K. (2007). Consumption and the yield of fish and other aquatic animals from the Lower Mekong Basin. 16, 1–88.

Howie, C. A. (2011). Co-operation and contestation: Farmer-state relations in agricultural transformation, An Giang Province, Vietnam. Royal Holloway, University of London.

https://pure.royalholloway.ac.uk/portal/files/25512782/Charles_Howie_PhD_thesis_2011_figure_4_removed.pdf

ICEM. (2010). Strategic Environmental Assessment of Hydropower on The Mekong Mainstream. Final report summary, Glen Iris: MRC.

Jacobi, John. (2013). "A tool for calculating the Palmer drought indices." Water Resources Research - Vol.49 6086-6089.

Judith Ehlert. (2010). Living with Flood—Local Knowledge in the Mekong Delta, Vietnam. WISDOM.

Kaukonen, Mira. (2008). "Mekong Delta at the Crossroads: More Control or Adaptation?" Ambio Vol. 37 205-212.

Khanal, U., Wilson, C., Hoang, V.-N., & Lee, B. (2018). Farmers' Adaptation to Climate Change, Its Determinants and Impacts on Rice Yield in Nepal. Ecological Economics, 144, 139–147. https://doi.org/10.1016/j.ecolecon.2017.08.006

Khong, T. D., Young, M. D., Loch, A., & Thennakoon, J. (2018). Mekong River Delta farm-household willingness to pay for salinity intrusion risk reduction. Agricultural Water Management, 200, 80–89. https://doi.org/10.1016/j.agwat.2017.12.010

Kummu, Matti. (2006). "Sediment-related impacts due to upstream reservoir trapping, the Lower Mekong River." Geomorphology 85 275–293.

Lamberts, D. (2008). Little impact, much damage: the consequences of Mekong River flow alterations for the Tonle Sap ecosystem. Modern myths of the Mekong, 3-18.

Le, A. T. (2011). "Climate Change in the Mekong River Delta and key concerns on future climate threads." Research Gate 206-217.

Lee, Ayeon. (2014). "Analysis of the effect of climate change on the Nakdong river streamflow using indicators of hydrological alteration." Journal of Hydro-environment Research 234-247.

Lem, A & Nghia, N. (2003). Module on Economic Modelling and Fish Consumption Report. FAO/DANIDA Fisheries Sector Programme Support.

Li, Zehua. (2016). "An agricultural drought index to incorporate the irrigation process and reservoir operations: A case study in the Tarim River Basin." Global and Planetary Change 10-20.

Louviere, J. J., & Islam, T., (2008). "A comparison of importance weights and willingness-to-pay measures derived from choice-based conjoint, constant sum scales and best-worst scaling," Journal of Business Research, 61 (9) (2008), pp. 903–911.

Louviere, J., Hensher, D., Swait, J., (2000). Stated Choice Methods—Analysis and Application.

Louviere, J.J., Flynn, T.N., and Marley, A.A.J. (2015). Best Worst Scaling: Theory, Methods and Applications. Cambridge University Press.

Lu, X. X., Li, S., Kummu, M., Padawangi, R., & Wang, J. J. (2014). Observed changes in the water flow at Chiang Saen in the lower Mekong: Impacts of Chinese dams? Large Asian Rivers VII, 336, 145–157. https://doi.org/10.1016/j.quaint.2014.02.006

Ma, Mingwei, Liliang Ren, Vijay P. Singh, Fei Yuan, Lu Chen, Xiaoli Yang, and Yi Liu. (2016). "Hydrologic model-based Palmer indices for drought characterization in the Yellow River basin, China." Stoch Environ Res Risk Assess 1401-1420.

Manh, N. V., Dung, N. V., Hung, N. N., Kummu, M., Merz, B., & Apel, H. (2015). Future sediment dynamics in the Mekong Delta floodplains: Impacts of hydropower development, climate change and sea level rise. Global and Planetary Change, 127, 22–33. https://doi.org/10.1016/j.gloplacha.2015.01.001

Marit Kitaw and Muluneh Yitayew. (2014). "Water Governance in the Nile Basin for Hydropower Development". In "Nile River Basin Ecohydrological Challenges, Climate Change and Hydropolitics". Page 499 – 515. DOI 10.1007/978-3-319-02720-3.

Minderhoud, P. S. J., Coumou, L., Erkens, G., Middelkoop, H., & Stouthamer, E. (2019). Mekong delta much lower than previously assumed in sea-level rise impact assessments. Nature Communications, 10(1), 3847. https://doi.org/10.1038/s41467-019-11602-1.

MONRE. (2017). Ministry of Natural Resources and Environment: http://www.monre.gov.vn. 2017

MRC. (1995). Mekong Agreement and Procedures. MRC.

MRC. (2016). IWRM- based Basin development strategy 2016-2020. For Sustainable Development,

MRC. (2017). 11 20. http://www.mrcmekong.org/about-mrc/history/.

MRC.(2005). Overview of Hydrology of the Mekong Basin. Vientiane: MRC.

NASA EOSDIS Land Processes DAAC. Accessed 2021-12-07 from https://doi.org/10.5067/MODIS/MCD12Q1.006

Nguyen Nghia, H., Delgado, J., Güntner, A., Merz, B., Bárdossy, A., & Apel, H. (2014). Sedimentation in the floodplains of the Mekong Delta, Vietnam Part II: Deposition and erosion. Hydrological Processes, 28. https://doi.org/10.1002/hyp.9855

Nguyen, K. V., & James, H. (2013). Measuring Household Resilience to Floods: A Case Study in the Vietnamese Mekong River Delta. Ecology and Society, 18(3), art13. https://doi.org/10.5751/ES-05427-180313

Nguyen, M. N., Nguyen, P. T. B., Van, T. P. D., Phan, V. H., Nguyen, B. T., Pham, V. T., & Nguyen, T. H. (2021). An understanding of water governance systems in responding to extreme droughts in the

Vietnamese Mekong Delta. International Journal of Water Resources Development, 37(2), 256–277. https://doi.org/10.1080/07900627.2020.1753500.

Nguyen, Quang M. (2017). "Is Vietnam in for Another Devastating Drought? Lessons learned from last year's disaster can shape a climate-resilient approach in the Mekong Delta." The Diplomat, 02 08.

Nguyen, Triet K.V., Dung V. Nguyen, Hideto Fujii, Matti Kummu, Bruno Merz, and Heiko Apel. (2017). "Has dyke development in the Vietnamese Mekong Delta shifted flood hazard downstream?" Hydrology and Earth System Science 3991-4010.

Nicholls, R.J. (2011). "Constructing Sea-Level Scenarios for Impact and Adaptation Assessment of Coastal Areas: A guidance document." IPCC.

NT Binh. (2015). Vulnerability and Adaptation to Salinity Intrusion in The Mekong Delta of Vietnam [Dissertation]. Rheinische Friedrich-Wilhelms-Universität Bonn. https://bonndoc.ulb.uni-bonn.de/xmlui/handle/20.500.11811/6230

Oluoch, S., Lal, P., Susaeta, A., & Wolde, B. (2021). Public preferences for renewable energy options: A choice experiment in Kenya. Energy Economics, 98, 105256. https://doi.org/10.1016/j.eneco.2021.105256

Orr, S., Pittock, J., Chapagain, A., & Dumaresq, D. (2012). Dams on the Mekong River: Lost fish protein and the implications for land and water resources. Global Environmental Change, 22(4), 925–932. https://doi.org/10.1016/j.gloenvcha.2012.06.002

Pham, Nam H. (2017). "Delta takes urgent steps to prevent drought." Viet Nam News, March 12.

Piman, T. and Shrestha, M. (2017). Case Study on Sediment in the Mekong River Basin: Current State and Future Trends. UNESCO and Stockholm Environment Institute (SEI)

Räsänen, Timo A. (2016). "Observed river discharge changes due to hydropower operations in the Upper." Journal of Hydrology.

Sebastian, L. S., Sander, B. O., Simelton, E., & Minh, D. N. (2016). The drought and salinity intrusion in the Mekong River Delta of Vietnam—Assessment Report [Assessment]. CGIAR Research Centers in Southeast Asia. https://www.researchgate.net/publication/309481170_The_drought_and_salinity_intrusion_in_the_Mekong_River_Delta_of_Vietnam_-_Assessment_report

Sebastian, L. S., Sander, B. O., Simelton, E., & Minh, D. N. (2016). The drought and salinity intrusion in the Mekong River Delta of Vietnam-Assessment Report [Assessment]. CGIAR Research Centers in Southeast Asia. https://www.researchgate.net/publication/309481170 The drought and salinity intrusion in the Mekong River Delta of Vietnam- Assessment report

Semu A. Moges and Mekonnen Gebremichael. 2014.” Climate Change Impacts and Development-Based Adaptation Pathway to the Nile River Basin”. In “Nile River Basin Ecohydrological Challenges, Climate Change and Hydropolitics”. Page 339 – 361. DOI 10.1007/978-3-319-02720-3.

Shrestha, Sangam. (2016). "Climate change impacts on groundwater resources in Mekong Delta under representative concentration pathways (RCPs) scenarios." Environmental Science & Policy 1-13.

Sithirith, M., and J. Gillen. (2017). "Furthering Mekong ontologies: On China and local uncertainties." Political Geography 139-141.

Smith, M., Lal, P., Oluoch, S., Vedwan, N., & Smith, A. (2021). Valuation of sustainable attributes of hard apple cider: A best-worst choice approach. Journal of Cleaner Production, 318, 128478. https://doi.org/10.1016/j.jclepro.2021.128478

Sokhem Pech & Kengo Sunada. (2008). Population Growth and Natural-Resources Pressures in the Mekong River Basin. AMBIO: A Journal of the Human Environment, 37(3), 219–224. https://doi.org/10.1579/0044-7447(2008)37[219:PGANPI]2.0.CO;2

Son, N.T. (2012). "Monitoring agricultural drought in the Lower Mekong Basin using MODIS NDVI and land surface temperature data ." Journal of Applied Earth Observation and Geoinformation 18 417–427.

Soto, J. R., Adams, D. C., & Escobedo, F. J. (2016). Landowner attitudes and willingness to accept compensation from forest carbon offsets: Application of best–worst choice modeling in Florida USA. Forest Policy and Economics, 63, 35–42. https://doi.org/10.1016/j.forpol.2015.12.004

Soto, J. R., Escobedo, F. J., Khachatryan, H., & Adams, D. C. (2018). Consumer demand for urban forest ecosystem services and disservices: Examining trade-offs using choice experiments and best-worst scaling. Ecosystem Services, 29, 31–39. https://doi.org/10.1016/j.ecoser.2017.11.009

Soto, J.R., Adams, D.C. and Escobedo, F.J., (2016). Landowner attitudes and willingness to accept compensation from forest carbon offsets: Application of best-worst choice modelling in Florida USA. Forest Policy and Economics, 63, pp.35-42.

Soukhaphon, A., Baird, I. G., & Hogan, Z. S. (2021). The Impacts of Hydropower Dams in the Mekong River Basin: A Review. Water, 13(3). https://doi.org/10.3390/w13030265

Tambo, J. A., & Wünscher, T. (2017). Farmer-led innovations and rural household welfare: Evidence from Ghana. Journal of Rural Studies, 55, 263–274. https://doi.org/10.1016/j.jrurstud.2017.08.018

Tanaka, M. 2003. "Flood–drought cycle of Tonle Sap and Mekong Delta area observed by DMSP-SSM/I." Int. J. Remote Sensing 1487-1504.

Tatsumi, K, and Y. Yamashiki. (2015). "Effect of irrigation water withdrawals on water and energy balance in the Mekong River Basin using an improved VIC land surface model with fewer calibration parameters." Agricultural Water Management (Elsevier) 159: 92-106.

Tessler, Z., Vörösmarty, C., Grossberg, M., Gladkova, I., Aizenman, H., Syvitski, J., & Foufoula-Georgiou, E. (2015). ENVIRONMENTAL SCIENCE. Profiling risk and sustainability in coastal deltas of the world. Science (New York, N.Y.), 349, 638–643. https://doi.org/10.1126/science.aab3574

Thanapon Piman & Manish Shrestha. (2017). Case study on sediment in the Mekong River Basin: Current state and future trends (Project Report No. 2017–03). Stockholm Enviromental Institute.

Thu, H.N., and U. Wehn. (2016). "Data sharing in international transboundary contexts: The Vietnamese perspective on data sharing in the Lower Mekong Basin." Journal of Hydrology 351-364.

Tong, Yen Dan. (2016). "Rice Intensive Cropping and Balanced Cropping in the Mekong Delta." Ecological Economics 205-212.

Tran, D. D., van Halsema, G., Hellegers, P. J. G. J., Hoang, L. P., & Ludwig, F. (2019). Long-term sustainability of the Vietnamese Mekong Delta in question: An economic assessment of water management alternatives. Agricultural Water Management, 223, 105703. https://doi.org/10.1016/j.agwat.2019.105703

Tran, D., Halsema, G. V. van, Hellegers, P., Ludwig, F., & Wyatt, A. (2018b). Questioning triple rice intensification on the Vietnamese Mekong delta floodplains: An environmental and economic analysis of current land-use trends and alternatives. Journal of Environmental Management, 217, 429–441.

Tran, D., Halsema, G., Hellegers, P., Ludwig, F., & Seijger, C. (2018a). Stakeholders' assessment of dike-protected and flood-based alternatives from a sustainable livelihood perspective in An Giang Province, Mekong Delta, Vietnam. Agricultural Water Management, 206, 187–199. https://doi.org/10.1016/j.agwat.2018.04.039

Tran, T. A., & Rodela, R. (2019). Integrating farmers' adaptive knowledge into flood management and adaptation policies in the Vietnamese Mekong Delta: A social learning perspective. Global Environmental Change, 55, 84–96. https://doi.org/10.1016/j.gloenvcha.2019.02.004

Tran, T. A., James, H., & Pittock, J. (2018). Social learning through rural communities of practice: Empirical evidence from farming households in the Vietnamese Mekong Delta. Learning, Culture, and Social Interaction, 16, 31–44. https://doi.org/10.1016/j.lcsi.2017.11.002

Tran, T. A., Nguyen, T. H., & Vo, T. T. (2019). Adaptation to flooding and salinity environments in the Vietnamese Mekong Delta: Empirical analysis of farmer-led innovations. Agricultural Water Management, 216, 89–97. https://doi.org/10.1016/j.agwat.2019.01.020

Trandem, A. (2015). "Dam diplomacy on the Mekong." The Phnom Penh Post, January 26. 2015.

Trung, Dang D. (2007). Agrarian reform in southern Vietnam from 1975 to the late 1980s: from small to large scale farming and back again. Australian National University, PhD dissertation.

Udmale, Rameshwar, Yutaka Ichikawa, Sujata Manandhar, Hiroshi Ishidaira, and Anthony S. Kiem. 2014. "Farmers' perception of drought impacts, local adaptation and administrative mitigation measures in Maharashtra State, India." Internal Journal of Disaster Risk Reduction 250-269.

UN. (2008). Design household survey samples: Practical Guidelines: Studies in Methods, Series F No.98, United Nations.

United Nations. (2020). Viet Nam: Drought and Saltwater Intrusion in the Mekong Delta Joint Assessment Report [Assessment]. Catholic Relief Services, Save The Children, UN Country Team in Viet Nam. https://reliefweb.int/report/viet-nam/viet-nam-drought-and-saltwater-intrusion-mekong-delta-joint-assessment-report

USGS (2017). The USGS Water Science School. https://water.usgs.gov/edu/qadroughts.html.

USGS. (2017). LP DAAC. https://lpdaac.usgs.gov/.

Van, T. P. D., Nguyen, H. T., & Vo, T. Q. (2013). Vulnerability to Flood in the Vietnamese Mekong Delta: Mapping and Uncertainty Assessment. Journal of Environmental Science and Engineering, B 2, 229–237.

Vigerstol, K., and E. J. Aukema. (2011). "A comparison of tools for modelling freshwater ecosystem services." Journal of Environmental Management (Elsevier) 1-7.

Wells, Nathan. (2003). PDSI User's Manual-Version 2.0. Lincoln, Nebraska: National Agricultural Decision Support System.

Widrow, B., Rumelhart, D. E., & Lehr, M. A. (1994). Neural Networks: Applications in Industry, Business, and Science. Communications of the ACM, 93-105.

Wilson, R. L., & Sharda, R. (1994). Bankruptcy prediction using neural networks. Decision Support Systems, 545-557.

Wolford, Wendy W., and Timothy Gorman. (2010). "Land Reform and Landless Movements ." The International Studies Encyclopedia: Blackwell Reference Online.

Zhang, Binghua. (2014). "Drought impact on vegetation productivity in the Lower Mekong Basin." International Journal of Remote Sensing 2835 - 2856.

Zhang, G., Patuwo, E. B., & Hu, M. H. (1998). Forecasting with artificial neural networks: The state of the art. International Journal of Forecasting, 35-62.

Zhang, Quiang. (2015). "Evaluation of ecological instream flow using multiple ecological indicators with consideration of hydrological alterations." Journal of Hydrology 711-722.

Zikmund, W.G., and B.J. Babin. (2010). "Exploring Marketing Research." In Exploring Marketing Research. Cengage Learning. http://primary.forestproductslocator.org/.

Ziv, Guy. (2012). "Trading-off fish biodiversity, food security, and hydropower in the Mekong River Basin." PNAS 5609-5614.